IRF3 is a Critical Regulator of Adipose Glucose and Energy Homeostasis

Dr. Evan Rosen Xun Wang

IRF3 is a Critical Regulator of Adipose Glucose and Energy Homeostasis

Abstract

Obesity is associated with a state of chronic inflammation, which is believed to contribute to insulin resistance. We previously identified interferon regulatory factor 3 (IRF3) as an anti-adipogenic transcription factor with high expression in adipocytes. Because IRF3 is known to drive expression of pro-inflammatory genes in immune cells, we hypothesized that it may also promote inflammation and insulin resistance in adipocytes. Consistent with our expectations, we found that the expression of inflammatory genes in adipocytes was induced by IRF3 overexpression, while knockdown of IRF3 had the opposite effect. Despite this effect on local adipocyte gene expression, we found that *Irf3*$^{-/-}$ mice did not show evidence of altered systemic inflammation. Nonetheless, *Irf3*$^{-/-}$ mice did display altered metabolism relative to their wild type (WT) littermates. For example, high fat diet (HFD) fed *Irf3*$^{-/-}$ mice exhibited increased lean mass and decreased fat mass compared to WT, accompanied by increased food intake and energy expenditure. Further investigation showed that the white adipose tissue (WAT) of *Irf3*$^{-/-}$ mice had increased expression of brown adipocyte selective genes compared to WT, and the inguinal WAT of the *Irf3*$^{-/-}$ mouse contain multilocular adipocytes that resemble brown adipocytes. These data suggest that IRF3 affects energy homeostasis by regulating the development of brown adipocyte-like cells

in WAT. Additionally, *Irf3*$^{-/-}$ mice are significantly more insulin sensitive and glucose tolerant compared to WT when kept on HFD. Consistent with *in vivo* observations, IRF3 knockdown in 3T3-L1 adipocytes resulted in enhanced insulin-stimulated glucose uptake and lipogenesis, while overexpression of constitutively active IRF3 had the opposite effect. Several IRF3 target genes in adipocytes were identified using transcriptional profiling. Interestingly, the expression level of *Slc2a4* (encoding the Glut4 protein) was inversely correlated with that of IRF3 in both WAT and cultured adipocytes. Analysis of the *Slc2a4* proximal promoter identified a putative IRF3 binding site upstream of the transcription start site, and luciferase assay in 3T3-L1 adipocytes showed that IRF3 negatively regulates *Slc2a4* expression via this site. Taken together, these data indicate that IRF3 plays a role in whole body glucose homeostasis by repressing thermogenic gene expression as well as the expression of adipose Glut4.

Table of Contents

List of Figures

Acknowledgements

This dissertation would not have been possible without the guidance and support of my advisor, Professor Evan Rosen. Thank you for your continued patience and encouragement throughout this project. Your advice has helped me grow both scientifically and professionally through my time in your lab.

Thank you to my dissertation advisory committee, Professors Ronald Kahn, Gokhan Hotamisligil, Guo-Ping Shi, and Michael Grusby. They provided invaluable insight into all aspects of my project. Their advice helped to point me in the right direction during the early stages of the project and kept me focused throughout my research.

I am especially grateful to Jun Eguchi for guiding me and helping me get started on my project during my early years in the lab. He taught me a great deal about the field of metabolism, and this project would not have been possible without his help.

I would also like to thank the past and present members of the Rosen lab. Throughout the years, my labmates shared excellent scientific ideas, provided helping hands during my experiments, and gave me encouragement to move forward on my project.

Additionally, I am thankful to Professor Bruce Spiegelman for his advice and expertise over the years. As a result of the close association between the Spiegelman and Rosen labs, I learned significantly more about the metabolism field. The members of the Spiegelman lab gave me excellent scientific insight and experimental help.

Moreover, I would like to thank the members of the BIDMC Division of Endocrinology. Through our countless conversations, I found invaluable advice both personally and scientifically. The encouragement of my division colleagues also helped to keep me moving forward throughout the years.

Thank you as well to the department of Biological and Biomedical Sciences for the opportunity to perform my graduate studies in this department.

Special thanks to my classmates. I am fortunate to have classmates whom I remained close with throughout my graduate studies. Their support and friendship was crucial for my success in graduate school.

Finally I would like to thank my family for their constant love and support throughout my graduate studies and prior. I owe my success to all of you.

Chapter 1

Introduction

Adipose tissue is an important metabolic organ

Adipose tissue was traditionally viewed as an inert tissue that merely provides a storage site for triglycerides. However, over the past twenty years, numerous studies have shown that adipose tissue is also an important endocrine organ that produces numerous hormones and cytokines that control metabolism, blood pressure, hemostasis, and immune responses throughout the body[1]. Leptin is an adipokine, a name referring to cytokines produced by the adipose tissue, which regulates food intake by binding specific neurons in the hypothalamus to decrease appetite and stimulate energy expenditure[2, 3]. Adiponectin, another major adipokine, acts on the liver and muscle to promote fatty acid oxidation and enhance insulin sensitivity. Adipose tissue also releases inflammatory cytokines such as TNFα and IL-6 that regulate and participate in inflammation[4]. Proteins of the renin-angiotensin system are released by the adipose tissue in response to changes in nutritional availability and can act on the vasculature to regulate blood pressure and fluid balance[5]. In addition to initiating efferent signals, adipose tissue can also respond to signals from the central nervous system and other peripheral organs via various receptors expressed by adipocytes. For instance, insulin secreted by pancreatic β-cells can act on the adipose tissue to stimulate glucose uptake during feeding, while glucagon secreted by pancreatic α-cells stimulate the adipose tissue to breakdown lipid storage and release fatty acids into the circulation during starvation[6, 7]. Thus, adipose tissue is an integral part of the metabolic regulatory machinery.

White vs. brown adipose tissue

Two distinct types of adipose tissue exist in mammals, i.e. white and brown adipose tissues. They have in common the ability to store lipid in the form of triglyceride; however, they are distinct both histologically and functionally, and they have different developmental origins[6]. The predominant form is the white adipose tissue (WAT), whose major constituents are white adipocytes, preadipocytes, endothelial cells, and immune cells. WAT is localized in many depots throughout the body, but is often characterized as belonging to one of two categories[8]. Subcutaneous fat can be found in relatively small depots under the skin, while visceral fat is located in large intra-abdominal depots[8]. Each WAT depot also serves distinct functions, with the intra-abdominal depots more closely associated with the onset of obesity, diabetes and cardiovascular diseases[9, 10]. Because of its primary function of energy storage and mobilization, WAT has the ability to greatly expand in size even in adulthood, surpassing any other tissue in the body in this regard[11]. White adipocytes are characterized by large unilocular lipid droplets occupying most of the cytoplasm, squeezing the nucleus into a thin rim at the plasma membrane[8].

In contrast, brown adipose tissue (BAT) specializes in energy expenditure[7]. Compared to WAT, BAT exists in much smaller depots and can be found in interscapular depots in mice and supraclavicularly in adult humans[12]. BAT is mostly made up of brown adipocytes, which are characterized by multilocular lipid droplets and abundant mitochondria in the cytoplasm, facilitating rapid fatty acid oxidation and heat production[8]. Compared to WAT, BAT is much better vascularized and innervated[8]. The

major function of BAT is to regulate energy expenditure via adaptive thermogenesis, a process unique to this tissue[7].

Adaptive thermogenesis is achieved through the function of uncoupling protein 1 (Ucp1), which is highly expressed in brown adipocytes and localizes to the inner mitochondrial membrane[7]. In most cell types, the mitochondrial electron transport chain establishes an electrochemical gradient across the inner mitochondrial membrane and ATP is synthesized as the protons rush back across the membrane[13]. In brown adipocytes, Ucp1 promotes thermogenesis by allowing dissipation of the mitochondrial proton gradient without concomitant ATP synthesis[14]. Thus, in brown adipocytes oxygen consumption results in heat generation instead of ATP production. Mice lacking Ucp1 protein are unable to maintain normal body temperature when exposed to a cold challenge; they are also susceptible to obesity when maintained under thermoneutrality[12]. Traditionally, it was thought that in humans BAT only exists in infants and disappears with age; however, recent clinical studies have identified active BAT depots in the interscapular region of adult human subjects[15-18]. Thus, BAT is a potential therapeutic target in the treatment of the metabolic syndrome by increasing energy dissipation via adaptive thermogenesis, and exploring methods to stimulate the generation and activation of BAT may result in new therapeutic approaches.

Adipocyte plasticity

Adipocytes are derived from a mesenchymal stem cell lineage[8]. It was previously believed that white and brown adipocytes originate from a common progenitor. Under

the appropriate stimulation, brown adipocytes can arise within WAT and vice versa[19]. For instance, ageing leads to replacement of BAT depots by WAT in both human and mice[20, 21]. High fat diet-induced obesity leads to morphological changes in BAT that leads to the appearance of white adipocyte-like cells[22]. Conversely, under thermogenically challenging conditions, such as chronic cold exposure or pharmacological treatment with β_3 adrenergic receptor agonists, brown adipocyte-like cells, also called "beige" or "BRITE" cells, can be found in WAT depots[8, 23]. These beige cells histologically resemble brown adipocytes in that they have multilocular lipid droplets. Functionally, beige cells also express Ucp1 and perform adaptive thermogenesis[19].

Recent work suggests that WAT and BAT are actually derived from distinct precursor populations. Brown adipocytes were found to be developmentally closer to skeletal muscle than white adipocytes[24-26]. Brown adipocytes are derived from dermatomyotomal precursor cells that express *Myf5*, which was previously thought to be exclusively expressed in committed skeletal muscle precursors[24-26]. These precursor cells differentiated into brown adipocytes upon induction of the PRDM16 transcription factor and turned into muscle cells if PRDM16 is absent. In contrast, these cells were unable to form white adipocytes even when treated with a pro-adipogenic cocktail[24-28]. Gene expression analysis also showed that brown adipocyte precursors and skeletal muscle cell precursors but not white adipocyte precursors express a closely related gene profile[29]. Lastly, proteomic analysis showed that BAT and skeletal muscle, but not WAT, have a highly related mitochondrial proteomic signature[30].

Although it is now clear that WAT and BAT are derived from distinct lineages, whether the beige cells appearing in WAT are derived from a BAT or WAT lineage is still under debate. Although these cells appear like brown adipocytes both histologically and functionally, they are not derived from a Myf5 positive lineage[25, 26, 28]. Recent data point to the possibility that they are derived from resident mesenchymal stem cells from the white adipocyte lineage but poised for "browning".

Transcriptional regulation of adipogenesis

Under conditions of excess nutrition, adipose tissue can generate more adipocytes for energy storage by inducing adipogenesis of resident mesenchymal stem cells, which have been primed to differentiate into adipocytes[7]. Adipogenesis is a complex but tightly controlled process that involves the interaction of numerous transcription factors. CCAAT/enhancer binding proteins C/EBPβ and C/EBPδ are two of the first major transcription factors to be turned on during adipogenesis. While their induction is early but transient, another family member, C/EBPα, is induced later during adipogenesis but remains highly expressed throughout the differentiation process as well as in mature adipocytes[31]. C/EBPβ, δ, and α in turn induces expression of peroxisome proliferator activated receptor γ (PPARγ). PPARγ is considered to be the master regulator of adipogenesis as it is both necessary and sufficient for differentiation to occur[32, 33]. PPARγ forms a heterodimer with retinoid X receptor α (Rxrα), which in turn activates transcription of downstream adipogenic genes[34, 35]. One of PPARγ's

transcriptional targets is C/EBPα, therefore these two transcription factors form a positive feedback loop, allowing both to maintain a high level of expression during the adipogenic process and throughout the life of the mature adipocyte[33, 36-38].

Both PPARγ and C/EBPα turn on the expression of additional transcription factors important for adipogenesis as well as mature adipocyte function. For instance, in adipose tissue PPARγ turns on the expression of *Pepck*, *Fabp4*, *CD36*, and lipoprotein lipase (*Lpl*)[39, 40]. Similarly, C/EBPα can enhance the expression of *Pepck* and *Fabp4* as well as *Scd1* and *Slc2a4*[41-43].

Although PPARγ and C/EBPα are the two major transcription factors regulating adipogenesis, this complex process requires the interaction of many other transcription factors, both pro-adipogenic and anti-adipogenic. One prominent pro-adipogenic transcription factor is kruppel like factor 15 (Klf15). It is up-regulated during adipogenesis and has been found to induce the expression of PPARγ and Glut4[44, 45]. Sterol regulatory element binding protein 1 (Srebp1) has also been found to induce PPARγ expression, as well as regulate fatty acid metabolism and cholesterol homeostasis[36]. In contrast, Gata2 and Gata3 negatively regulate adipogenesis by transcriptionally down-regulating PPARγ; expression of Gata factors also decreased during adipogenesis[38, 46].

Unbiased search for transcription factors regulating adipogenesis

Although many major nodes in the complex adipogenic transcriptional cascade have been described, many relevant factors have yet to be identified[38]. To further

understand adipogenesis our lab set out to find additional transcription factors regulating this process. One way to predict transcription factor involvement in biological processes is to analyze chromatin structure changes throughout the process[47]. Thus we employed DNase hypersensitivity assay followed by computational motif finding to identify transcription factors involved in adipogenesis.

The DNase hypersensitivity assay takes advantage of the ability of small amounts of DNase I to digest regions of open chromatin while leaving compact heterochromatin intact[47, 48]. Open chromatin is known to be associated with promoters, enhancers, silencers, insulators, and other regions with active transcription factor binding[47-49]. Because we were specifically interested in adipogenesis we focused on studying the changes in chromatin state in 3T3-L1 preadipocytes and adipocytes. To find chromatin regions active during adipogenesis, we reviewed relevant literature to identify 27 key genes that showed relatively adipocyte-specific expression and whose expression levels were induced during adipogenesis. These 27 genes are all well known players in adipogenesis, e.g. *Pparγ*, *Cebpα*, *Fabp4*, etc. We restricted our search to highly conserved regions within 50kb upstream and in the first intron of the 27 selected genes and designed primers specific for each of the identified regions. Q-RTPCR on DNase I digested chromatin from 3T3-L1 preadipocytes and adipocytes identified 32 regions that had reduced copy numbers in DNase I digested adipocyte chromatin compared to preadipocyte chromatin, or in other words, were DNase I hypersensitive[50]. Computational motif finding was employed to identify overrepresented motifs in these 32 regions[50-52].

From this assay, we identified the orphan nuclear receptor chicken ovalbumin upstream promoter transcription factor II (COUP-TFII) as a regulator of adipogenesis[53]. We performed *in vitro* assays using 3T3-L1 preadipocytes to confirm this finding. Overexpression of COUP-TFII in 3T3-L1 preadipocytes suppressed adipogenesis, while knockdown enhanced adipogenesis[53]. These results indicate that the combination of DNase hypersensitivity assay and computational motif finding is a valid approach to identify novel transcription factors in adipogenesis. In addition to COUP-TFII, one of the top scoring motifs identified was a binding site for interferon regulatory factors (IRFs), known as interferon stimulated regulatory element (ISRE)[50].

IRFs

IRFs are a family of transcription factors that play a variety of critical roles in the immune system. There are nine members in the mammalian IRF family, IRF1 through IRF9, each serving distinct roles in host defense, growth control, and immunomodulation[54]. All nine IRFs contain a well conserved helix-turn-helix DNA binding domain (DBD) in their N-terminus, which binds the ISRE in the promoter region of target genes[55]. The C-terminus domain of IRFs consists of an IRF association domain (IAD), mediating interactions with other IRFs and additional transcriptional co-modulators, as well as clusters of phosphorylation sites conferring post-translational regulation. This region is distinct for each IRF family member[55] (Figure 1.1).

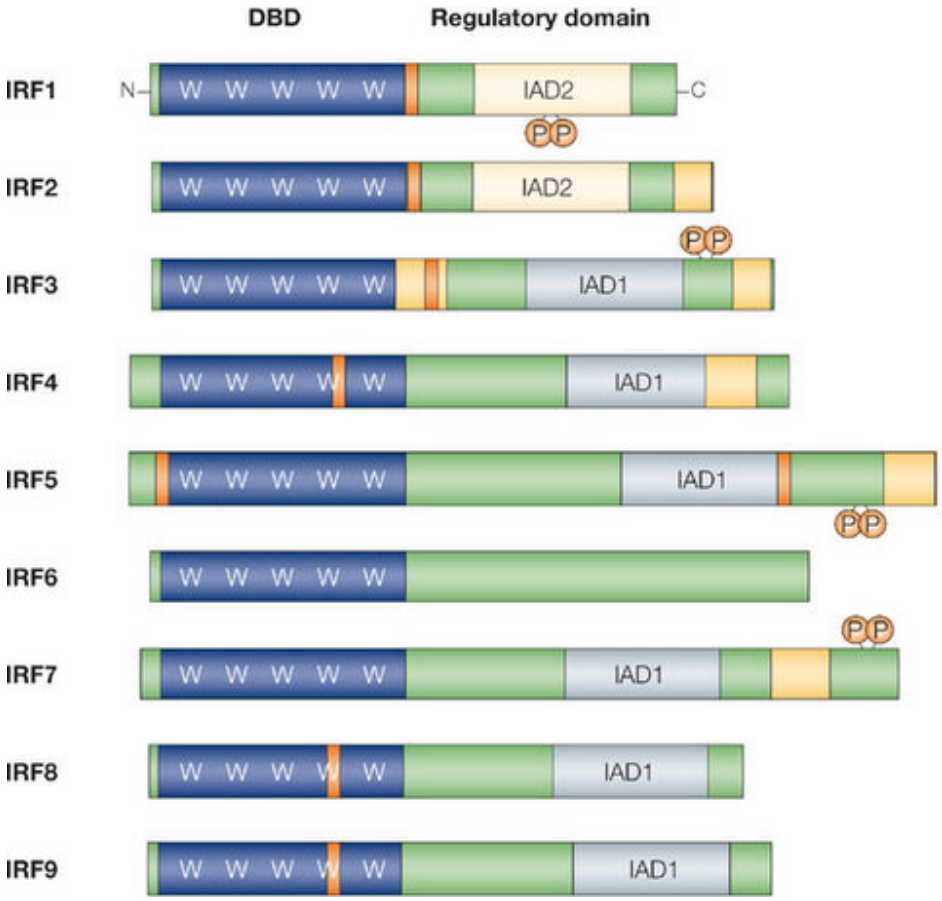

Figure 1. 1 The interferon regulatory factor protein family.

The structure of the nine proteins in the mammalian IRF family. All IRFs contain a well-conserved DNA binding domain (DBD, blue) defined by five tryptophan residues (W). The regulatory domain (green) is in the C-terminus. Most IRFs also contain either IRF association domain type 1 (IAD1) or type 2 (IAD2). Some members of the IRF family also contain repression domains (yellow) or nuclear-localization signals (orange). Some IRFs are regulated by phosphorylation (P) in their regulatory domains. Figure adapted from Lohoff and Mak, Nature Reviews Immunology 2005[55].

IRFs were originally named for their ability to induce type I interferons upon infection[56]; however, further studies revealed IRFs to be involved in a diverse group of immune functions. They are important players in the regulation of innate immune response, cell growth, apoptosis, and oncogenesis, and the development and maturation of various immune cells including dendritic cells, myeloid cells, natural killer cells, B cells, T cells, and erythroid cells[54, 55, 57].

Although IRFs are very well studied in the context of immunity, there have been no previous reports of their function in adipocytes. We found all nine IRFs to be expressed in 3T3-L1 adipocytes, in a developmentally-regulated fashion, as well as in the adipose tissue of mice (Figure 1.2)[50]. Additionally we performed a combination of ChIP, EMSA, and luciferase assays in 3T3-L1 preadipocytes versus adipocytes. These results confirmed the adipocyte specific binding of several IRFs to the ISRE sites predicted by the DNase I hypersensitivity assay[50].

Gene expression analysis in 3T3-L1 adipocytes showed that all nine IRFs are expressed in adipocytes. However, IRF3 and IRF4 were particularly interesting in that they exhibited low expression levels in preadipocytes and were significantly induced in the mature adipocyte (Figure 1.2A)[50], indicating that in addition to adipogenesis they may also play an important role in mature adipocyte function.

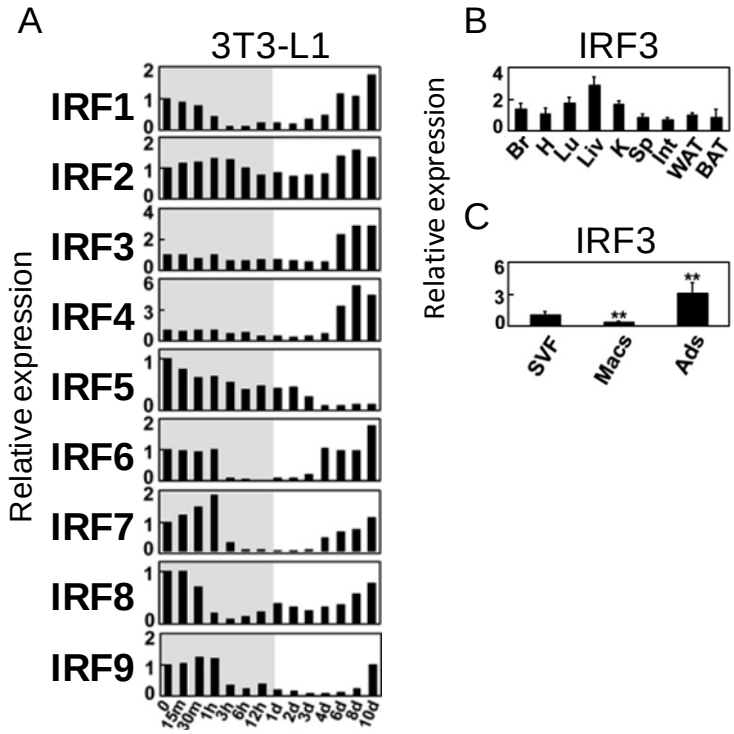

Figure 1. 2 IRFs are expressed in adipocytes.

A) Expression of all nine IRFs during 3T3-L1 differentiation as determined by Q-RTPCR. The shaded area indicates time points <24hr after induction of adipogenesis, n=3. B) IRF3 expression in tissues from male FVB mice as determined by Q-RTPCR. Br: brain, H: heart, Lu: lung, Liv: liver, K: kidney, Sp: spleen, Int: intestine, WAT: epididymal white adipose tissue, BAT: interscapular brown adipose tissue, n=3. C) IRF3 expression in the fractionated epididymal fat pads of C57BL/6 mice. SVF: stromal vascular fraction, Macs: F4/80 positive macrophages, Ads: adipocytes, n=6, **P < 0.01 versus SVF, n.d. = not detectable. Figure adapted from Eguchi et al. Cell Metabolism 2008[50].

We studied the role of IRF4 in adipocytes by characterizing the metabolic phenotype of mice lacking IRF4 in adipocytes. These mice exhibit increased adiposity

and deficient lipolysis[58]. Mechanistic studies showed IRF4 to be a critical determinant of the transcriptional response to nutrient availability in adipocytes. Fasting induces IRF4 in an insulin- and FoxO1-dependent manner, and IRF4 is required for lipolysis, at least in part due to direct effects on the expression of adipocyte triglyceride lipase (ATGL) and hormone-sensitive lipase (HSL) (Figure 1.3)[58].

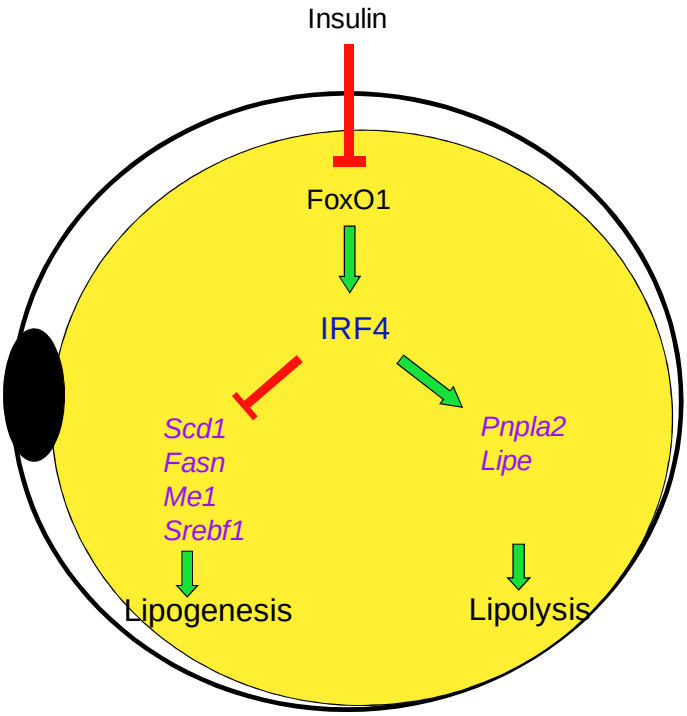

Figure 1. 3 IRF4 is a transcriptional regulator of adipose nutrient response.

In addition to IRF4, IRF3 expression is also upregulated in the mature 3T3-L1 adipocytes (Figure 1.2A)[50]. We found IRF3 to be expressed in all tissues tested, including WAT and BAT (Figure 1.2B). When the epididymal WAT was fractionated, the expression level of IRF3 was higher in the adipocytes compared to the infiltrating macrophages, as well as the stromal vascular fraction (SVF) (Figure 1.2C)[50].

IRF3 was also found to be an important player in adipogenesis. In 3T3-L1 preadipocytes over-expressing IRF3, adipogenesis was greatly attenuated as measured by both Oil-Red-O staining of triglyceride content (Figure 1.4A) and gene expression analysis of key markers of adipogenesis such as *Pparγ*, *Cebpα*, *Fabp4*, etc. (Figure 1.4B). Conversely, shRNA-mediated IRF3 knockdown in 3T3-L1 adipocytes resulted in enhanced adipogenesis (Figure 1.4C and D)[50]. These data indicate IRF3 to be a transcription factor regulating both adipogenesis and adipocyte function.

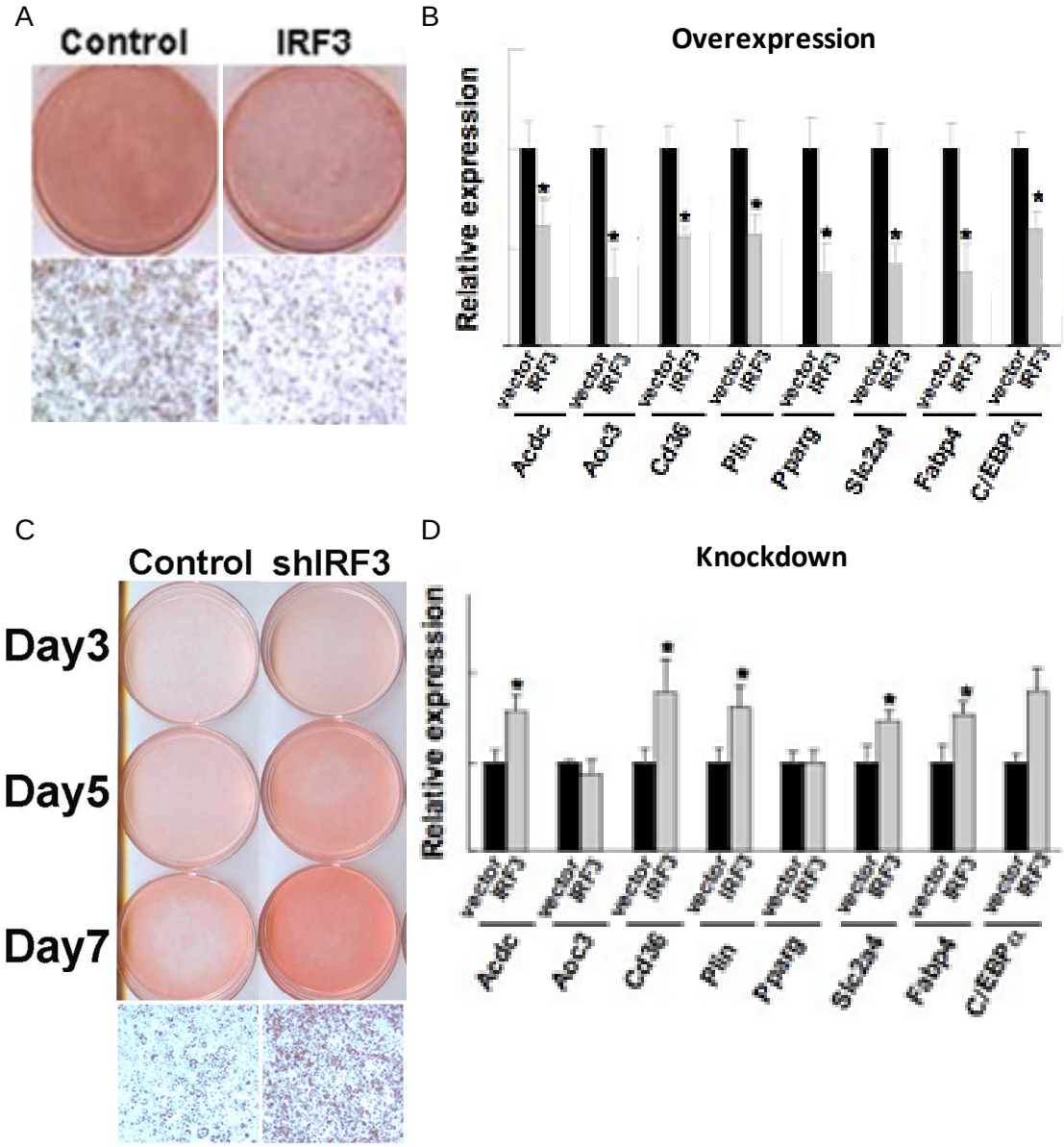

Figure 1. 4 IRF3 is anti-adipogenic in 3T3-L1 cells.

A - B) 3T3-L1 preadipocytes were transduced with retrovirus expressing IRF3, then differentiated with a dexamethasone, IBMX, and insulin cocktail (DMI). Experiments were performed seven days post-differentiation. A) Oil-Red-O staining. B) Q-RTPCR of adipocyte selective genes. C - D) 3T3-L1 preadipocytes were transduced with lentivirus

Figure 1.4 (Continued). expressing shIRF3 and differentiated with DMI. C) Oil-Red-O staining was performed at three, five, and seven days post differentiation. D) Q-RTPCR of adipocyte selective genes was performed seven days after differentiation. *P<0.05, **P<0.01, n=3. Figure adapted from Eguchi et al. Cell Metabolism 2008[50].

IRF3

Although its role in metabolism has not been characterized, IRF3 has been well studied in the context of immunity. It is recognized as the major effector of the induction of interferon gene expression as part of the innate immune response to viral infection[59-61]. Additionally, IRF3 has also been implicated in viral as well as bacterial mediated apoptosis[57].

IRF3 is a unique member of the IRF family in that it is constitutively expressed in all cells and tissues, while its activity in innate immune response is regulated post-translationally[61]. There are two clusters of phosphorylation sites in the C-terminus region of IRF3. The first region is located at Ser385/Ser386, while the second region is at Ser396/Ser398/Ser402/Thr404/Ser405[62, 63]. Upon viral infection, IRF3 is phosphorylated at its C-terminus. Although the precise residue critical for IRF3 activation is still a subject of intense debate[64-67], it is widely accepted that phosphorylation must occur within the 385-405 amino acid region for IRF3 to be activated[68-70], and mutation of the serine residues in this region into aspartic acid results in a constitutively active IRF3 mutant[69] (Figure 1.5). Phosphorylated IRF3 undergoes a conformational change that exposes the DBD and the IAD, facilitating homo-dimerization as well as interaction with

the CREB/p300 cofactor[62, 63, 71]. Binding with CREB/p300 allows IRF3 to shuttle into the nucleus where it forms a complex with other viral response proteins such as NF-κB[72-75]. This complex can then bind to ISRE sequences and induce transcription of genes critical for the antiviral response, including *Ccl5*, *Ifnβ*, and *Ifit1*[59, 61, 76, 77]. Activated IRF3 is shuttled out of the nucleus via its nuclear export sequence, after which it rapidly undergoes proteasomal degradation, thus ensuring the timely termination of the inflammatory response[70, 75, 78, 79].

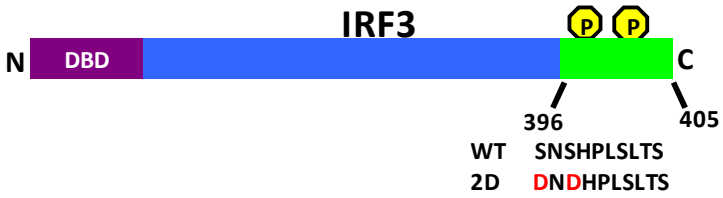

Figure 1. 5 Schematic of the IRF3 protein.

The IRF3 protein has a cluster of phosphorylation sites in its C-terminus. Mutation of amino acids 396 and 398 from serine to aspartic acid results in the 2D mutant that is constitutively active.

The signaling pathways leading to IRF3 activation in the adipocyte have not been identified, but it is well studied in immune cells. IRF3 activation is initiated by pathogen associated molecular patterns binding to toll like receptor 4 (TLR4), located on the cell surface[54, 61]. TLR4 recognizes a diverse group of ligands including lipopolysaccharide (LPS), the fusion protein of respiratory syncytial virus, and certain free fatty acids (FFAs)[80-82], while its signaling depends on four adaptor molecules, including myeloid

differentiation factor 88 (MyD88)[83, 84], TIR domain containing adaptor protein (TIRAP)[85, 86], TIR containing adaptor molecule 1 (TICAM1)[87, 88], and TRIF related adaptor molecule (TRAM)[89, 90]. Ligand binding activates two pathways downstream of TLR4: the MyD88-dependent and the MyD88-independent pathways. Signaling through the MyD88-independent pathway activates Iκβ kinase ε (IKKε) and TANK binding kinase 1 (TBK1), which together phosphorylate IRF3, leading to its dimerization and translocation[91-93] (Figure 1.6).

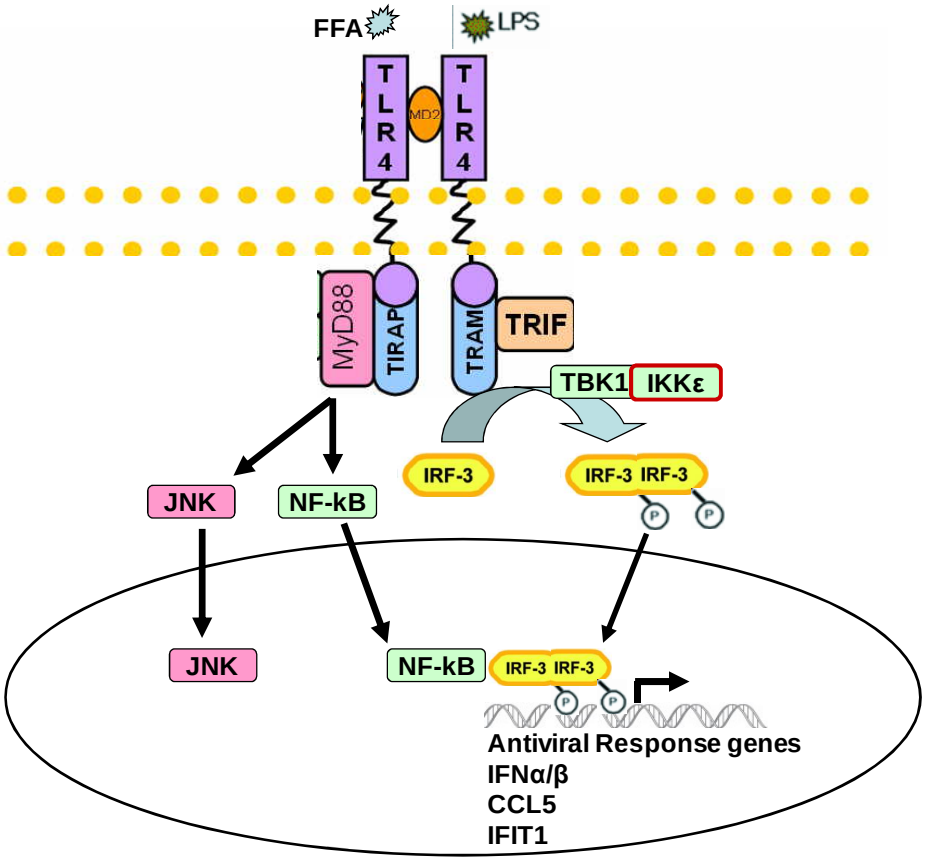

Figure 1. 6 IRF3 signaling pathway in immune cells.

Interestingly, TLR4 has been implicated in the crosstalk of innate immunity and metabolism as well. TLR4 is expressed in adipocytes and has been shown to be a target of free fatty acids, which are present at increased levels during obesity[80]. FFAs increase the expression of inflammatory cytokines downstream of TLR4, such as IL-6 and TNFα, while deletion of TLR4 substantially decreases levels of inflammatory cytokines and ameliorates the FFA-mediated insulin resistance[80, 94]. Hematopoietic cell-specific deletion of TLR4 via bone marrow transplantation results in protection from HFD induced insulin resistance[94]. This is exemplified by decreased serum insulin and enhanced glucose clearance in the insulin tolerance test. Hematopoietic cell-specific TLR4 deletion also results in improved hepatic insulin resistance and decreased hepatic and adipose inflammation on HFD[94]. Thus TLR4 in hematopoietic-derived cells is a regulator of whole body insulin response.

IKKε has also been found to play a role in metabolism. Diet induced obesity increases the expression of IKKε in adipose tissue and liver[95]. IKKε knockout mice are protected from diet induced obesity and show increased body temperature, energy expenditure, and food intake. The IKKε mouse also exhibits enhanced insulin sensitivity compared to WT when challenged with high fat diet (HFD), with decreased serum glucose, insulin, and cholesterol levels, as well as better performance in both the glucose tolerance test and the insulin tolerance tests. Additionally, IKKε knockout mice are also protected from HFD induced hepatic steatosis and obesity induced systemic inflammation[95].

Because IRF3 is a major downstream transcription factor of both TLR4 and IKKε[61, 91], it is likely to be involved in the gene regulation events leading to the downstream effects of both proteins. Thus we hypothesize IRF3 to be a player in the transcriptional regulations mediating the crosstalk between immunity and metabolism.

Obesity and inflammation are closely linked

The actions of the immune system and the metabolic machinery are closely linked. Clinical observations show that obese patients exhibit 2-3 fold elevated circulating levels of proinflammatory cytokines including TNFα, IL-6, and C-reactive protein (CRP) corresponding to decreased insulin sensitizing hormones, such as adiponectin[96-98]. Obesity is not only associated with chronic low grade systemic inflammation, peripheral tissues including adipose tissue, liver, and muscle are also found to be in an inflamed state during obesity[99]. This state of inflammation is a crucial contributing factor to the comorbidities of obesity, including insulin resistance and type 2 diabetes (T2D)[97, 100, 101].

Obesity is characterized by the expansion of the adipose tissue[102, 103]. This expansion is due to both adipocyte hyperplasia and hypertrophy to accommodate the need for storage space for the excess fuel[102, 104]. Rapid WAT expansion results in hypoxia in poorly vascularized regions of the tissue which eventually become necrotic. Macrophages are recruited to the necrotic regions to remove dying adipocytes[105, 106]. Activated macrophages surround the dying cells, forming “crown like structures,” which are now recognized as a classic sign of obesity associated inflammation[105-108].

Even though macrophages were the first immune cells discovered to infiltrate WAT, recent data have demonstrated that WAT becomes infiltrated by many other groups of immune cells, including T cells[109, 110], B cells[111], mast cells[112], and eosinophils[113]. These resident immune cells, as well as the adipocytes themselves, contribute to the WAT inflammatory milieu[114].

In obese mouse models, adipocytes and resident immune cells exhibit increased expression of inflammatory cytokines including TNFα, IL-6, IL-10, and IL-1β[4, 7]. Mouse studies have shown TNFα to be a major factor in obesity-associated insulin resistance. TNFα protein and mRNA levels are increased in obese humans as well as in mouse models of obesity[115-121]. Expression of TNFα is positively correlated with the level of obesity as measured by the body mass index and insulin resistance as assessed by serum insulin[118, 119]. Conversely, TNFα expression is negatively correlated with lipoprotein lipase activity in the adipocyte[122]. Antibody neutralization of TNFα can lower serum glucose levels and improve insulin resistance in obese mice[123-125]. TNFα deficient mice develop diet-induced obesity similar to WT. Despite a similar degree of obesity, TNFα deficient mice are protected from obesity-induced insulin resistance, exhibited by lower serum insulin and enhanced glucose clearance in both the glucose and insulin tolerance tests[126]. Alternatively, when the genetically obese model of *ob/ob* mice are crossed with mice harboring a loss-of-function mutation in the p55 and p75 TNFα receptors, the resulting animals exhibit decreased serum glucose and insulin, as well as enhanced performance in the insulin and glucose tolerance tests compared to ob/ob mice with WT

TNFα receptors[126]. *In vitro*, TNFα treatment also hinders insulin stimulated glucose uptake in 3T3-L1 adipocytes[117, 127].

Functional studies show that TNFα interferes with the metabolic function of the adipocyte via multiple pathways. First, it can increase reactive oxygen species (ROS) in adipocytes, which induces insulin resistance[128, 129]. TNFα treatment of 3T3-L1 adipocytes results in the upregulation of ROS-related genes, and the addition of antioxidants can prevent 25-65% of the insulin resistance caused by TNFα[127]. These results indicate that TNFα induces adipose insulin resistance at least in part via elevating ROS. Secondly, it can impair insulin signaling by interfering with insulin receptor substrate 1 (IRS1) tyrosine phosphorylation, thus inhibiting subsequent PI-3 kinase (PI-3k) activation and insulin stimulated glucose uptake[117, 130-132]. In addition, it can interfere with lipid storage by down-regulating fatty acid transport and lipoprotein lipase, resulting in increased lipolysis[100, 133].

Another inflammatory cytokine, IL-1β, is also a mediator of obesity-induced inflammation. Mice lacking IL-1β or the IL-1β receptor are protected from diet induced obesity induced insulin resistance[134, 135]. Clinically, type 2 diabetic patients also show increased IL-1β, while weight loss in type 2 diabetic patients results in reduced adipose IL-1β expression[136]. Mechanistically, IL-1β directly inhibits insulin signaling via negative regulation of IRS-1 expression and hindrance of IRS-1 tyrosine phosphorylation, which together contribute to insulin resistance[137].

IL-1β is a component of the NOD-like receptor family pyrin domain-containing 3 (NLRP3) inflammasome protein complex, which plays a role in the innate immune

response to infection[138]. Activation of the NLRP3 inflammasome leads to caspase-1-dependent cleavage of the latent pro-IL-1β into the active IL-1β[139]. Studies indicate Caspase-1 to also be involved in whole body metabolism. Metabolic characterization of Caspase-1 deficient mice show protection from diet-induced obesity and improved insulin sensitivity on HFD[140].

In addition to TNFα and IL-1β, numerous other cytokines have been implicated in obesity associated inflammation[97]. For instance, IL-6 expression is increased in both the adipocytes and infiltrating immune cells in WAT during obesity, and elevated IL-6 levels have been found to promote insulin resistance[97].

In addition to proinflammatory cytokines such as TNFα and IL-1β, many kinases involved in the inflammatory signaling pathway are also activated in obese adipose tissue. This includes the kinase c jun N terminal kinase (JNK)[141], inhibitor of NF-κB kinase (IKKβ)[142, 143], and protein kinase C (PKC)[144-146]. Previous studies have also implicated these signaling molecules in obesity associated insulin resistance. For instance these kinases can activate NF-κB, resulting in further increase in proinflammatory cytokine expression[97, 100].

Interestingly, the actions of NF-κB are closely related to that of IRF3 in immunity. NF-κB is a key player in the innate immune response[147]. Like IRF3, latent NF-κB is sequestered in the cytoplasm. Signaling through TLR4 leads to activation and nuclear translocation of NF-κB[148]. Nuclear NF-κB can form a heterodimer with IRF3 to activate transcription of downstream genes, including inflammatory cytokines such as TNFα and IL-6[147, 148]. Obese patients show chronically increased activation of NF-κB in the adipose

tissue[149]. Treating mice with glucose or lipid infusions can also increase adipose tissue NF-κB activity[142, 146, 150, 151]. *In vitro*, palmitate treatment activates NF-κB in cultured 3T3-L1 adipocytes[152]. Conversely, stimulation with adiponectin or PPARγ, which are both insulin sensitizers, suppresses NF-κB activity in adipocytes[153-155].

JNK, IKKβ, and PKC also directly interfere with insulin signaling by serine/threonine phosphorylating IRS1, thus preventing its activation and downstream PI-3K recruitment, resulting in the inability to activate the insulin signaling pathway[97, 144, 145]. Metabolic characterization of JNK1 deficient mice shows that they are protected from diet induced obesity and insulin resistance[141]. Mice heterozygous for IKKβ exhibit enhanced insulin sensitivity[143]. Clinical studies show that treatment with salicylates, which are known IKKβ inhibitors, enhances insulin sensitivity in patients with type 2 diabetes[97, 100, 133].

The interaction between the metabolic and the immune system has been a field of intense study in the past two decades. It is now well accepted that many signaling molecules can both activate inflammatory pathways while inhibiting metabolic function and many cytokines can signal to both immune and metabolic organs. However, the transcriptional pathways regulating this crosstalk are still unknown. We believe that studying the role of IRF3 in adipocytes will shed light on this question.

Overview of Dissertation

Chapter 2 of this dissertation will discuss the role of IRF3 in promoting the inflammatory milieu in both WAT and cultured adipocytes. We employed lentiviral

mediated IRF3 overexpression and knockdown in 3T3-L1 adipocytes followed by gene expression analysis to study the effect of IRF3 on the adipocyte inflammatory profile. The inflammatory state of WAT in *Irf3*$^{-/-}$ mice is characterized by studying the extent of WAT macrophage infiltration. Chapter 3 focuses on discovering how IRF3 regulates energy homeostasis. We studied the thermogenic profile of IRF3 whole body knockout mice. The effect of IRF3 on adipocyte "browning" is also characterized using cultured primary adipocytes from the SVF of the inguinal WAT of WT vs. *Irf3*$^{-/-}$ mice. Chapter 4 looks into the role of IRF3 on insulin action. We characterized the metabolic phenotype of the *Irf3*$^{-/-}$ mice. Additionally we studied the effect of IRF3 on insulin action in cultured adipocytes. In summary we found IRF3 to strongly elevate inflammatory genes in adipocytes. Furthermore, it also influences energy homeostasis by suppressing adipose tissue "browning" and regulates glucose homeostasis by transcriptional control of adipose *Slc2a4*.

Chapter 2

IRF3 regulates adipocyte inflammation

Introduction

IRFs are transcription regulators of type I interferon and interferon-inducible genes[57]. Specifically, IRF3 is recognized as the major effecter of the induction of interferon gene expression as part of the innate immune response to viral infection[61]. Upon viral infection, TLRs recognize pathogen-associated molecular patterns, and then activate the innate immune response pathway[54]. IRF3 acts downstream of TLR4, which recognizes a diverse group of ligands, including bacterial LPS, the fusion protein of respiratory syncytial virus, and FFAs[54, 80]. Ligand binding to TLR4 causes IRF3 to become phosphorylated, after which it dimerizes and translocates into the nucleus, where it activates downstream genes including *Ccl5, Ifnβ, and Ifit1*[69, 91]. Activation of these interferon response genes results in the mounting of the host innate immune response[54]. In addition to activating the innate immune response, IRF3 is a mediator of bacteria-induced apoptosis in macrophages, which is triggered upon TLR4 activation[60]. Lastly, IRF3 is also a downstream mediator of DNA dependent protein kinase, which activates DNA damage induced apoptosis[57].

Sato et al. created the *Irf3*$^{-/-}$ mouse in 2000 and characterized its immunological phenotype[156]. Consistent with IRF3's role in the innate immune response, the *Irf3*$^{-/-}$ mouse was found to be susceptible to encephalomyocarditis virus infection[156]. Additionally, the *Irf3*$^{-/-}$ mouse was also found to be resistant to LPS-induced endotoxic shock, which is expected since IRF3 is a mediator of LPS induced TLR4 signaling[157].

However, no abnormalities were observed in the size, behavior, or reproduction of *Irf3*$^{-/-}$ mice[156].

In the past 20 years there has been a growing recognition of the close link between the immune system and the metabolic system. Obesity is associated with chronic low grade systemic inflammation, and peripheral metabolic tissues including adipose tissue, liver, and muscle also show signs of inflammation during obesity[97].

Under obese conditions the adipose tissue quickly expands in order to store the excess energy in the form of lipids[102, 103]. Rapid WAT expansion results in hypoxia in poorly vascularized regions of the tissue which eventually becomes necrotic[106]. Macrophages are recruited to the necrotic regions to remove the dying adipocytes[97, 105]. Resident macrophages also switch from the M2 polarized anti-inflammatory state during lean conditions toward a M1 polarized pro-inflammatory state during obese conditions[158, 159]. Additionally, obesity also elevates the secretion of inflammatory cytokines in the adipose tissue including TNFα, IL-6, IL-10, and IL-1β[4, 7].

Interestingly, IRF3 has been implicated in the crosstalk between immune response and metabolic function. Activation of IRF3 during viral infection inhibits liver X receptor (LXR) activation and downstream induction of Abca1 in macrophages. This leads to an inability of macrophages to rid themselves of excess cholesterol during an infection[160]. Additionally, statins, which are inhibitors of the HMG-CoA reductase enzyme in cholesterol production, have also been found to inhibit IRF3 activation in macrophages[161].

One the other hand, IRF3 function in macrophages can also be inhibited by nuclear receptor signaling. Treatment with the Pparγ ligand troglitazone inhibits IFN-β production in mice following LPS injection[162]. *In vitro* studies in macrophages found that troglitazone prevents IRF3 binding to the ISRE site in the *Ifnβ* promoter while enhancing Pparγ binding to the same site. This results in a reduction of IFN-β production in macrophages during microbial infection[162].

Since IRF3 is highly expressed in adipocytes, we hypothesized that IRF3 is also a transcriptional regulator of the inflammatory pathway in adipocytes. We speculated that deletion of IRF3 may hamper activation of the inflammatory pathway in adipocytes of *Irf3*$^{-/-}$ mice, and would subsequently lead to reduced overall systemic inflammation during the obese state, with beneficial metabolic consequences.

Materials and methods

3T3-L1 adipocytes

3T3-L1 cells (ATCC) were cultured in high glucose DMEM (Invitrogen) supplemented with 10% bovine calf serum (Hyclone). Proliferating cells were maintained at or below 70% confluency. For adipogenic differentiation, cells were grown until two days after confluency then stimulated with an adipogenic cocktail including dexamethasone, insulin, and isobutylmethylxanthine in high glucose DMEM supplemented with 10% fetal bovine serum (FBS) (Atlas Biologicals)[163, 164]. Cells were stimulated for 48 hours, after which they were maintained on high glucose DMEM/FBS

until further experimentation. All experiments were performed at least seven days after adipogenic differentiation to ensure that adipogenesis was complete.

IRF3 knockdown and overexpression in 3T3-L1 adipocytes

IRF3 knockdown and overexpression experiments were performed by lentiviral transduction into mature 3T3-L1 adipocytes. For overexpression experiments, IRF3 cDNA was cloned into the pCDH-CMV-MCS-EF1-puro lentiviral construct (System Biosciences). For knockdown experiments shIRF3 hairpin designed by the Broad Institute RNAi Consortium (TRCN0000085242) was cloned into pSIH1-H1-copGFP lentiviral construct (System Biosciences).

Lentivirus was generated by transient transfection of the appropriate viral construct and two packaging vectors pMD2.g and psPAX2 (Addgene) in a mass ratio of 10µg:5µg:5µg respectively into ~80% confluent HEK293T cells using the ProFection calcium phosphate transfection kit (Promega). Transfected HEK293T cells were changed into fresh high glucose DMEM medium (Gibco) containing 10% FBS (Atlas Biologicals) 16 hours later. The viral-laden media was collected 48 hours after the transfection, filtered through a 0.4uM filter (BD Biosciences), and frozen down at -80^{o}C for later use.

3T3-L1 adipocytes were transduced with lentivirus 7 days after adipogenic differentiation. Viral-laden media was warmed to room temperature and mixed with 7ug/ml polybrene then applied to 3T3-L1 adipocytes for 12hr. To achieve optimal transduction efficiency, 3T3-L1 adipocytes were subjected to 2 successive rounds of viral transduction. At the end of a total of 24hr of viral transduction 3T3-L1 adipocytes were

switched back to fresh DMEM media containing 10% FBS. Subsequent experiments were performed 6-10 days after viral transduction.

Microarray

Microarray was performed using cDNA from 3T3-L1 adipocytes after IRF3 overexpression or knockdown. All experiments were performed in duplicates. Illumina mouse whole genome microarray was used for this experiment, and all procedures were performed by the Broad Institute genetic analysis platform.

Normalization: All data were normalized using the quantile algorithm implemented in the 'limma' package in R. All signal intensities were log2 transformed.

Differentially expressed genes: We first set the cutoff of fold-change as 0.35. There were < 0.1% probes with fold-change > 0.35 or < -0.35 in pairs of biological repeats. We then set the cutoff of signal intensity as 6.6. Only < 0.1% probes in background may have signal intensity > 6.6 according to Illumina's array image scanning results.

The differentially expressed genes met the following criteria:

1. Maximal signal intensity > 6.6 in EGFP, IRF3, shLuc, or shIRF3 samples

2. Absolute value of fold-change was greater than 0.35 in both IRF3 vs. EGFP comparison and shLuc vs. shIRF3 comparison.

3. The directions of differential expression in EGFP vs. IRF3 comparison and in shLuc vs. shIRF3 comparison are the opposite.

Pathway analysis: Gene Set Enrichment Analysis (GSEA) algorithm was used to identify KEGG pathways significantly associated with the expression profile alteration between different conditions.

Heatmap: All signals in heatmaps were pseudo-relative signals. For the purpose of visualization, we artificially normalized signals so that pseudo-signals at each row in heatmaps have a mean value of 0 and standard deviation of 1.

Q-PCR

Tissue was harvested from mice and homogenized in Trizol (Invitrogen). Total RNA was harvested using the manufacturer's suggested protocol. mRNA concentration was measured using a NanoDrop ND-1000 spectrophotometer and 1ug of mRNA was then used to synthesize cDNA using the RETROscript 2-Step RT-PCR Kit (Ambion). The resulting cDNA product was diluted by 10-fold with water and subjected to real time qPCR with the SybrGreen reagent (ABI) in the ABI 7900-HT qPCR apparatus. 36B4 was utilized as an internal control for each sample. Relative expression of each gene was calculated using the ΔΔCt method.

Animals

All animal procedures used in this study were approved by the Institutional Animal Care and Use Committee (IACUC) of Beth Israel Deaconess Medical Center. All mice were kept under 12 hr light : dark conditions at an ambient temperature of 73^{o}F (22.8^{o}C). Mice were housed at 1-5 per cage and were fed *ad libitum* on chow diet

consisting of Purina Diet #5008. High fat diet (HFD) fed animals were given Research Diets #D12331i with 58% kcal from fat beginning at three weeks of age.

The *Irf3*$^{-/-}$ mice were purchased from Riken BioResource Center. These mice have been completely backcrossed onto a C57BL/6 background, and all subsequent generations were maintained on a C57BL/6 background.

Mice cohorts were generated by mating heterozygous males and females with each other, and offsprings were born in genotypes in the expected Mendelian ratios. WT and *Irf3*$^{-/-}$ littermates were used for all studies.

Serum cytokine measurements

Mice were fasted overnight and fasting serum was collected from cheek bleed using a 5.5mm sterile animal lancet (Goldenrod). Fasting serum was separated from whole blood by centrifugation at 3000 rpm for 5 min at 4^{o}C in BD Microtainer serum separator tubes (BD Bioscience #365956). Serum MCP-1 was measured using the Quantikine mouse MCP-1 immunoassay kit (R&D Systems #MJE00).

Tissue histology

WAT and BAT were collected from chow and HFD-fed mice. Fresh tissue was fixed by incubating in 4% paraformaldehyde in PBS overnight at 4^{o}C. Fixed tissue was paraffin embedded, sectioned, and mounted onto microscope slides. Slides were stained with hematoxylin-eosin (H&E), anti-F4/80, or anti-UCP1 (Abcam #ab10983). All tissue histology was performed by the BIDMC histology core facility.

Tissue slides were visualized using a Zeiss Axio Imager A1 microscope fitted with a Zeiss Axiocam at 10 times magnification.

Statistical analysis

Unpaired t-tests or one-way ANOVA were applied to the data with either Bonferroni or Fisher-post hoc tests.

Results

Lentiviral transduction can effectively manipulate IRF3 expression in 3T3-L1 adipocytes.

We sought to study the effects of IRF3 on inflammatory gene expression in adipocytes using gain- and loss-of-function models. We began our analysis in 3T3-L1 cells, one of the best characterized models of adipocytes in culture[165, 166]. We and others have long used retroviral vectors to manipulate gene expression in proliferating cell lines such as 3T3-L1 preadipocytes. However, we have previously identified IRF3 as an inhibitor of adipogenesis, and so to study the role of IRF3 in mature adipocytes, all manipulations must be performed after differentiation is complete. Since mature 3T3-L1 adipocytes are notoriously difficult to transfect with reagents such as calcium phosphate or lipofectamine, we chose lentiviral-mediated transduction for this study.

The mouse IRF3 cDNA was cloned into the pCDH lentiviral vector for overexpression experiments. Previous studies in immune cells have shown that under basal conditions IRF3 resides in the cytoplasm and is inactive. Under appropriate

stimulation, such as during viral infection, IRF3 becomes phosphorylated, undergoes dimerization, and subsequently translocates into the nucleus, where it can activate transcription of downstream genes[61, 91]. A cluster of key phosphorylation sites involved in this process has been identified in the C-terminus of the IRF3 protein, and mutation of amino acids 396 and 398 from serine to aspartic acid has been found to result in a constitutively active form of IRF3 that can translocate into the nucleus and activate transcription of downstream genes without additional stimulation[62, 63, 69]. Therefore, to mimic active IRF3 we mutated amino acids 396 and 398 to create a constitutively active pCDH lentiviral IRF3 construct.

Overexpression of IRF3 was performed by lentiviral transduction into 3T3-L1 mature adipocytes seven days after differentiation, which we consider to represent the mature state. An EGFP-expressing viral vector was used as control. Two days after viral transduction, visualization of EGFP shows very high transduction efficiency of ~90% (Figure 2.1A). Six days after viral transduction, RNA and protein were harvested and Q-RTPCR and Western blot experiments were performed to assess IRF3 overexpression efficiency. Q-RTPCR showed significant overexpression of constitutively active IRF3 (IRF3-2D), but the wild type IRF3 (wtIRF3) overexpression was much stronger (Figure 2.1B). Despite this, IRF3-2D overexpression induced greater expression of *Ifit1* and *Ccl5*, two IRF3 downstream target gene, than wtIRF3 (Figure 2.1C and D). This indicates that IRF3-2D can indeed act as a potent constitutively active form of IRF3 in adipocytes. The inability to overexpress IRF3-2D and wtIRF3 to an equal level may be due to a negative feedback mechanism initiated by active IRF3 protein. Although previous studies have

not identified any negative feedback mechanism in IRF3 action, IRF4 has been implicated in the negative feedback suppression of TLR signaling[167]. Therefore, we hypothesize that IRF3 may be involved in a similar mechanism of negative feedback so that active IRF3 levels cannot be grossly overexpressed.

On the protein level, Western blot experiments showed that both wtIRF3 and IRF3-2D protein were highly overexpressed (Figure 2.1E). It is interesting to note that although on the mRNA level, wtIRF3 overexpression is much stronger compared to IRF3-2D overexpression, on the protein level the extent of overexpression is similar in both wtIRF3 and IRF3-2D. One possible cause for this discrepancy is that the IRF3-2D mutation may increase the translational efficiency of the protein in adipocytes. Although we did not further explore this possibility, it is a future area to explore in studying the regulation of IRF3 activation in adipocytes.

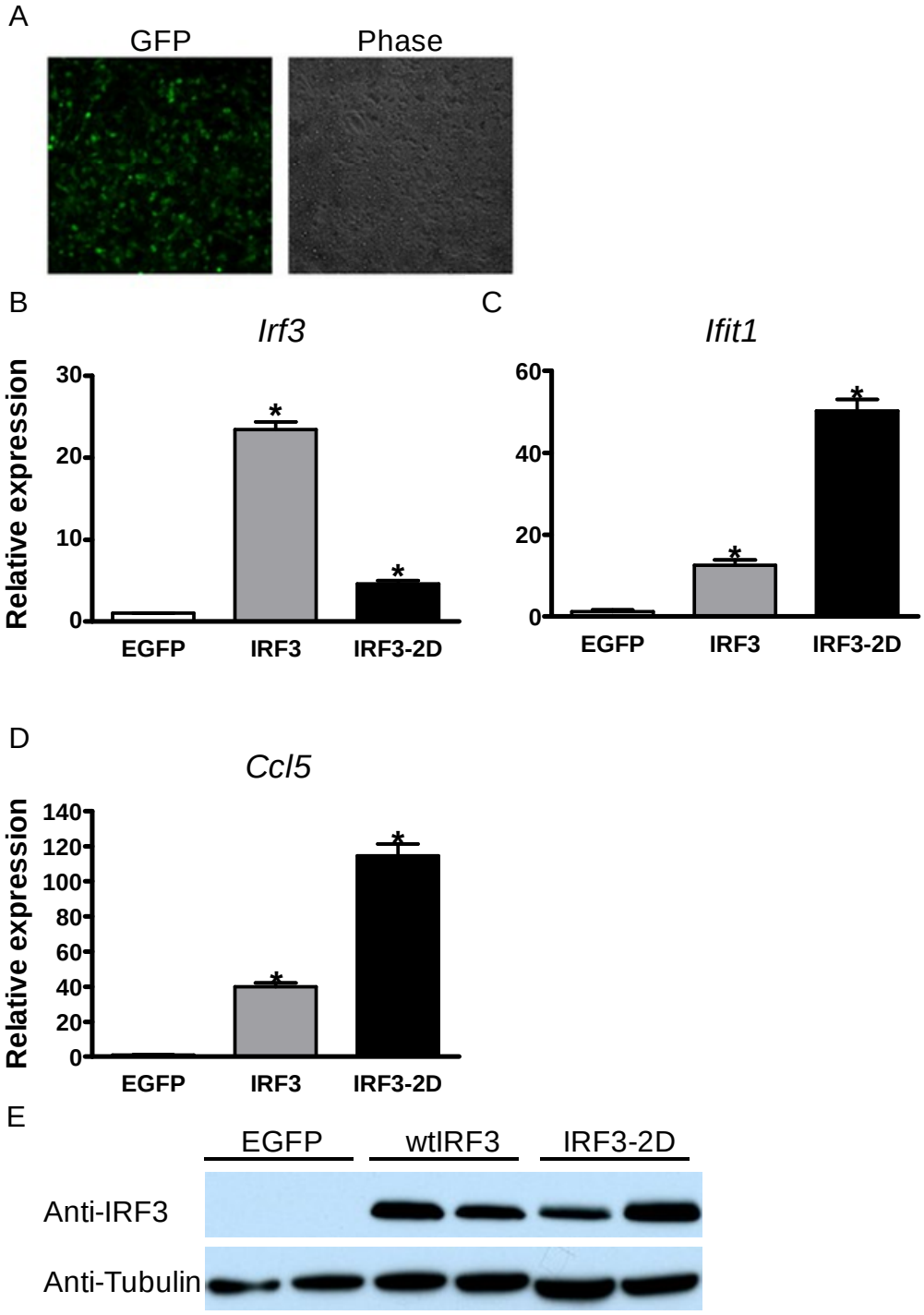

Figure 2. 1 Lentiviral transduction can overexpress IRF3 in 3T3-L1 adipocytes.

Figure 2.1 (Continued). 3T3-L1 adipocytes were transduced with pCDH virus expressing EGFP, IRF3, or IRF3-2D seven days after adipogenesis. A) Live visualization of pCDH-EGFP transduced cells. B-D) Q-RTPCR of IRF3 and representative target genes in transduced cells *P<0.05. E) Western blot of transduced cells.

For IRF3 knockdown experiments, a shIRF3 hairpin was cloned into the pSIH1 lentiviral vector, which encodes GFP in its backbone for easy assessment of transduction efficiency. Lentiviral transduction into 3T3-L1 mature adipocytes was performed seven days after differentiation, and transduction efficiency was assessed two days later by visualization of GFP (Figure 2.2A). Eight days after transduction, cells were harvested for Q-RTPCR and Western blot experiments. Both Q-RTPCR and Western blot showed IRF3 knockdown efficiency to be ~60-70% (Figure 2.2B and C). We were never able to achieve a greater amount of knockdown efficiency, likely due to intrinsic limitations of the specific shIRF3 hairpin sequence, since GFP visualization showed very high transduction efficiency (Figure 2.2A). To overcome this limitation, several other shIRF3 hairpin sequences were assessed but none could achieve a higher knockdown efficiency. Therefore we chose to proceed with this shIRF3 hairpin. As discussed later, we used *Irf3*$^{-/-}$ mouse embryonic fibroblast (MEF)-derived adipocytes as an additional genetic loss-of-function model to confirm our experimental results.

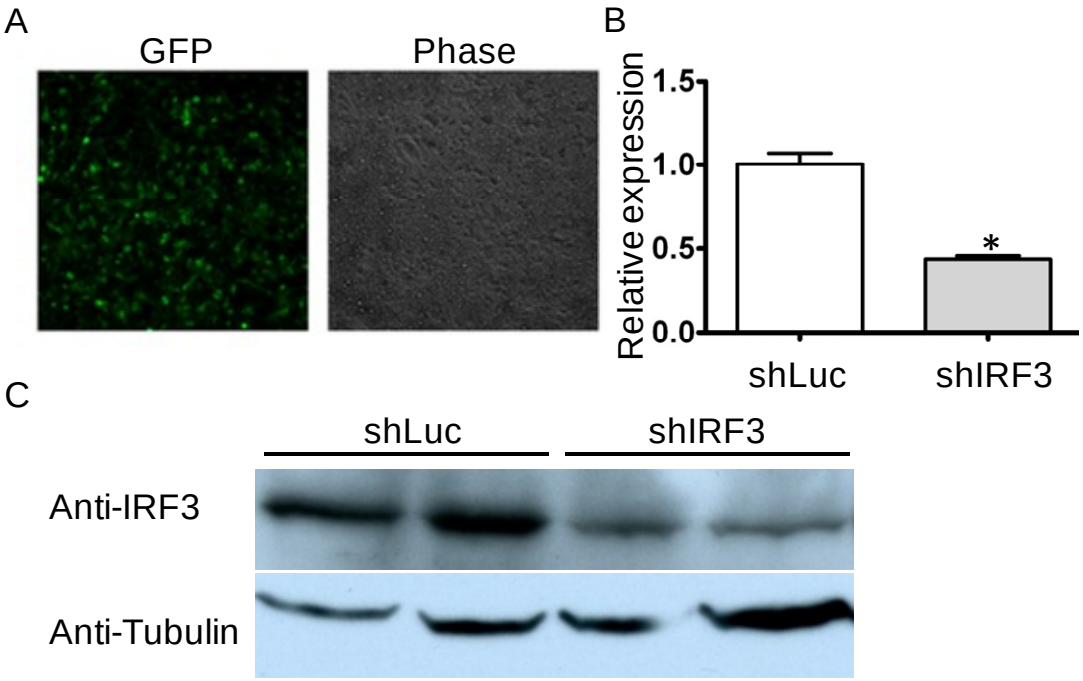

Figure 2. 2 Lentiviral transduction of shIRF3 causes knockdown of IRF3 RNA and protein levels in 3T3-L1 adipocytes.

3T3-L1 adipocytes were transduced with pSIH1 virus expressing either shLuc or shIRF3 seven days after adipogenesis. A) Live visualization of pSIH1-shLuc transduced cells. B) Q-RTPCR of IRF3 gene expression in transduced cells *P<0.05. C) Western blot of IRF3 in transduced cells.

IRF3 regulates inflammatory genes in adipocytes.

We performed transcriptional profiling using Illumina mouse whole genome microarrays to assess the effect of IRF3 knockdown and overexpression in adipocytes. RNA was harvested from 3T3-L1 adipocytes transduced with IRF3-2D or EGFP control, as well as from cells transduced with shIRF3 or shLuc control. Gene set enrichment

analysis (GSEA)[168] showed that the genes most strongly regulated by IRF3 were those in the immune response pathway (Figure 2.3A and B). This cluster of genes was coordinately upregulated by IRF3 overexpression and downregulated by IRF3 knockdown. The second most strongly regulated group of genes was involved in GTPase activity (Figure 2.3B). GTPase activation is a part of the inflammatory response pathway[169], and many of the GTPase activity genes identified in the microarray were those involved in inflammatory response, indicating that IRF3 is indeed a critical regulator of adipocyte inflammatory response.

A

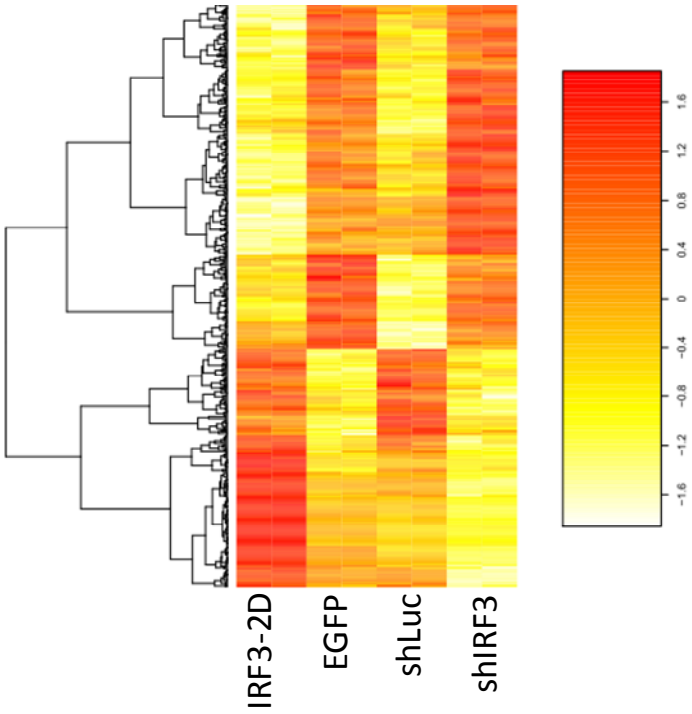

B

Up-regulated by IRF3-2D	P-value	Down-regulated by shIRF3	P-value
Immune response	1.3×10^{-14}	Immune response	1.4×10^{-6}
GTPase activity	3.3×10^{-6}	GTPase activity	4.7×10^{-4}
Cytokine production	2.7×10^{-3}	Endocytosis	2.2×10^{-2}
Ubiquitin	3.0×10^{-2}	Lipoprotein	2.0×10^{-1}
DNA damage response	4.5×10^{-2}	Protein kinase activity	6.0×10^{-1}

Figure 2. 3 Immune response genes are among the top group of genes regulated by

Figure 2.3 (Continued). IRF3 in adipocytes.

Whole genome transcriptional profiling of 3T3-L1 adipocytes transduced with pCDH-EGFP, pCDH-IRF3-2D, pSIH1-shLuc, or pSIH1-shIRF3. A) Heat map of microarray. B) Top five clusters of genes most highly upregulated by IRF3-2D or downregulated by shIRF3 in the microarray identified by GSEA.

To confirm the results from the microarray, Q-RTPCR was performed on several of the top genes identified in the immune response cluster, including *Ifnβ*, *Ifit1*, *Ccl5*, and *Mcp1*. We focused on these four genes because they showed some of the largest fold inductions by IRF3-2D overexpression in the microarray, and previous studies in immune cells indicate that *Ifnβ, Ccl5,* and *Ifit1* are direct transcriptional targets of IRF3[69, 91]. Indeed, these genes were strongly induced by IRF3 overexpression, while suppressed by IRF3 knockdown (Figure 2.4A and B). Additionally, the expression of these genes in epididymal WAT from WT and *Irf3*$^{-/-}$ mice was assessed; as expected, *Irf3*$^{-/-}$ WAT showed marked reduction in the expression of these genes compared to WT littermates, in both chow and HFD-fed conditions (Figure 2.4C and D).

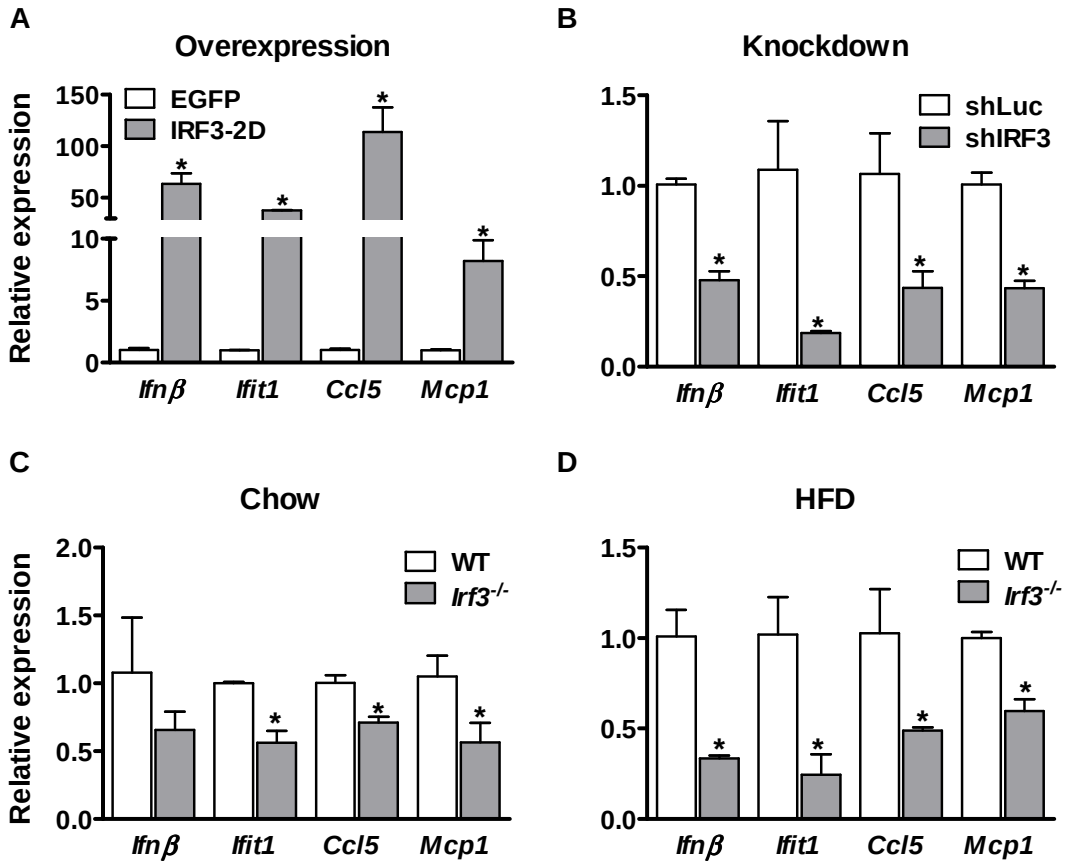

Figure 2. 4 IRF3 is a regulator of inflammatory gene expression in adipocytes *in vitro* and *in vivo.*

Expression analysis of immune response genes by Q-RTPCR in adipocytes. A) IRF3-2D overexpression in 3T3-L1 adipocytes. B) IRF3 knockdown in 3T3-L1 adipocytes. C) Chow-fed male epididymal WAT. D) HFD-fed male epididymal WAT. *P<0.05

IRF3 deletion does not reduce systemic MCP-1 level.

To assess whether loss of IRF3 affects the systemic inflammatory state, the serum level of inflammatory cytokine MCP-1 was measured in *Irf3*$^{-/-}$ and WT mice after

16 weeks of either chow or HFD feeding. As expected, HFD feeding increased the serum MCP-1 level since diet induced obesity is known to be an inducer of systemic inflammation. However, *Irf3*$^{-/-}$ and WT mice showed similar levels of MCP-1 (Figure 2.5), indicating that while IRF3 has potent effects at the level of the adipocyte, it may not be a critical regulator of the systemic inflammatory state.

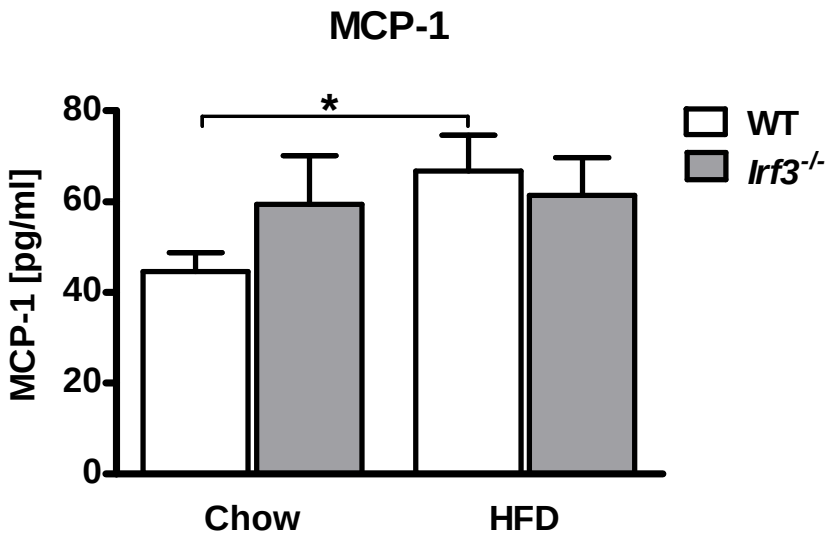

Figure 2. 5 IRF3 deletion does not affect serum MCP-1 level.

Fasting serum MCP-1 ELISA, *P<0.05.

IRF3 deletion does not reduce macrophage infiltration in WAT.

Adipose tissue-derived MCP-1 is involved in the recruitment of macrophages to white adipose tissue in obesity[106, 108]. Since IRF3 regulates MCP-1 expression in WAT, we asked whether deletion of IRF3 would reduce macrophage recruitment under high fat fed conditions. Male *Irf3*$^{-/-}$ and WT mice were subjected to 16 weeks of high-fat

feeding after which their epididymal WAT was harvested and sectioned. Staining with H&E showed no difference in the appearance of adipocytes between the two genotypes (Figure 2.6A). To assess for macrophage infiltration, sections were subjected to immunohistochemistry against the macrophage marker F4/80. Comparison between *Irf3*$^{-/-}$ and WT did not show any difference in the number of crown-like structures, which are formed by macrophages surrounding an inflamed adipocyte (Figure 2.6A and B).

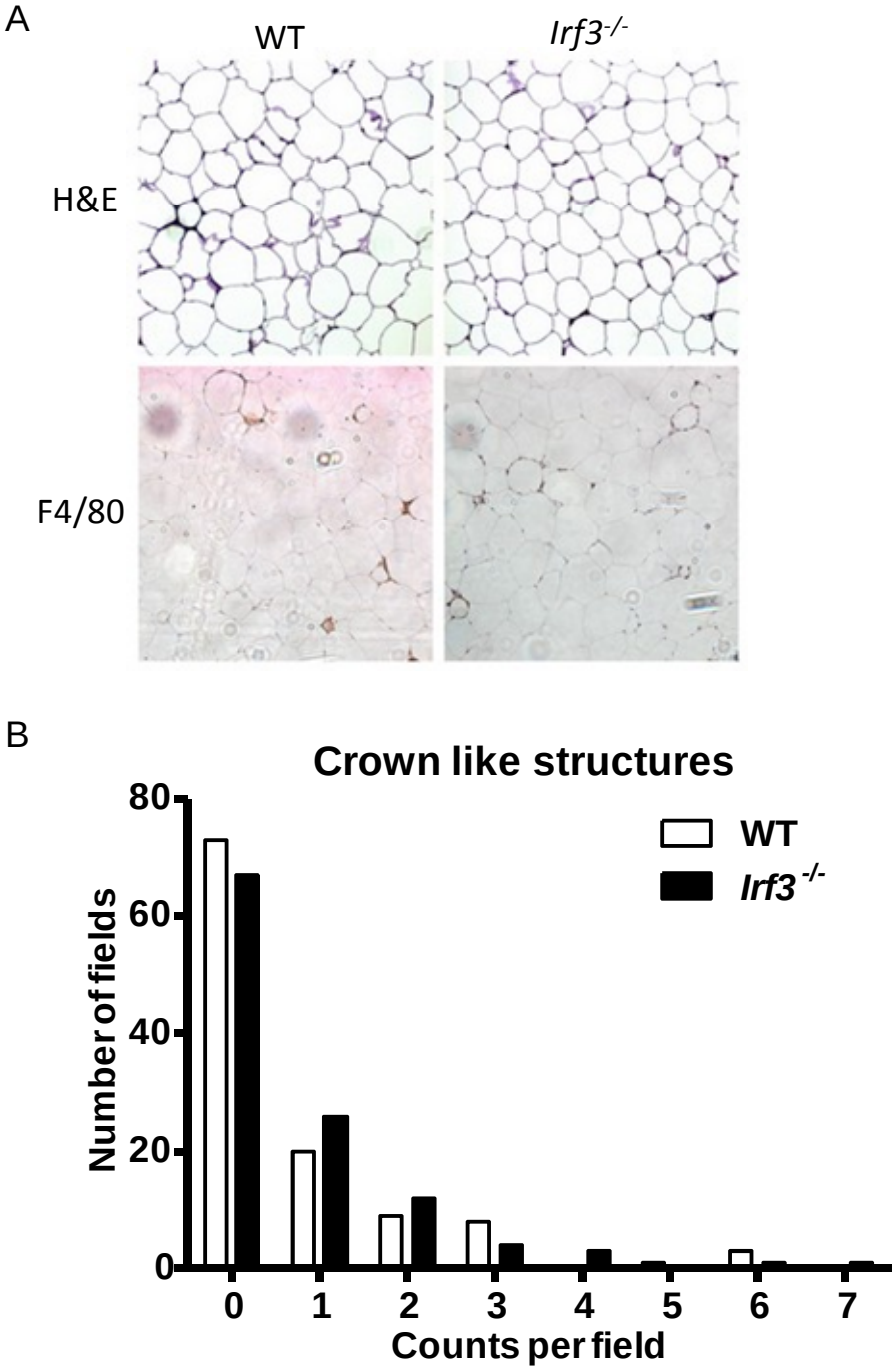

Figure 2. 6 Loss of IRF3 does not affect adipose tissue macrophage infiltration in high fat fed mice.

Figure 2.6 (Continued). Immunostaining of epididymal WAT from male HFD fed mice. A) H&E and F4/80 staining. B) Quantification of the number of crown-like structures per low power field in F4/80 stained WAT. N=114 fields per genotype.

Discussion

IRF3 is an important transcriptional regulator of innate immunity. Therefore we hypothesized that IRF3 can also regulate inflammatory gene expression within adipocytes. To this end we employed lentiviral mediated IRF3 knockdown and overexpression in 3T3-L1 adipocytes, and then used whole genome microarray analysis to find IRF3-regulated genes. Indeed, the top cluster of genes showing coordinate up-regulation by IRF3 overexpression and down-regulation by IRF3 knockdown were those in the immune response pathway. This result indicates that IRF3 plays a similar transcriptional role in adipocytes as noted by others in immune cells. Interestingly Kopp et al. found that IRF3 is not a mediator of LPS-induced inflammation in 3T3-L1 adipocytes[170]. However, in the Western blot used to demonstrate this, Kopp et al. did not use a positive control[170]. Therefore, this experiment is inconclusive because one cannot determine whether the LPS stimulation produced a proper inflammatory response in the 3T3-L1 adipocytes, or if the antibody worked properly.

To our surprise, further analysis of the inflammatory state of *Irf3*$^{-/-}$ mice found no difference between in the extent of macrophage infiltration of WAT between *Irf3*$^{-/-}$ mice

and WT littermates. The state of systemic inflammation was also indistinguishable between the two genotypes, shown by the similar serum levels of the inflammatory cytokine MCP-1 in the serum.

We used MCP-1 as a marker of systemic inflammation because it is an important chemokine secreted by adipocytes during obesity-induced inflammation. Increased MCP-1 secretion in the adipose tissue recruits monocytes into the adipose tissue, where they differentiate into macrophages[171, 172]. These macrophages themselves also secrete MCP-1 which help build up even more macrophages in the adipose tissue, resulting in a positive feedback mechanism perpetuating the increase of adipose tissue macrophages during obesity induced inflammation[106].

Although MCP-1 is an important player in inflammation, many other chemokines and cytokines are involved in this process. For instance, leukotriene B4 (LTB4) is another chemokine secreted by adipocytes during obesity induced inflammation to recruit neutrophils into the adipose tissue[173, 174]. Mice lacking the LTB4 receptor, BLT1, are protected from obesity-induced inflammation and insulin resistance[175]. Additionally, many inflammatory cytokines are also upregulated during obesity induced inflammation. The expression of TNFα, a proinflammatory cytokine, is increased in the adipose tissue during obesity, while serum TNFα is also elevated in obese individuals[118, 119, 121, 123]. Another proinflammatory cytokine, IL-6 is also elevated in obese individuals and reduced with weight loss[96]. These and other proinflammatory chemokines and cytokines may be regulated by IRF3. Therefore, to gain a more complete understanding of the systemic inflammatory state of *Irf3*$^{-/-}$ mice we will need to measure the serum

concentrations of additional chemokines and cytokines. Since IRF3 is a positive regulatory of innate immunity we hypothesize that certain inflammatory markers will be decreased in the *Irf3*$^{-/-}$ mice.

Obesity induced inflammation is manifested as both an increase in systemic inflammation as well as local adipose tissue inflammation[97]. In this study we used the number of F4/80+ macrophages as an indicator of adipose tissue inflammatory state. Obesity induced inflammation leads to macrophage infiltration in the adipose tissue[106]. These adipose tissue macrophages secrete proinflammatory cytokines such as TNFα, IL-1β, and IL-6, all of which can impair insulin action, leading to insulin resistance[98, 134, 140, 176, 177]. However, two groups of macrophages reside in the adipose tissue, namely classically activated macrophages (CAMs), also called M1 macrophages, and alternatively activated macrophages (AAMs), also called M2 macrophages[158]. Although moth M1 and M2 macrophages are F4/80+, they are differentiated by the expression of CD11c. While M1 macrophages are CD11c+, M2 macrophages are CD11c-[158, 159, 178]. M1 and M2 macrophages are also distinct in their inflammatory milieu. While M1 macrophages mainly secrete proinflammatory cytokines such as TNFα and CXCL5, M2 macrophages secrete a signature of anti-inflammatory cytokines such as IL-10 and IL-1Ra[158].

During obesity-induced inflammation a majority of the adipose tissue infiltrating macrophages are M1[159, 178]. Mice depleted of all CD11c+ macrophages are protected from HFD-induced insulin resistance[179]. These data indicate that the obesity-associated inflammation positively correlates with the amount of M1 macrophage infiltration as

oppose to that of M2 macrophages. In this study we assessed the total number of adipose tissue macrophages; however, there may still be a difference between the number of M1 macrophages between WT and *Irf3*$^{-/-}$ mice, which will cause a difference in adipose tissue inflammation between the two genotypes. To study this possibility we can count the number of F4/80+, CD11c+ and F4/80+, CD11c- cells in the adipose tissue of these mice.

While we assessed the number of adipose tissue macrophages, many other immune cell types have been found to be recruited to the adipose tissue during obesity and can contribute to the adipose tissue inflammatory state. Regulatory T cells (T_{reg} cells) secrete anti-inflammatory cytokines that inhibit macrophage recruitment and also induce the development of M2 macrophages[109, 110]. Clinical studies show that obese patients have reduced number of adipose tissue T_{reg} cells[110]. In contrast CD8+ T helper cells (T_H1 cells) produce proinflammatory cytokines and are found to be increased in obese adipose tissues[110]. Adipose T_H1 cells recruit monocytes to the adipose tissue and promote M1 macrophage activation during obesity[180].

In addition to T cells, B cells are also recruited to the adipose tissue during obesity. Adipose tissue B cells can activate proinflammatory T cells, which in turn promote insulin resistance through M1 macrophage activation[111]. Mast cells are also increased in the obese adipose tissue in both human and mouse, and found to play a role in obesity induced metabolic disregulation[112]. Depletion of mast cells in mice results in protection from diet induced obesity and improved glucose homeostasis on HFD[112]. Recently, adipose tissue eosinophils have also been found to affect obesity

induced inflammation. Eosinophils are the main producers of anti-inflammatory cytokines IL-4 and IL-13 in adipose tissue, which promote the development of M2 macrophages[181]. Obesity results in the reduction of adipose tissue eosinophils, leading to a reduction of adipose tissue M2 macrophages. Mice deficient for eosinophils exhibit elevated diet induced inflammation and insulin resistance[113].

These studies indicate that the inflammatory state of the adipose tissue cannot be determined only by the extent of macrophage infiltration. For a more complete picture of the *Irf3*$^{-/-}$ adipose tissue inflammatory state we can fractionate the adipose tissue to collect the stromal vascular fraction and use FACS to sort and count the number of different immune cells present, including macrophages, T cells, B cells, mast cells, and eosinophils. Since IRF3 is a positive regulator of inflammatory response we hypothesize that there will be a decrease in proinflammatory immune cells and / or an increase in anti-inflammatory immune cells in *Irf3*$^{-/-}$ mice.

Our results so far indicate that although IRF3 can activate transcription of immune response genes in the adipocyte, it is likely not sufficient to alter the chronic inflammatory state associated with obesity. This finding is consistent with previous observations made in *Irf3*$^{-/-}$ mice, which respond normally to most immune challenges other than the aforementioned susceptibility to encephalomyocarditis virus infection and resistance to LPS-induced endotoxic shock[157]. Additionally, *Irf3*$^{-/-}$ dendritic cells are still able to respond to viral RNA stimulation by inducing downstream interferon gene expression[156]. This indicates that other factors must play important roles in the innate immune response in the absence of IRF3. One such transcription factor may be IRF7,

which has the closest sequence homology to IRF3 among the nine IRF proteins[54]. Similar to IRF3, IRF7 is activated by TLR4 signaling and can dimerize with NF-κB to induce downstream activation of interferon genes[156]. To study this possibility one could look at the level of IRF7 expression and activity in 3T3-L1 adipocytes after IRF3 knockdown. If IRF7 is indeed compensating for IRF3 we would expect to see elevated IRF7 expression and activation after IRF3 knockdown. Furthermore one can assess the expression of key immune response genes after IRF7 knockdown in cultured *Irf3*$^{-/-}$ adipocytes, which we expect to decrease even more compared to that of *Irf3*$^{-/-}$ adipocytes.

We found *Irf3*$^{-/-}$ mice to exhibit a decrease in intra-adipocyte inflammation. However, since IRF3 is deleted in all cells, whether this change is caused by IRF3 action within the adipocyte or by the effect of IRF3 in adipose tissue immune cells is unclear. We performed *in vitro* experiments using IRF3 overexpression or knockdown in 3T3-L1 adipocytes to show that at least a part of the phenotype is due to cell autonomous effects in adipocytes. To definitively answer this question one can use tissue specific knockout models of IRF3, specifically IRF3 adipocyte-specific knockout and IRF3 macrophage-specific knockout mice. If the decrease in adipocyte inflammation is manifested in the IRF3 adipocyte-specific knockout mouse but not in the IRF3 macrophage-specific knockout model, then one can conclude that this phenotype is due to IRF3 action in the adipocyte but not in the macrophage. Additionally one can study IRF3 tissue-specific knockout models in other immune cells present in the adipose tissue such as T cells, B cells, and eosinophils to determine whether they are contributors to IRF3's effects on adipocyte inflammation.

We can also use bone marrow transplant models to answer this question. We can irradiate WT mice and replace their bone marrow with that from *Irf3*$^{-/-}$ mice and vice versa. If *Irf3*$^{-/-}$ mice with WT bone marrow show a decrease in adipocyte inflammation while WT mice with *Irf3*$^{-/-}$ bone marrow do not, then we can conclude that this phenotype is not due to the action of IRF3 in hematopoietic-derived cells such as macrophages.

Despite the fact that global immune function appears to be intact in *Irf3*$^{-/-}$ mice, these animals do not have normal metabolic function. This will be described and discussed in the next two chapters.

Chapter 3

IRF3 affects energy homeostasis by repressing "browning" of white adipose tissue

Introduction

Obesity is a result of the imbalance between energy intake and energy expenditure[182]. When the energy content from food consumption outweighs the energy expended in everyday activities to maintain life, the excess energy is stored in the body in the form of lipids and leads to an increase in body weight[182].

Whole body energy expenditure consists of three different components including resting energy expenditure (REE), thermic effect of food (TEF), and activity energy expenditure (AEE)[182]. REE makes up the largest portion of energy expenditure. It is the energy expenditure at rest required to maintain life. TEF is the energy expenditure required for the digestion and processing of food. AEE is the energy expenditure associated with physical activity, and is made up of two subcomponents, namely exercise energy expenditure and non-exercise activity thermogenesis[182].

One component of non-exercise activity thermogenesis is adaptive thermogenesis, which is a specific function of BAT. BAT is found in the interscapular depot in mice and supraclavicularly in adult humans[12, 16-18]. In contrast to WAT, which stores excess energy in the form of lipids, BAT dissipates energy through adaptive thermogenesis[7]. The process of adaptive thermogenesis is achieved through the function of UCP-1, a BAT-specific protein that localizes to the inner mitochondrial membrane. UCP-1 alters the ATP production process in the mitochondria by allowing dissipation of the mitochondrial proton gradient without concomitant ATP synthesis[7, 12].

Thus, in brown adipocytes, a significant percentage of oxygen consumption results in heat generation instead of ATP production[12].

It was previously believed that white and brown adipocytes originate from a common progenitor cell, and clinical evidence point to the possible trans-differentiation of brown to white adipocyte and vice versa. For instance, during cold challenge or pharmacological treatment with β_3-adrenergic receptor agonists, brown adipocyte-like cells that can perform adaptive thermogenesis are found in WAT depots[7]. These cells are also called "BRITE" or "beige" cells.

However, recent work suggests that WAT and BAT are actually derived from distinct precursor populations. "Classic" brown adipocytes found in the interscapular BAT of mice were found to be derived from Myf5 positive precursor cells that also give rise to skeletal muscle cells. Although WAT and BAT are derived from distinct lineages, the origin of the beige cells is still under debate, because these cells appear like brown adipocytes, but are not Myf5 positive. Recent data point to the possibility that they are derived from WAT resident mesenchymal stem cells from the white adipocyte lineage, but poised for "browning"[25, 26]. However, whether the exact origins of these cells come from resident stem cells, committed preadipocytes, or white adipocytes undergoing trans-differentiation remains to be determined.

Human newborn infants have BAT surrounding the great vessels of the thorax that helps them maintain normal body temperature; however, this BAT regresses with age[183]. Until recently, it was believed that humans lose BAT completely by adulthood[183]. Recently, however, three groups employed positron-emission tomography and

computed tomography (PET-CT) to identify active Ucp1-expressing BAT in the supraclavicular region of adult humans[16-18]. Although the exact lineage of the brown adipocytes in the supraclavicular BAT is still unclear, these findings validate the physiological relevance of BAT in human metabolism, and present BAT, as well as adaptive thermogenesis as a valid target for novel anti-obesity treatments in human.

Chiang et al. identified a potential role for IKKε in thermogenesis. When kept on HFD, *IKKε*$^{-/-}$ mice were found to have increased food intake coupled with an increase in O_2 consumption compared to WT, suggesting an overall increase in energy expenditure. Additionally, *IKKε*$^{-/-}$ mice on HFD also show up-regulation of Ucp1 in WAT as well as a 1.5^{o}C increase in body temperature compared to WT, pointing to an increase in adaptive thermogenesis[95]. IKKε is an immediate upstream kinase of IRF3 in the innate immune response pathway[54]. Upon antigen binding to TLR4, IKKε and TBK1 are activated downstream of the MyD88-independent signaling pathway. Together IKKε and TBK1 phosphorylate IRF3, which leads to its dimerization and translocation into the nucleus. Nuclear IRF3 activates the transcription of downstream genes including interferon response genes crucial for the innate immune response[54].

Since IRF3 acts downstream of IKKε, we hypothesized that IRF3 may also play a role in energy homeostasis. Therefore we studied the thermogenic phenotype of *Irf3*$^{-/-}$ mice as well as the potential development of beige cells in *Irf3*$^{-/-}$ WAT.

Materials and methods

Animals

Please refer to Materials and Methods in Chapter 2 to see a complete description of animal housing conditions and diet, as well as breeding schemes.

Body weight and composition

Body weight of mice was recorded weekly beginning at three weeks of age. Body mass composition was measured using an Echo-MRI 3-in-1 Composition Analyzer (Echo Medical Systems, Houston, TX) at 20 weeks of age. Individual conscious animals were placed in a glass tube and placed in the MRI for brief scanning.

For tissue weight, each tissue was carefully dissected and weighed on a Mettler Toledo AG140 analytical scale.

Food intake

Mice food intake was measured daily over a one week period at 21 weeks of age. Mice were housed individually and provided the same amount of either chow diet or HFD *ad libitum*. The amount of food placed into the cage was weighed everyday and the amount remaining was weighed again 24hr later, and the daily food intake was calculated by taking the difference between the two values. Food was replaced every day after weighing. Food intake was measured at the end of the daily light cycle. Data were analyzed using two-way ANOVA.

CLAMS

Mice metabolic rate was measured by indirect calorimetry in open-circuit Oxymax chambers that are a component of the Comprehensive Lab Animal Monitoring System (CLAMS, Columbus Instruments). All mice were acclimatized to monitoring cages for 48 hours prior to the beginning of an additional 72 hours of hourly automated recordings of physiological parameters. Mice were housed singly and maintained at 73^{o}F (22.8^{o}C) under a 12:12 light dark cycle. Food and water were available *ad libitum*. Data were analyzed using two-way ANOVA.

Cold exposure

Mice were individually housed and given free access to food and water. Cages were placed in an air ventilated 4^{o}C cooler and subjected to 12hr light : dark conditions.

Body temperature of each mouse was measured individually using a rectal probe attached to a Precision Thermometer 4600 (YSI).

Thermoneutral treatment

Ten week old male mice were housed 5 per cage and given free access to food and water. Cages were placed in an air ventilated 30^{o}C incubator and subjected to 12hr light : dark conditions. Tissues were harvested 3 weeks later.

Tissue histology

Please refer to the Materials and Methods section in Chapter 2 for a complete description of procedures used for tissue histology.

Inguinal WAT SVF isolation

Inguinal WAT was dissected from pairs of WT vs. *Irf3*$^{-/-}$ littermates at 5-6 weeks of age. The SVF was dissociated from adipocytes by 1hr incubation in PBS buffer supplemented with Collagenase D (Roche) and Dispase II (Roche). The SVF was further purified by filtering through a cell strainer. The resulting cells were cultured in 1:1 DMEM/F12 media with Glutamax (Invitrogen) supplemented with 10% FBS and Pen/Strep. Primary SVF cells were maintained no more than five passages.

For adipogenic differentiation, cells were pretreated with 20ng/ml BMP-4 at one day before confluency. Adipogenesis was induced one day post confluency with an adipogenic cocktail containing dexamethasone, insulin, isobutylmethylxanthine, and rosiglitazone. Cells were induced for 48 hours, after which they were maintained in DMEM/F12/Glutamax/FBS/Pen/Strep media supplemented with 5ug/ml insulin. Adipocytes were harvested for experiments 7 days after adipogenesis.

Q-PCR

Please refer to the Materials and Methods section in Chapter 2 for a complete description of procedures for Q-RTPCR.

Statistical analysis

Please refer to the Materials and Methods section in Chapter 2 for a complete description of methods used for statistical analysis.

Results

Male Irf3$^{-/-}$ mice have reduced fat mass on HFD.

To determine the role of IRF3 in metabolism, we characterized the metabolic phenotype of *Irf3*$^{-/-}$ mice. When kept on chow diet, the body weights of both male and female *Irf3*$^{-/-}$ mice were indistinguishable from their WT littermates (Figure 3.1A and B). Body composition analysis was performed using Echo-MRI after 16 weeks of chow diet, and revealed no differences in either the lean or fat mass distribution between the two genotypes (Figure 3.1C and D).

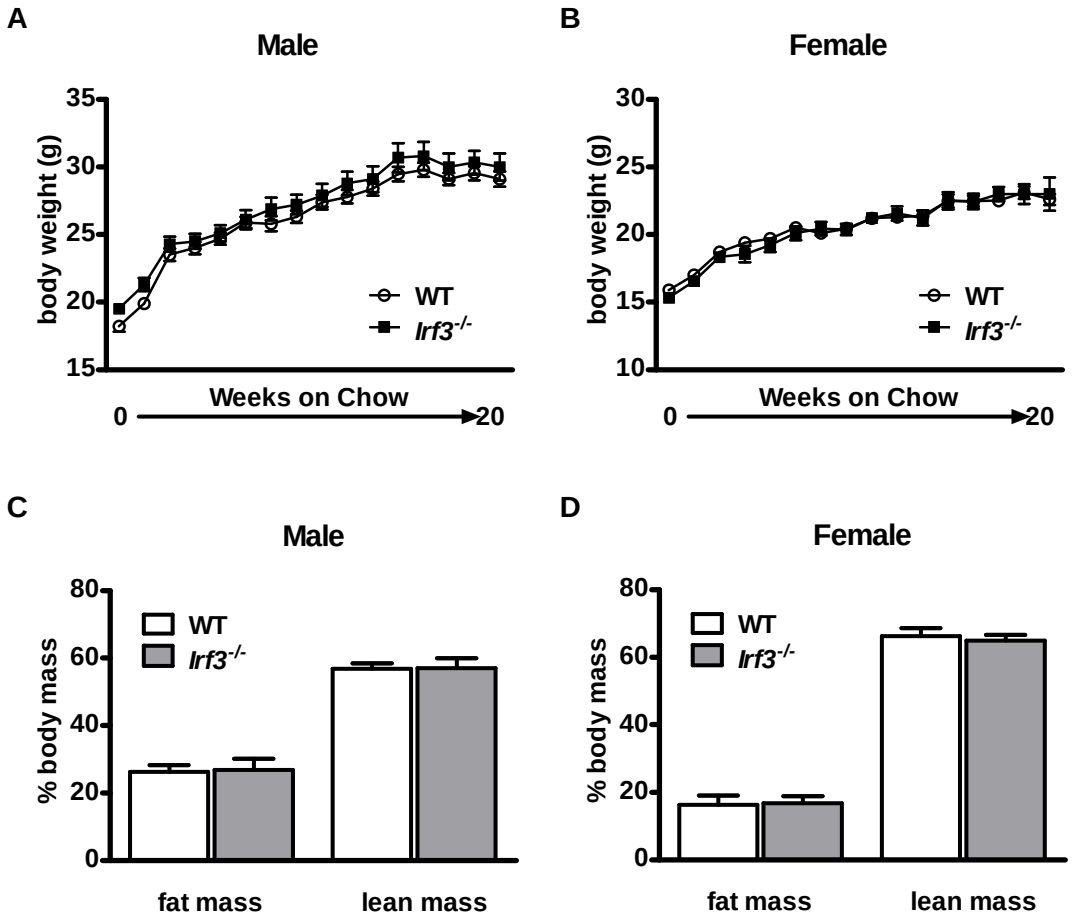

Figure 3. 1 *Irf3*$^{-/-}$ mice do not show a body weight or body mass composition phenotype on chow diet.

A-B) Weekly body weight of chow-fed A) male and B) female mice. C-D) Body mass composition of chow-fed mice as measured by MRI of A) males and B) females. N=9-12.

A second cohort of mice was challenged with HFD (58% kcal from fat). After 24 weeks of HFD feeding, there was no divergence in the overall body weight between *Irf3*$^{-/-}$ mice and WT littermates in both male and females (Figure 3.2A and B). However, after 20 weeks of high-fat feeding male *Irf3*$^{-/-}$ mice showed a slight but statistically significant

decrease in fat mass and an increase in lean mass compared to WT littermates (Figure 3.2C). Consistent with this observation, high fat fed female *Irf3*$^{-/-}$ mice also displayed a trend toward decreased fat mass and increased lean mass, but this did not reach statistical significance (Figure 3.2D).

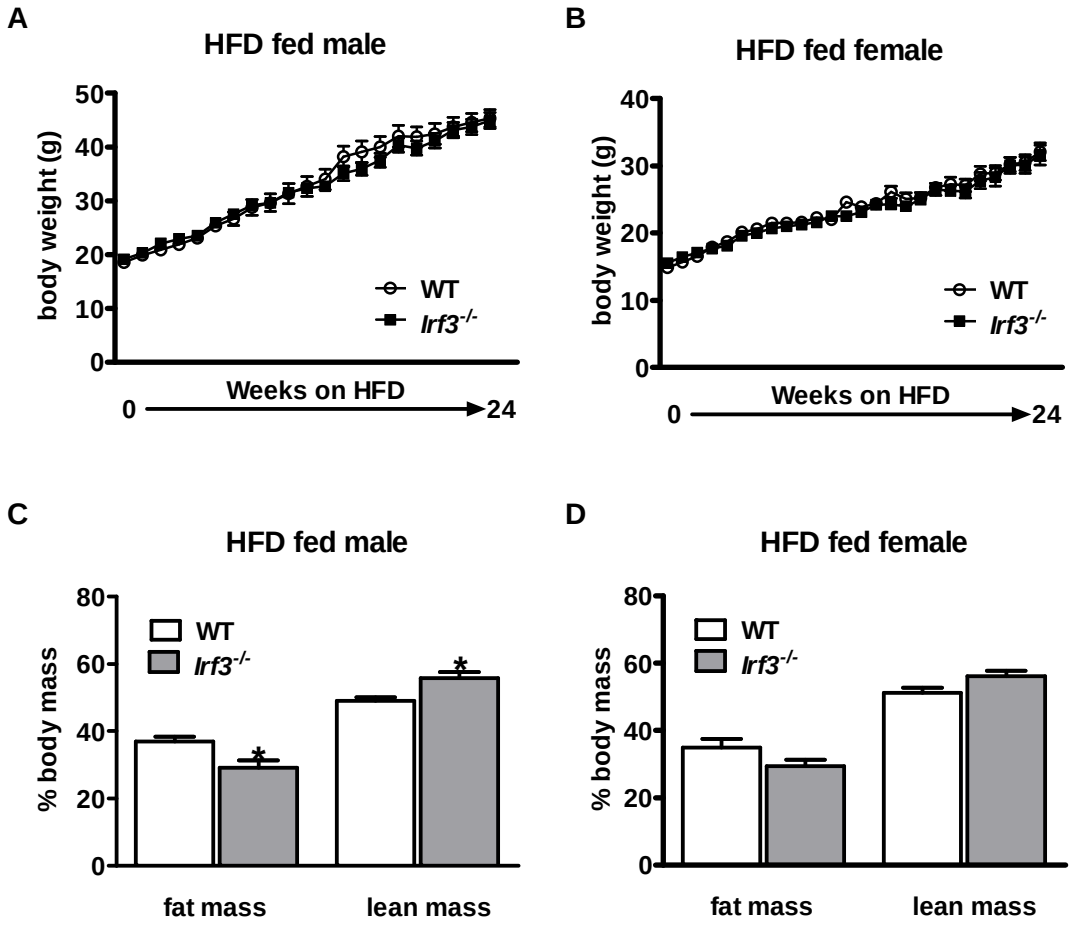

Figure 3. 2 *Irf3*$^{-/-}$ mice have decreased fat mass and increased lean mass on HFD.

A-B) Weekly body weight of HFD-fed A) male and B) female mice. C-D) Body composition analysis of HFD-fed mice as measured by Echo-MRI of A) males and B) females. N=9-12 *P<0.05.

To determine whether IRF3 affects the mass of different fat depots, inguinal WAT, epididymal WAT, and BAT were dissected and weighed on an analytical scale. The weights of these three fat pads were indistinguishable between *Irf3*$^{-/-}$ mice and WT littermates (Figure 3.3A and B). The spleen was used as a negative control organ because it is a non-metabolic tissue in which IRF3 is highly expressed.

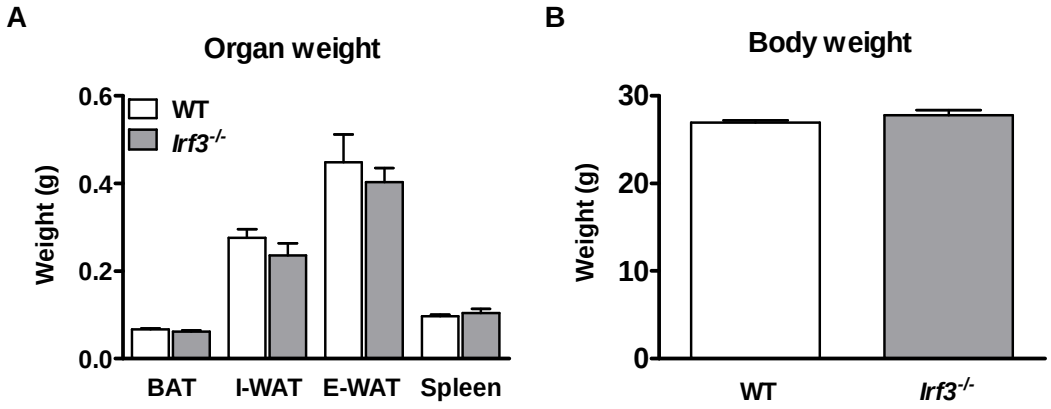

Figure 3. 3 IRF3 deletion does not affect the mass of fat depots.

A) Tissue weight of 12 week-old male chow-fed mice. BAT: brown adipose tissue, I-WAT: inguinal white adipose tissue, E-WAT: epididymal white adipose tissue. B) Body weight of the mice used in panel A. N=6.

We thus had to reconcile the observations that the MRI showed decreased adiposity, while actual fat pad weights (and body weight) were unchanged. This led us to hypothesize that lack of IRF3 may promote the development of brown adipocyte-like cells within the WAT. These cells, also called 'beige' or 'BRITE' cells, can develop within white fat pads in certain conditions, such as cold exposure or β_3-adrenergic stimulation.

Classic BAT, as well as these brown-adipose like cells, have reduced lipid content and can possibly be recognized as lean mass by the Echo-MRI machine.

Irf3$^{-/-}$ mice develop beige cells in the inguinal WAT.

To determine whether *Irf3$^{-/-}$* mice are predisposed to develop beige cells in WAT, subcutaneous adipose tissue from the inguinal depot was dissected from 12 week-old male mice maintained at room temperature (22.8^{o}C), sectioned and stained with hematoxylin-eosin (H&E). One simple way to identify beige cells is to look for the presence of multilocularity, which is a hallmark of brown adipocytes. Indeed, the inguinal WAT of *Irf3$^{-/-}$* mice had many clusters of multilocular adipocytes, while the inguinal WAT of WT mice contained predominantly unilocular adipocytes (Figure 3.4A). Interestingly, the histological appearance of classic interscapular BAT from *Irf3$^{-/-}$* mice was not different from that of WT mice (Figure 3.4B). Inguinal WAT and BAT sections were subjected to immunohistochemistry using a UCP-1 antibody. Again, many clusters of UCP-1 positive adipocytes were found in the inguinal WAT from *Irf3$^{-/-}$* mice, while very few were present in the inguinal WAT from WT mice (Figure 3.4A). No difference was found in the number of UCP-1 positive adipocytes in the interscapular BAT of *Irf3$^{-/-}$* and WT mice (Figure 3.4B).

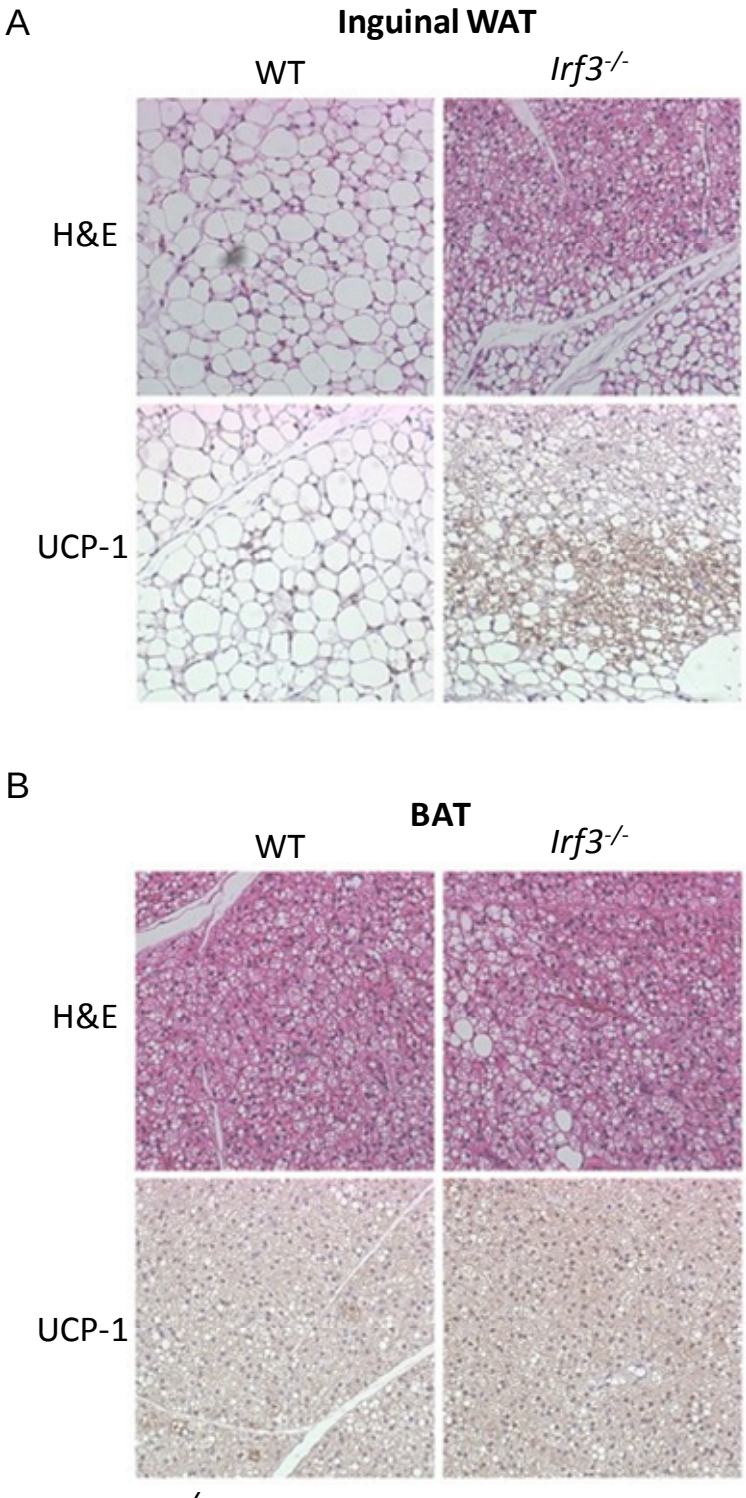

Figure 3. 4 *Irf3*$^{-/-}$ mice have increased beige cells in inguinal WAT.

Figure 3.4 (Continued). Tissue section immunostaining from chow fed male mice kept at ambient temperature. A) Inguinal WAT. B) Interscapular BAT.

Previous research has shown that cold challenge can stimulate the development of beige cells in the inguinal WAT of mice[12, 19]. To determine whether IRF3 deletion can further enhance the development of beige cells under cold challenged conditions, ten week-old male mice were exposed to 4^{o}C for three days, and their inguinal WAT and BAT was analyzed histologically. Interestingly, H&E staining revealed that multilocular cells were equally abundant in the inguinal WAT of both *Irf3*$^{-/-}$ and WT mice, while immunohistochemistry against UCP-1 showed a similar amount of UCP-1 positive adipocytes between the two groups (Figure 3.5A). The interscapular BAT also did not differ histologically between the two genotypes (Figure 3.5B). These results suggest that IRF3 represses the formation of beige cells under basal (i.e. warm) conditions, and that cold exposure relieves this inhibition.

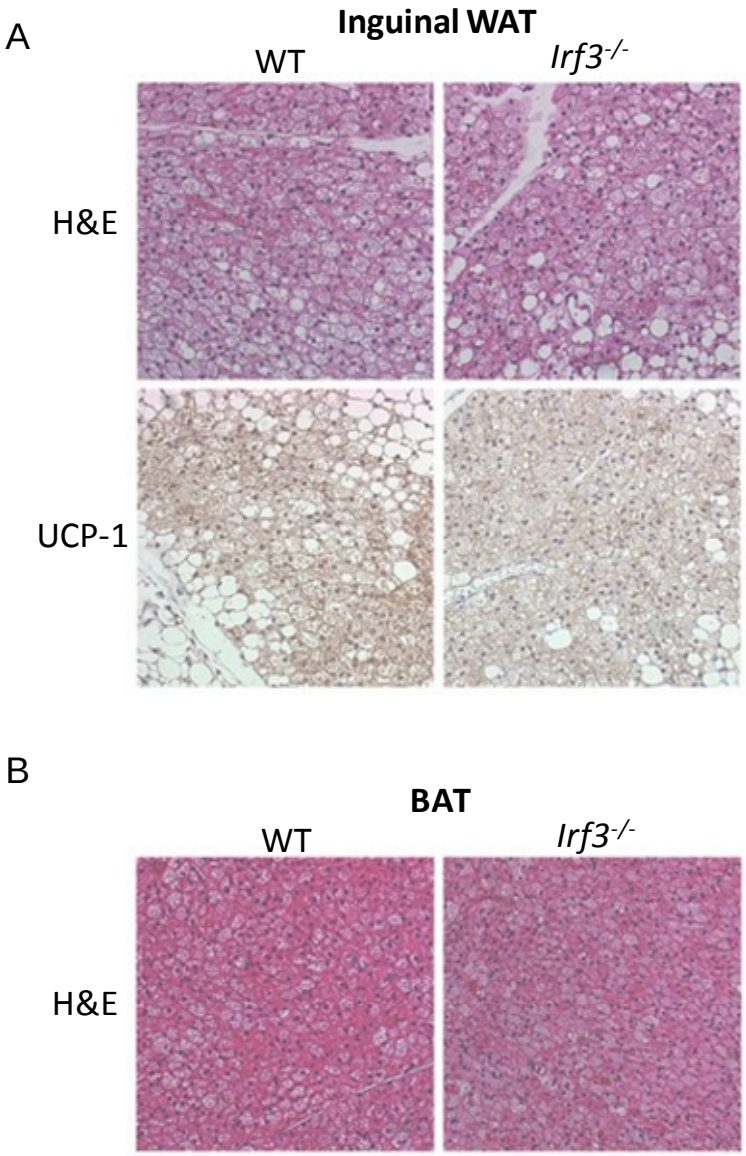

Figure 3. 5 Loss of IRF3 does not increase the number of beige cells in the inguinal WAT under cold challenged conditions.

Tissue section immunostaining of chow fed male mice after 3 days exposure to 4^{o}C conditions. A) Inguinal WAT B) interscapular BAT.

Although laboratory mice are studied at room temperature, their thermoneutral temperature is actually 30^{o}C. To determine if deletion of IRF3 can stimulate the development of beige cells in mice at thermoneutrality, ten week old *Irf3*$^{-/-}$ and WT mice were housed in a 30^{o}C chamber for 3 weeks and their inguinal WAT and BAT were studied. H&E staining showed that the inguinal WAT of *Irf3*$^{-/-}$ mice contained clusters of multilocular adipocytes, while the inguinal WAT from WT mice was made up of predominantly unilocular adipocytes. Immunohistochemistry against UCP-1 showed that many of the multilocular cells detected in *Irf3*$^{-/-}$ inguinal WAT were UCP-1 positive, while barely any UCP-1 positive cells could be detected in WT inguinal WAT (Figure 3.6A). H&E staining of interscapular BAT showed that exposure to thermoneutral conditions increased lipid accumulation in both *Irf3*$^{-/-}$ and WT mice, while no difference was found in the abundance of UCP-1 positive cells (Figure 3.6B). Together these results indicate that IRF3 prevents the development of beige cells in the inguinal WAT under basal conditions, and that deletion of IRF3 is sufficient to release this inhibition.

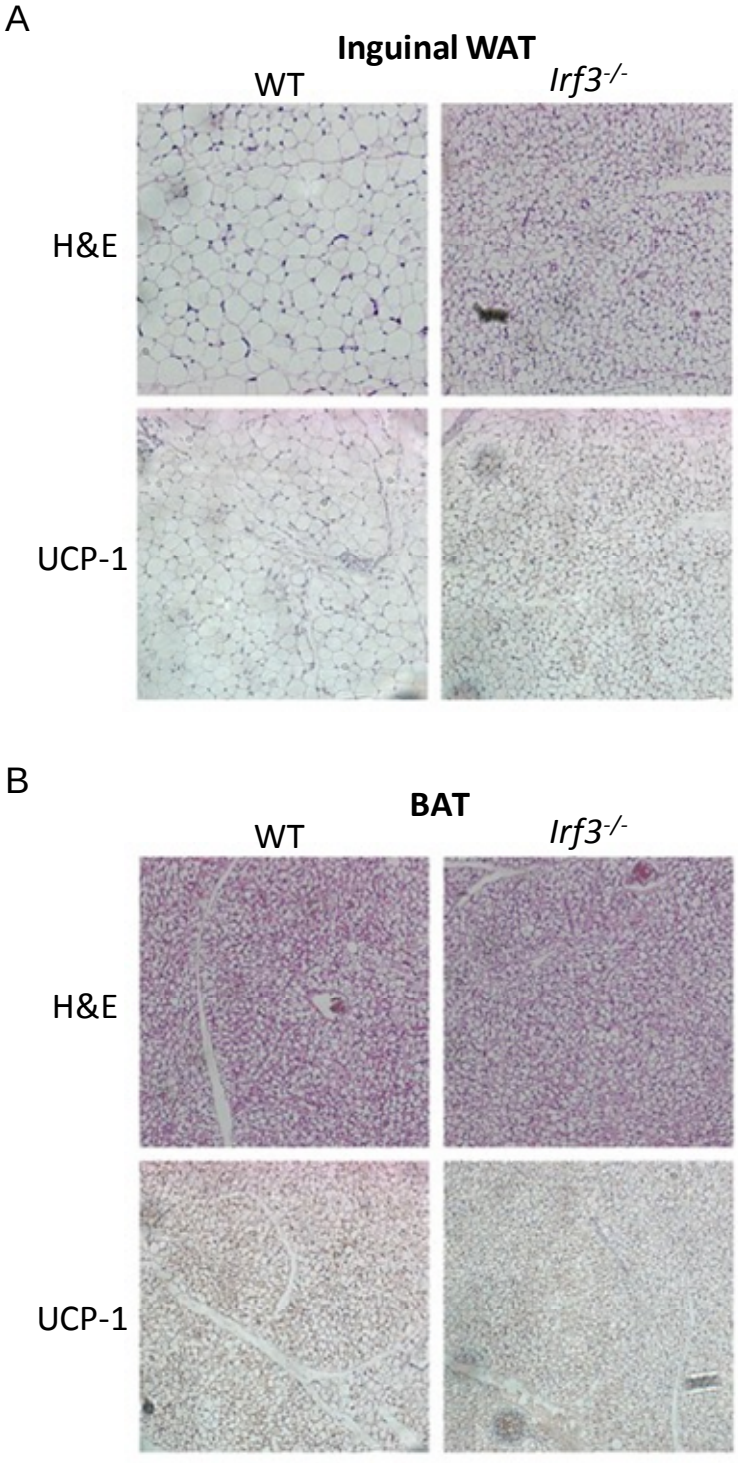

Figure 3. 6 *Irf3*$^{-/-}$ mice have increased beige cells under thermoneutral conditions.

Figure 3.6 (Continued). Tissue section immunostaining of chow fed male mice after 3 weeks exposure to 30°C. A) Inguinal WAT B) interscapular BAT.

Brown adipocyte genes are induced in the white adipocytes of Irf3$^{-/-}$ mice.

We next assessed whether these histologically identified beige cells express brown adipocyte signature genes in the inguinal WAT and BAT of *Irf3*$^{-/-}$ and WT mice. We assessed the expression of *Prdm16*, a critical determinant of brown adipogenesis[24-26, 28]; *Pgc1α* and *Ucp1*, both important players in adaptive thermogenesis[12, 16, 17, 26]; *Cox7a1*, an indicator of mitochondrial activity[184]; and *CideA*, a regulator of Ucp1 activity[185]. Key brown adipocyte genes were significantly up-regulated in both tissues of *Irf3*$^{-/-}$ mice compared to WT (Figure 3.7). These results suggest that the histologically identified beige cells in the *Irf3*$^{-/-}$ inguinal WAT are indeed functional.

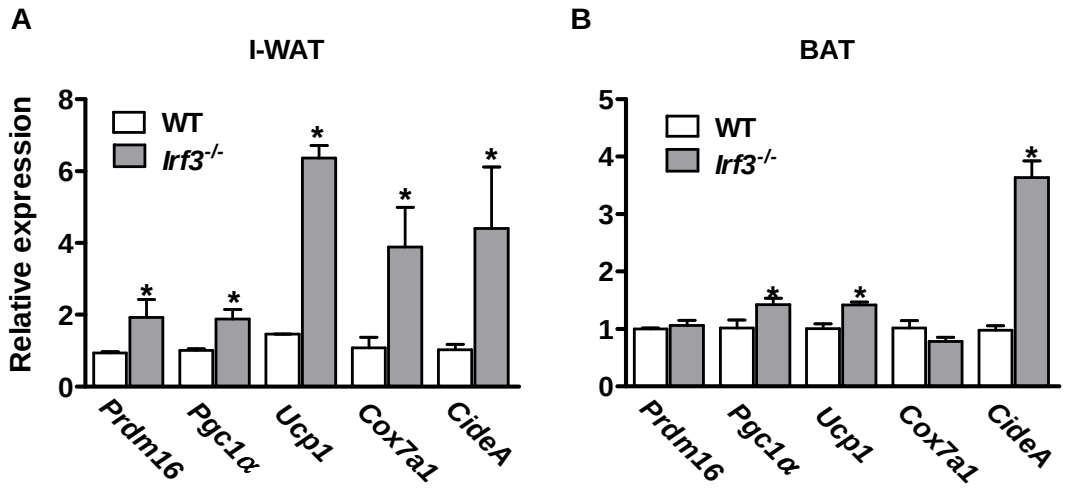

Figure 3. 7 Loss of IRF3 elevates the expression of brown adipocyte-selective genes in white and brown adipose tissue.

Figure 3.7 (Continued). Q-RTPCR of brown adipocyte genes. A) Inguinal WAT from HFD-fed male mice. B) Interscapular BAT from HFD-fed male mice. N=4, *P<0.05.

In addition to studying inguinal WAT tissue, an *in vitro* model was also employed to determine whether the observed "browning" effect was cell autonomous. The stromal-vascular fraction (SVF) of inguinal WAT was fractionated from *Irf3*$^{-/-}$ and WT mice. Pre-adipocytes from the SVF were briefly propagated and then differentiated into adipocytes. This model allows us to study the role of IRF3 in beige cell development independent of other tissues. Since IRF3 is anti-adipogenic, we need to ensure both *Irf3*$^{-/-}$ and WT cells are equally differentiated. Pre-adipocytes were treated with BMP-4 before adipogenic differentiation, and rosiglitazone was applied during the differentiation process to drive adipogenesis to completion. Differentiated adipocytes were treated with Oil-Red-R, which stains neutral lipids, to assess the extent of differentiation (Figure 3.8A). The expression of key adipocyte genes was also measured using Q-RTPCR (Figure 3.8B). Results from both Oil-Red-O and gene expression analysis indicate that both *Irf3*$^{-/-}$ and WT cells underwent adipogenic differentiation to an equal extent.

The expression of key brown adipocyte selective genes was assessed by Q-RTPCR in cultured SVF-derived adipocytes. In agreement with results from adipose tissue, these key brown adipocyte selective genes were significantly upregulated in *Irf3*$^{-/-}$ adipocytes compared to WT (Figure 3.8C).

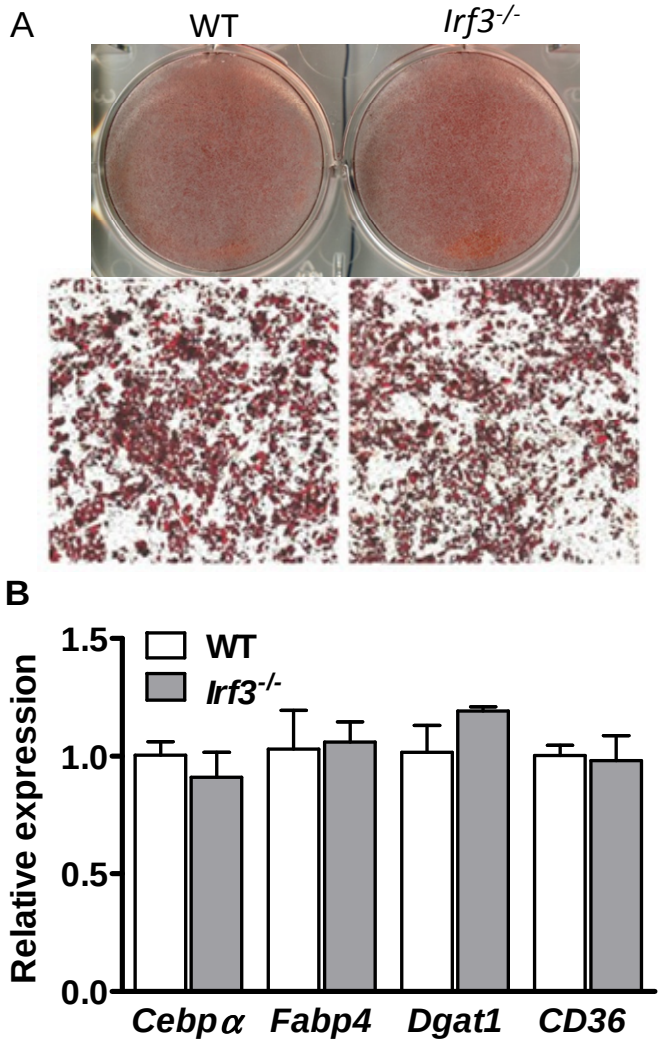
A
WT
Irf3-/-
B
Relative expression
1.5
1.0
0.5
0.0
WT
Irf3-/-
Cebpα
Fabp4
Dgat1
CD36
C
Relative expression
5
4
3
2
1
0
WT
Irf3-/-
*
Prdm16
Pgc1α
Ucp1
Cox7a1
CideA

Figure 3. 8

Figure 3.8 (Continued). Brown adipocyte-selective genes are elevated in cultured *Irf3*$^{-/-}$ adipocytes.

Inguinal SVF-derived adipocytes 7 days after adipogenic differentiation. A) Oil-Red-O staining. Whole field scan (top) and 10X magnified image (bottom). B) Q-RTPCR of adipocyte genes. C) Q-RTPCR of brown adipocyte selective genes. N=4 *P<0.05.

Irf3$^{-/-}$ *mice are partially protected from cold challenge.*

One of the major functions of brown adipocytes is to perform adaptive thermogenesis. An increase in the number of beige cells in *Irf3*$^{-/-}$ mice should promote adaptive thermogenesis, and thus ameliorate the drop in body temperature of these mice during cold exposure. Twelve week-old male *Irf3*$^{-/-}$ and WT mice were exposed to 4^{o}C, and the change in their rectal temperatures was measured over time. Although both *Irf3*$^{-/-}$ and WT mice dropped to 31^{o}C after two hours, the rate of drop in temperature was slower in *Irf3*$^{-/-}$ mice compared to WT, suggesting at least partial protection from cold (Figure 3.9).

One may expect "browning" of the white adipocyte to confer greater protection from cold induced body temperature drop for *Irf3*$^{-/-}$ mice than what we observed. However, adaptive thermogenesis is just one mechanism of thermogenesis under cold challenge. For instance, shivering is another mechanism to maintain physiological body temperature[186]. We hypothesize that the increase in the number of beige adipocytes allows *Irf3*$^{-/-}$ mice to confer faster response to cold challenge in maintaining their body

temperature. However, as time progresses other mechanisms of thermogenesis such as shivering allow WT mice to eventually reach the same body temperature.

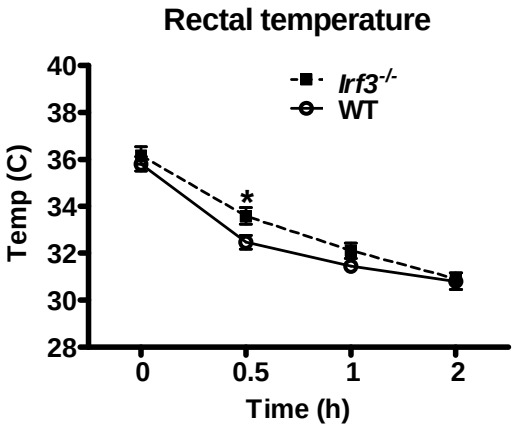

Figure 3. 9 *Irf3*$^{-/-}$ mice are partially protected from cold-induced drop in body temperature.

Rectal temperature of 12 week old male mice exposed to 4^{o}C. N=6, *P<0.05.

Irf3$^{-/-}$ *mice exhibit increased food intake and energy expenditure on HFD.*

If *Irf3*$^{-/-}$ mice have increased numbers of beige cells at room temperature, we might expect them to show increased energy expenditure. These mice were placed in open-circuit Oxymax chambers that are a component of the Comprehensive Lab Animal Monitoring System (CLAMS) to monitor their metabolic rate. No difference was observed in the amount of physical activity between *Irf3*$^{-/-}$ and WT mice (Figure 3.10B). However, *Irf3*$^{-/-}$ mice displayed significantly increased O_2 consumption and CO_2 production compared to WT, which together caused a marked shift in the respiratory exchange ratio (RER) (Figure 3.10C-E), suggesting a movement away from glucose as a

main source of fuel towards a fatty acid burning scheme. This is consistent with an increase in beige cells, which rely on fatty acid oxidation for adaptive thermogenesis. *Irf3*$^{-/-}$ mice displayed increased body heat compared to WT, again consistent with increased adaptive thermogenesis (Figure 3.10F). Given that energy expenditure was increased, we were puzzled to note that the *Irf3*$^{-/-}$ mice did not weigh less than WT littermates. We therefore measured daily food intake in male mice after 18 weeks of HFD feeding. *Irf3*$^{-/-}$ mice consumed approximately 0.4 g more food everyday compared to WT littermates (Figure 3.10A), which likely counterbalances the effect of the increased energy expenditure on body mass. Although the decrease in RER in *Irf3*$^{-/-}$ mice indicates that they are burning a smaller percentage of glucose in favor of fatty acids, their increase in food intake suggests that overall, *Irf3*$^{-/-}$ mice are burning more energy than WT mice, only with a change in preference for the source of energy.

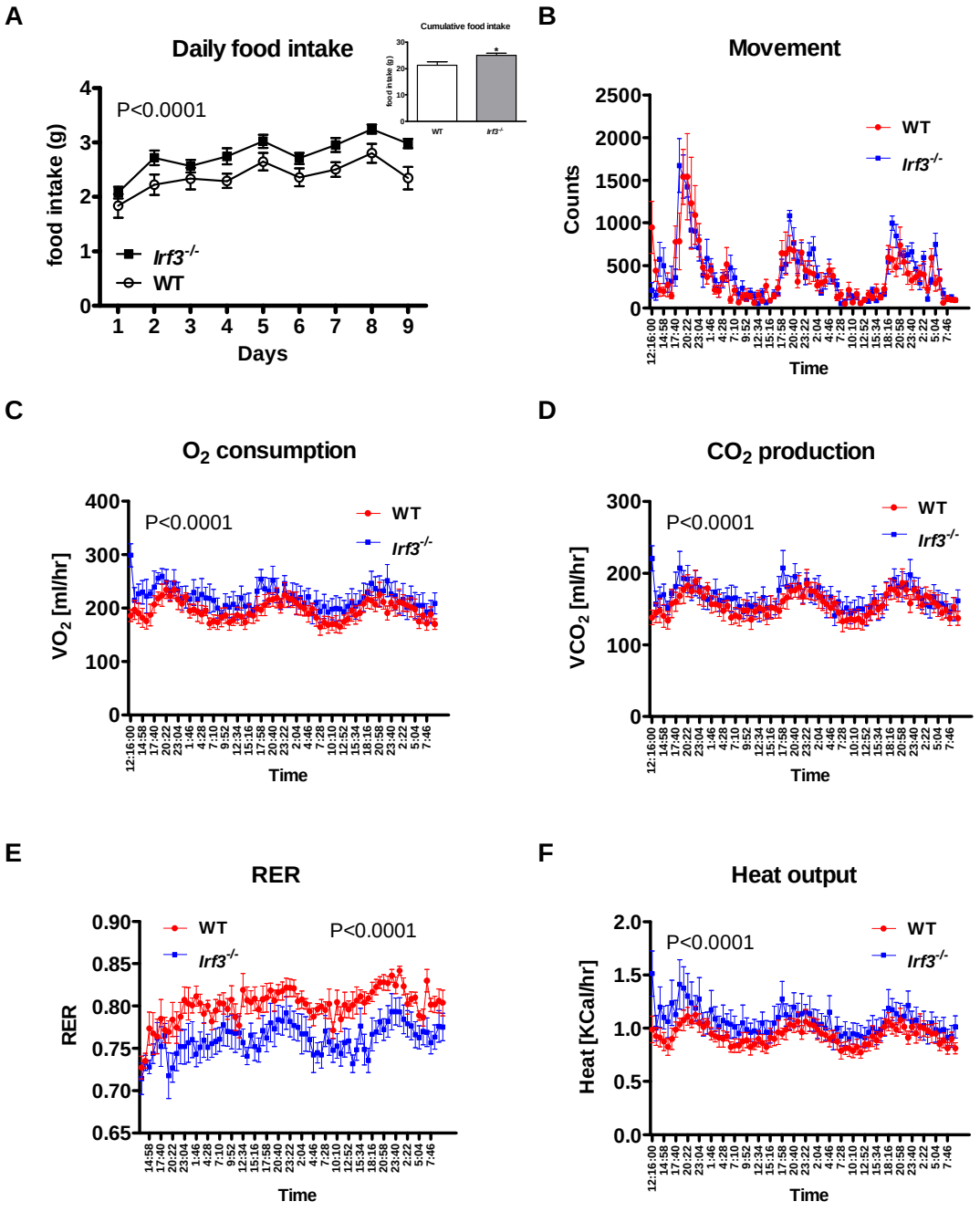

Figure 3.10 *Irf3*$^{-/-}$ mice have increased food intake and energy expenditure on HFD.

A) Daily food intake and cumulative food intake (inset) of male mice after 18 weeks on HFD, *P<0.05. B-F) Metabolic rate as measured by CLAMS B) Movement, C) O_2

Figure 3.10 (Continued). consumption, D) CO_2 production, E) Respiratory exchange ratio, F) Total body heat output. N=8.

Discussion

We found IRF3 to be a potent suppressor of beige cell development in inguinal WAT (Figure 3.11). Specifically, *Irf3*$^{-/-}$ mice were found to have increased numbers of beige cells in the inguinal WAT compared to WT mice at both room temperature and thermoneutral conditions, but not in cold challenged conditions. Interscapular BAT showed no histological difference between *Irf3*$^{-/-}$ and WT mice at any condition. This suggests that IRF3 may act as a brake for the development of WAT resident beige cells. Under basal conditions deletion of IRF3 allows the development of resident precursor cells into mature beige cells, while cold challenge overcomes the brake put into place by IRF3. This would explain why beige cell number and thermogenic capacity are not different between WT and *Irf3*$^{-/-}$ mice after prolonged exposure to 4°C.

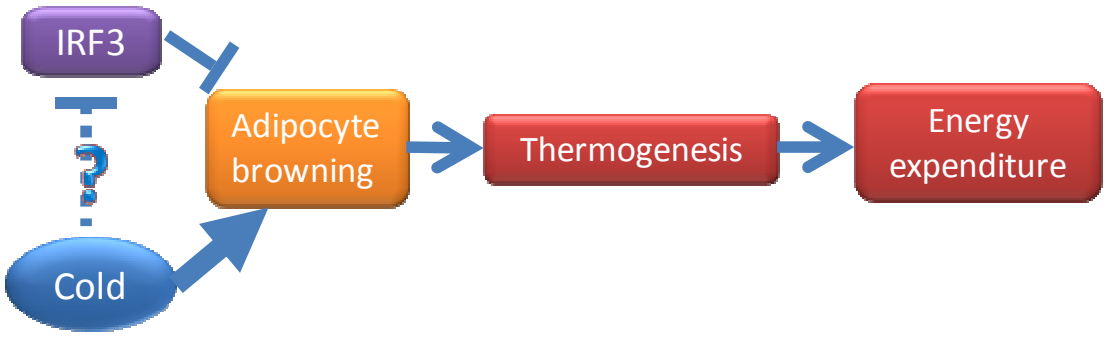

Figure 3. 1 1 IRF3 regulates energy homeostasis by inhibiting adipocyte browning.

Further characterization under HFD-fed conditions show that *Irf3*$^{-/-}$ mice exhibit increased food intake, increase energy expenditure, and a shift away from glucose toward fatty acid as a source of fuel. These characteristics are all consistent with enhanced adaptive thermogenesis due to an increase in the number of beige cells. Lastly, adaptive thermogenesis by these beige cells also conferred short-term protection from cold-induced body temperature drop in *Irf3*$^{-/-}$ mice. Additional *ex vivo* experiments will need to be performed to assess the functional characteristics of the beige cells appearing in the WAT of *Irf3*$^{-/-}$ mice, such as the rate of cellular respiration and mitochondrial density, which should both be increased due to a more brown adipocyte-like phenotype.

One of the unexplained phenotypes observed in the *Irf3*$^{-/-}$ mice is a small but significant increase in lean mass accompanied by a similar decrease in fat mass compared to WT littermates when fed HFD. One possible explanation for this observation is the inability of the Echo-MRI analyzer to properly classify BAT. The Echo-MRI analyzer distinguishes fat mass from lean mass via the difference in their density[187, 188]. Because BAT is denser than WAT we hypothesize that BAT may be recognized as lean mass by the Echo-MRI analyzer. Since the *Irf3*$^{-/-}$ mice exhibit browning of the WAT, this phenotype may be manifested as an increase in lean mass with decrease in fat mass. One way to test this hypothesis is to analyze pure BAT and see if the Echo-MRI analyzer recognizes it as lean mass.

One might wonder if *Irf3*$^{-/-}$ mice exhibit increased "browning" of the WAT, why did we not detect an elevation of brown adipocyte specific genes in the microarray of 3T3-L1 adipocytes after lentiviral mediated IRF3 knockdown (Figure 2.3)? This inconsistency can be explained by the inability of 3T3-L1 adipocytes to become brown adipocytes. Among the many *in vitro* adipocyte models, 3T3-L1 cells are one of the most white adipocyte-like[189, 190]. Key brown adipocyte selective genes such as Ucp1 and Pgc1α are undetectable in 3T3-L1 adipocytes (data not shown). Due to this reason, we employed an alternative *in vitro* model of adipocytes, namely preadipocytes isolated from the SVF fraction of the inguinal fat pad, to study the cell autonomous effect of IRF3 on adipocyte "browning" (Figure 3.8).

We observed increased "browning" of the WAT in chow fed *Irf3*$^{-/-}$ mice; however, we found increased thermogenesis in high fat-fed *Irf3*$^{-/-}$ mice. This may be due to the fact that under the metabolic challenge of HFD a small increase in energy expenditure may be more easily detectable. Further experiments are underway to study adipocyte "browning" in high fat-fed *Irf3*$^{-/-}$ mice. These are similar experiments performed to study adipocyte browning in chow diet-fed mice, such as tissue histology to look for multilocular and Ucp1 positive cells in the inguinal WAT. We hypothesize that lack of IRF3 will also induce "browning" of WAT in high fat-fed mice.

One interesting phenotype of the *Irf3*$^{-/-}$ mice is their increased food intake compared to WT littermates. This phenotype cannot be explained by increase adipocyte "browning." One adipokine that regulates food intake is leptin. Leptin reports peripheral nutritional information such as the energy store level of the adipose tissue to

the central nervous system[3]. Leptin expression increases with feeding and decreases with starvation. Elevation of leptin levels acts as a satiety signal and initiates a negative feedback loop to the hypothalamus to suppress food intake[1, 3, 191]. When leptin levels drop, the hypothalamus initiates a feeding response to increase energy intake[3, 192]. Studies of the *ob/ob* mouse, which is deficient of the *obese* gene encoding leptin, show massive weight gain and hyperphagia[191, 193, 194]. Alternatively, the *db/db* mouse, which expresses a mutant leptin receptor effectively abolishing leptin signaling, exhibit massive adipose tissue depots and produces excessive leptin[193, 195]. Similar to the *ob/ob* mouse, *db/db* mice are also extremely obese, hyperphagic, as well as diabetic[193, 195].

Leptin action is mediated by receptors present in the brain as well as peripheral organs such as the pancreas, liver, and the immune system[3, 196]. Leptin receptor binding in the hypothalamus results in downstream activation of the JAK-STAT3 signaling pathway, leading to an increase in anorexigenic neuropeptides such as proopiomelanocortin (POMC), as well as the expression of orexigenic neuropeptides neuropeptide Y (NPY) and agouti-related protein (AgRP)[196, 197]. Therefore, we hypothesize that IRF3 may be affecting food intake through its effects on adipose leptin expression. To test this hypothesis we can begin by measuring the serum leptin levels of WT and *Irf3*$^{-/-}$ mice. We expect serum leptin to be decreased in *Irf3*$^{-/-}$ mice. Additionally we can inject leptin into WT and *Irf3*$^{-/-}$ mice. If a difference in leptin level is causing the differences in food intake then leptin injection should equalize this difference.

An alternative possibility is that IRF3 plays a role in the central nervous system that regulates feeding behavior. We have previously shown that IRF3 is expressed in the

brain (Figure 1.2B), and previous studies have also shown that IRF3 plays an important role in immune response in the brain[198, 199]. IRF3 was found to be a mediator of interferon response to corneal infection with herpes simplex virus[198] as well as response to viral double stranded RNA in astrocytes[199]. Interestingly, IRF3 and the interferon response pathway which it regulates has also been implicated in protecting the brain against ischemic injury post stroke[200]. Therefore it is possible that IRF3 plays a role on the central nervous system to regulate feeding behavior.

One possible way to test this hypothesis is to knockout IRF3 specifically in the hypothalamus and assess whether this still leads to an increase in food intake. To perform this experiment we can first create a floxed IRF3 mouse model, then inject adeno-associated virus (AAV) expressing the Cre protein into the hypothalamus of the floxed IRF3 mouse[201]. This will result in a mouse with IRF3 deleted only in the hypothalamus. If IRF3 is indeed acting on the hypothalamus to regulate food intake then this mouse will exhibit increase food intake just as in the *Irf3*$^{-/-}$ mouse.

Further studies could focus on fully characterizing the role of IRF3 in beige cell development. We do not know which stage of beige cell development IRF3 is acting upon, but it is intriguing that Prdm16, one of the earliest known transcriptional activators of the brown as well as beige cell fate, is altered by loss of IRF3. This suggests that IRF3 plays a role very early in the developmental process of beige adipogenesis. Since IRF3 is a transcription factor it is possible that it is transcriptionally regulating the expression of Prdm16. One possible way to test this is to perform a luciferase reporter assay of the Prdm16 promoter with IRF3 overexpression. If IRF3 is transcriptionally

regulating the IRF3 promoter we would expect IRF3 overexpression to reduce Prdm16 promoter luciferase activity.

In addition to possible transcription regulation of brown adipocyte selective genes, it is also possible that IRF3 affects the adipose sympathetic tone, and thus lack of IRF3 may lead to activation of the sympathetic tone, which can lead to increased adaptive thermogenesis. Activation of the sympathetic tone can lead to increased noradrenaline release in the adipose tissue[202, 203]. Noradrenaline can stimulate the expression of brown adipocyte selective genes such as *Ucp1* and *Pgc1α* in adipocytes and thus result in "browning" of white adipocytes[204-206]. To test this hypothesis we can measure the level of noradrenaline in the WAT of WT and *Irf3*$^{-/-}$ mice, and we would expect to find higher noradrenaline levels in *Irf3*$^{-/-}$ mice.

Our results also suggest that cold might inhibit the expression or activity of IRF3 in WAT, a possibility that we are currently investigating (Figure 3.11). We are performing two experiments to test this hypothesis. We investigated the expression of IRF3 mRNA in inguinal WAT after cold exposure but did not detect any change (data not shown). However, in immune cells it is known that IRF3 is regulated post-translationally but not transcriptionally[69], therefore it is possible that this is also true in the adipocyte. We plan to study IRF3 protein level in inguinal WAT after cold exposure to determine whether cold challenge decreases IRF3 protein. It is also possible that cold exposure affects the phosphorylation state of IRF3, and we plan to use mass spectrometry to determine the phosphorylation state of adipose IRF3 before and after cold exposure.

Chapter 4

IRF3 hinders adipocyte glucose homeostasis through transcriptional regulation of GLUT4

Introduction

IRF3 is an important transcriptional regulator of the innate immune response. It acts downstream of TLR4 to initiate interferon response to pathogen infection. Upon antigen recognition, TLR4 signaling leads to the downstream activation of IKKε and TBK1, which act together to phosphorylate IRF3, leading to its dimerization and nuclear translocation. Nuclear IRF3 then binds to the promoter and activates transcription of interferon response genes such as *Ccl5* and *Ifnβ*, ultimately resulting in the activation of the interferon response pathway[54].

Characterization of *Ikkε*$^{-/-}$ mice show them to be protected from HFD-induced obesity. Additionally they exhibit decreased fasting serum insulin as well as better glucose tolerance compared to WT mice on HFD conditions. Interestingly, studies of the *Tlr4*$^{-/-}$ mice also found them to be more insulin tolerant compared to WT mice on HFD[95].

Adipose tissue is an important regulator of insulin stimulated glucose uptake. It influences the glucose uptake ability of peripheral tissues by secreting adipokines that act on muscle and liver[7]. For instance, adiponectin, a major adipokine, which has been found to be down-regulated during obesity, enhances insulin sensitivity[207-209]. Conversely, adipose tissue can also secrete insulin-desensitizing cytokines. TNFα, a pro-inflammatory cytokine secreted by WAT, is up-regulated during obesity and decreases insulin sensitivity[125]. Resistin, another major cytokine found to be up-regulated in obesity, hinders glucose uptake while elevating hepatic glucose output[210, 211].

In addition to influencing liver and skeletal muscle glucose homeostasis, adipose tissue itself also accounts for ~10-15% of systemic glucose uptake via insulin stimulated glucose uptake into adipocytes[1]. Following nutritional intake, pancreatic β-cells secrete insulin in response to elevated glucose in the circulation[212]. Insulin stimulates glucose uptake in peripheral tissues, including skeletal muscle and adipose tissue[212]. Insulin binds to the insulin receptor (IR) on the plasma membrane of target cells, resulting in IR dimerization and auto-phosphorylation[213-215]. Activated IR subsequently phosphorylates insulin receptor substrates IRS1 and IRS2, which then recruit Pl-3 kinase (PI-3k) to the cell surface[216, 217]. PI-3k converts phosphatidylinositol 4, 5 bisphosphate (PIP_2) to phosphatidylinositol 3, 4, 5 triphosphate (PIP_3)[218, 219], resulting in the activation of 3-phosphoinositide dependent kinase (Pdk1), which ultimately leads to protein kinase B (Akt) phosphorylation[220, 221]. Akt promotes the exocytosis of glucose transporter 4 (Glut4) containing vesicles to the plasma membrane, allowing the import of glucose into the cell via an ATP-independent, facilitative diffusion mechanism[221-225]. Imported glucose serves distinct purposes in different tissues. In skeletal muscle cells, glucose is metabolized to generate ATP, while in the adipose tissue excess glucose is stored as triglycerides[212].

Glut4 is a 12-transmembrane protein that is the major transporter responsible for insulin stimulated glucose transport in adipocyte and muscle cells[226]. Under basal conditions Glut4 undergoes idle cycling among several intracellular compartments including Glut4 storage vesicles (GSV), endosomal recycling compartment (ERC), and Trans-golgi network (TGN)[226]. Without insulin stimulation, Glut4 is prevented from

translocation to the plasma membrane (PM) by proteins that promote intracellular retention such as AS160 and Sortilin. Under insulin stimulation Glut4 vesicles bud from GSV, quickly translocate to the cell surface and fuses with the plasma membrane[227]. While new Glut4 protein synthesized by the endoplasmic reticulum are modified in the TGN, then sorted directly into GSV. Post insulin stimulation cell surface Glut4 is recycled via clathrin-mediated endocytosis or cholesterol-dependent, clathrin-independent endocytosis[226]. Endocytosed Glut4 accumulates in the endosomal recycling compartment (ERC). From the ERC a small amount of Glut4 is sorted back to the plasma membrane, while a majority of the Glut4 is sorted into the GSV or TGN where it undergoes idle cycling until the next insulin stimulation[226].

In addition to the tight intracellular regulation of its localization, GLUT4 is also regulated transcriptionally[228]. GLUT4 is encoded by the *Slc2a4* gene. Mice studies show that *Slc2a4* transcription is decreased in obesity and T2D models[229, 230]. Many transcription factors have been found to upregulate *Slc2a4* expression in adipocytes, including sterol response element binding protein-1c (Srebp-1c) and liver X receptor α (LXRα)[228]. Additionally thyroid hormone receptor α1 (TRα1) and kruppel-like factor 15 (Klf15) can regulate *Slc2a4* expression in both muscle and adipocytes[44, 228]. Conversely, tumor necrosis factor α (Tnfα), nuclear factor 1 (Nf-1), and nuclear factor-kappa B (Nf-κB) are negative regulators of *Slc2a4* expression[132, 176, 228].

Since IRF3 acts downstream of both TLR4 and IKKε we hypothesized that it too, may play a role in glucose homeostasis. To this end we characterized the metabolic phenotype of *Irf3*$^{-/-}$ mice. Skeletal muscle and adipose tissue are the two major players

in peripheral glucose uptake, which is tightly regulated by insulin secreted from pancreatic β cells. Both tissues utilize glucose in different ways; skeletal muscle cells metabolize glucose to generate ATP, while in the adipose tissue excess glucose is stored as triglycerides[7, 222]. Therefore, to elucidate the role of IRF3 in glucose homeostasis we must carefully dissect the different roles played by each tissue, which can best be done by studying tissue-specific knockout models of IRF3. However, at present the floxed IRF3 mouse model is unavailable. To overcome this difficulty we employed *in vitro* models of IRF3 overexpression and knockdown to supplement *in vivo* data from global knockout mice. Specifically, we chose to study IRF3 in cultured adipocytes because IRF3 is highly expressed and its expression is induced during adipogenic differentiation. This suggests that IRF3 may play a critical role in mature adipocytes, an excellent model for studies of cellular glucose uptake.

Materials and methods

Animals

Please refer to Materials and Methods in Chapter 2 to see a complete description of animal housing conditions and diet, as well as breeding schemes.

Insulin tolerance test

Mice were fasted for 6hr then injected intraperitoneally with human insulin (Humulin, Eli Lilly). Insulin doses range from 0.6-1 units/kg body weight depending on

whether the animals were on chow diet or HFD. The blood glucose level was measured before and at multiple time points after insulin injection by taking tail bleeds from each mouse. Glucose readings were taken with OneTouch handheld glucometers (Johnson and Johnson).

Glucose tolerance test

Mice were fasted overnight and fasting serum was collected from cheek bleed using a 5.5mm sterile animal lancet (Goldenrod). Mice were then injected intraperitoneally with a solution of 20% glucose at a dose of 1g/kg body weight. The blood glucose level was measured before and at multiple time points after insulin injection by taking tail bleeds from each mouse.

Serum cytokine measurements

Mice were fasted overnight and fasting serum was collected from cheek bleed using a 5.5mm sterile animal lancet (Goldenrod). Fasting serum was separated from whole blood by centrifugation at 3000 rpm for 5 min at 4^{o}C in BD Microtainer serum separator tubes (BD Bioscience #365956). Serum adiponectin was measured using the Chemicon Mouse Adiponectin ELISA Kit (Millipore #EZMADP-60K).

3T3-L1 adipocytes

Please refer to the Materials and Methods section in Chapter 2 for a complete description of the procedures followed for 3T3-L1 cell culture and adipogenesis.

IRF3 knockdown and overexpression in 3T3-L1 adipocytes

Please refer to the Materials and Methods section in Chapter 2 for a complete description of the procedures used for lentiviral production and lentiviral mediated IRF3 overexpression and knockdown in 3T3-L1 adipocytes.

MEFs

Pairs of WT vs. *Irf3*$^{-/-}$ embryos from the same litter were harvested on E13.5. After trypsinization and dissociation the fibroblasts are plated in high glucose DMEM/FBS. The 3T3 protocol was followed for immortalization[231]. Briefly, cells were subcultured every 3 days at a density of 1.17 million cells per 10cm dish, and after 30 passages MEFs were considered immortalized.

For adipogenic differentiation, immortalized WT and *Irf3*$^{-/-}$ MEFs were transduced with retrovirus encoding Pparγ. After puromycin selection for transduced cells, differentiation was induced with an adipogenic cocktail, including dexamethasone, insulin, isobutylmethylxanthine, and rosiglitazone. After 3 days of induction cells were maintained in high glucose DMEM/FBS until further experiments.

Glucose uptake assay

3T3-L1 adipocytes and MEF-derived adipocytes were subjected to glucose uptake assay either 10 days after adipogenic differentiation or 8 days after lentiviral transduction. Cells were serum-starved in high glucose DMEM for 4 hours and then

stimulated with 100nM insulin or vehicle for 15 min in KRH buffer at 37°C, after which [^{3}H] 2-deoxyglucose (2-DG) were added to the cells and incubated for 4 min. Glucose uptake is terminated by the addition of ice cold KRH with 25mM glucose and 10uM cytochalasin B (Sigma Aldrich). Excess [^{3}H] 2-DG was eliminated by repeated washing with ice cold KRH buffer. Cell lysates were solubilized in 0.1%SDS, mixed with EcoLite scintillation fluid (MP Biomedicals), and [^{3}H] 2-DG uptake was measured by liquid scintillation counting. All glucose uptake experiments were performed with six replicates for each sample.

Lipogenesis assay

3T3-L1 adipocytes and MEF-derived adipocytes were subjected to lipogenesis assay either 10 days after adipogenic differentiation or 8 days after lentiviral transduction. Cells were serum-starved in low glucose DMEM (Invitrogen) supplemented with 0.5% FBS for 3 hours then treated with 100nM insulin for 15 min at 37°C. Lipogenesis was then stimulated by adding [^{14}C] glucose and terminated after 45 min by repeated washing with ice cold PBS. Cells are harvested in PBS and mixed with EcoLite scintillation fluid. After overnight phase separation, 200ul of the lipid top layer is extracted for scintillation counting. All lipogenesis experiments were performed with six replicates for each sample.

Q-PCR

Please refer to the Materials and Methods section in Chapter 2 for a complete description of the procedures used for Q-RTPCR.

Tissue western blot

Mice were fasted overnight before tissue harvest. Tissues were frozen in liquid nitrogen immediately after dissection. For Western blots, tissues were homogenized in RIPA buffer supplemented with MiniComplete Protease Inhibitor (Roche) and phosphatase inhibitor cocktail II (Boston BioProducts). Total protein was quantified using the DC method (Bio-Rad) and 50ug of each protein sample was used for Western blot. Each sample was mixed with Laemmli buffer and boiled for 5 min at 95^{o}C. Samples were loaded into 10% polyacrylamide denaturing gels (Bio-Rad). Each gel was transferred onto PVDF membrane (Millipore). After transfer each membrane was blocked in 5% milk in PBS-T for 1 hr then incubated in primary antibody overnight at 4^{o}C. On the next day each membrane is washed in PBS-T before incubating with secondary antibody for 1 hr at room temperature. Lastly each membrane was washed in PBS-T before being developed with SuperSignal West Pico Maximum Sensitivity Substrate (Pierce) and exposed to film.

Luciferase assay

3T3-L1 adipocytes were transfected using the Amaxa Nucleofection II transfection device following manufacturer's protocol 7 days after adipogenesis. Briefly, one 10cm plate of adipocytes were trypsinized, pelleted, and then resuspended in 100µl

of Amaxa Nucleofector Solution V (Lonza #VCA-1003). Cell solution was then mixed with DNA containing 4µg pGL3 basic vector, 2µg pCDH IRF3 overexpression vector, and 50ng of pRL Renilla luciferase control reporter vector. The resulting mixture was placed in the transfection device and transfected with program A33. Transfected cells were immediately replated in high glucose DMEM with 10% FBS. Cells were allowed to attach overnight and the media was replaced 18hr later.

Luciferase assay was performed 48hr after transfection using Dual Luciferase Reporter Assay Kit (Promega #E1960) following the manufacturer's protocol. Luciferase activity was measured using FluoStar Optima fluorescence plate reader (BMG Labtech). Luciferase activity was normalized with Renilla, and all experiments were performed in quadruplicates.

Statistical analysis

Please refer to the Materials and Methods section in Chapter 2 for a complete description of the procedures followed for statistical analysis.

Results

Male Irf3$^{-/-}$ mice exhibit enhanced glucose metabolism on HFD.

We sought to determine whether IRF3 plays a role in glucose homeostasis. When kept on a chow diet, male *Irf3*$^{-/-}$ and WT mice at 22 weeks of age were found to be equally glucose tolerant (Figure 4.1A). However, after 22 weeks of HFD, male *Irf3*$^{-/-}$ mice

exhibited an enhanced ability to clear glucose compared to WT in a glucose tolerance test (GTT) (Figure 4.1B).

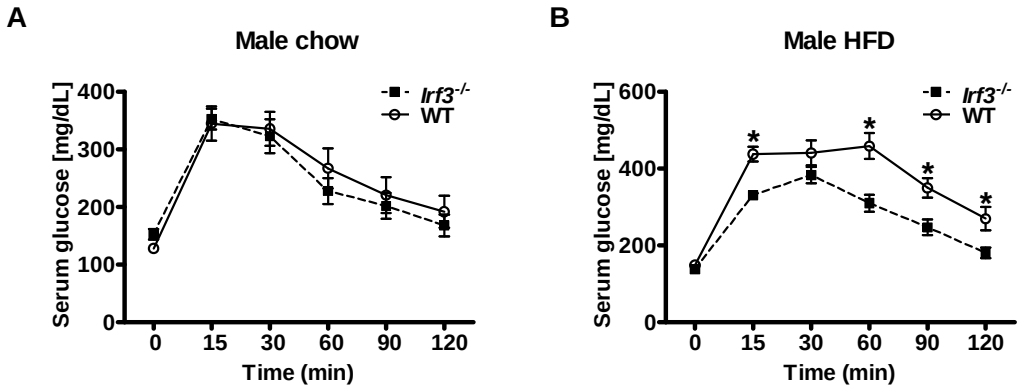

Figure 4. 1 Male *Irf3*$^{-/-}$ mice have enhanced glucose tolerance on HFD.

Glucose tolerance test of male mice on A) chow or B) HFD. N=9-12, *P<0.05.

To test whether the improved glucose tolerance of *Irf3* $^{-/-}$ mice is associated with increased insulin sensitivity, we performed insulin tolerance tests (ITT). At 21 weeks of age, chow fed male *Irf3*$^{-/-}$ mice displayed comparable insulin tolerance as their WT littermates (Figure 4.2A). However, male *Irf3*$^{-/-}$ mice maintained on 21 weeks of HFD showed significantly improved insulin tolerance compared to WT (Figure 4.2B).

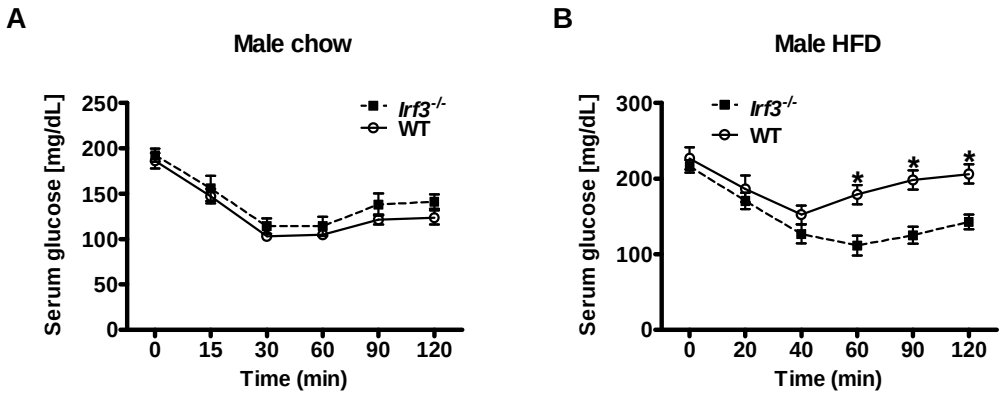

Figure 4. 2

Figure 4.2 (Continued). Male *Irf3*$^{-/-}$ mice have enhanced insulin tolerance on HFD.

Insulin tolerance test of male mice on A) chow or B) HFD. N=9-12, *P<0.05.

Fasting serum glucose and insulin levels were measured in male mice after an overnight fast. For both chow and HFD cohorts, no difference was observed in the serum glucose levels of *Irf3*$^{-/-}$ and WT mice (Figure 4.3A). *Irf3*$^{-/-}$ and WT mice kept on chow diet exhibited similar levels of fasting serum insulin. Under HFD conditions, however, *Irf3*$^{-/-}$ mice had significantly lower serum insulin compared to their WT littermates, consistent with their improved performance in the GTT and ITT (Figure 4.3B).

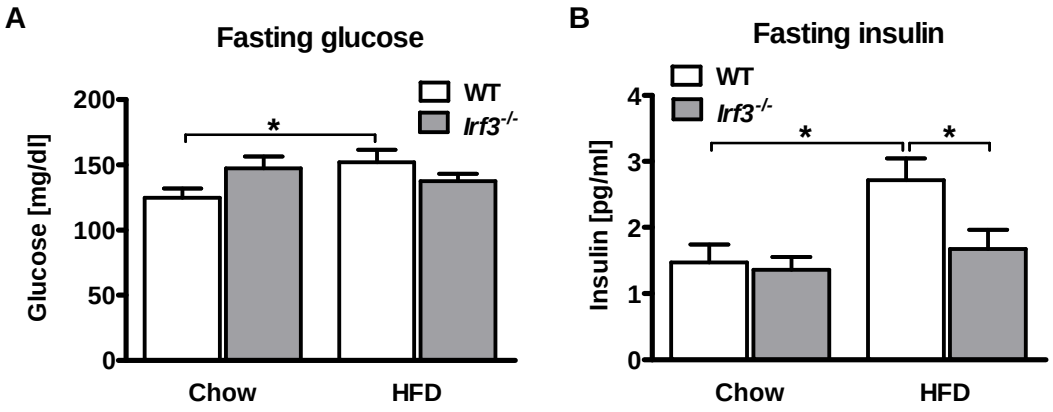

Figure 4. 3 Male *Irf3*$^{-/-}$ mice have reduced fasting serum insulin on HFD.

Fasting serum A) glucose or B) insulin of chow and HFD fed male mice. N=9-12, *P<0.05.

Female Irf3$^{-/-}$ *mice do not display enhanced glucose metabolism on HFD.*

Interestingly, the enhanced glucose metabolism exhibited by male *Irf3*$^{-/-}$ mice on HFD, was not seen in female mice. GTT performed on female mice after 22 weeks of HFD did not show any difference in glucose tolerance between *Irf3*$^{-/-}$ mice and their WT

littermates (Figure 4.4A). Similarly, female *Irf3*$^{-/-}$ and WT mice had similar insulin tolerance (Figure 4.4B). The fasting glucose and insulin levels were also indistinguishable between female high fat-fed WT and *Irf3*$^{-/-}$ mice (data not shown).

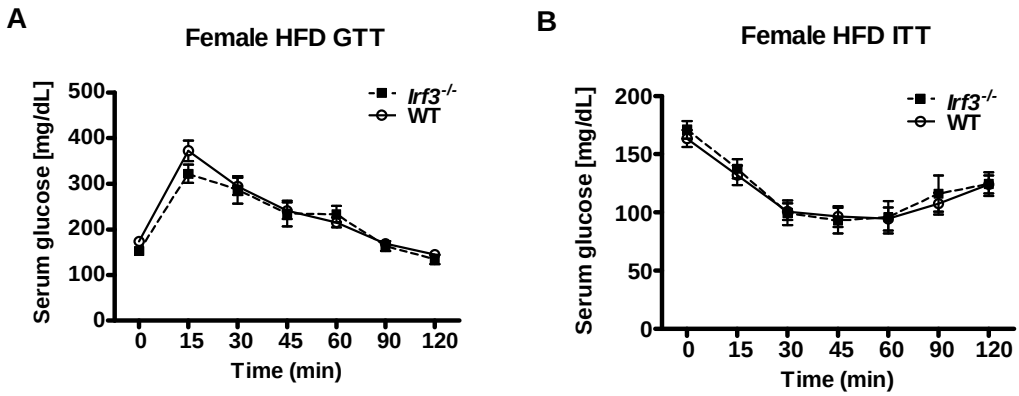

Figure 4. 4 Female *Irf3*$^{-/-}$ mice do not display enhanced glucose homeostasis on HFD.

A) Glucose tolerance test and B) Insulin tolerance test of female mice on HFD. N=9-12, *P<0.05.

IRF3 hinders insulin action in 3T3-L1 adipocytes.

Glucose homeostasis is regulated through the interaction of peripheral tissues such as the adipose tissue, liver, and muscle. The enhanced glucose homeostasis phenotype in male *Irf3*$^{-/-}$ mice on HFD may be due to the role of IRF3 in any or all of these three organs. Because IRF3 is highly expressed in adipocytes and its expression level is elevated in mature 3T3-L1 adipocytes, we hypothesized that at least part of this phenotype is due to IRF3's role in adipocytes. One way to test this hypothesis *in vivo* is to study the metabolic phenotype of adipocyte-specific IRF3 knockout mice. Unfortunately, conditional (i.e. floxed) *Irf3* mice are not currently available, so we used

an *in vitro* adipocyte model to study the role of IRF3 in cell autonomous adipocyte glucose homeostasis.

Mature 3T3-L1 adipocytes were transduced with lentiviral constructs mediating IRF3 overexpression or knockdown as described earlier. Insulin-stimulated glucose uptake and lipogenesis assays were performed 10 days later. While both wtIRF3 and IRF3-2D overexpression did not change basal glucose uptake, insulin-stimulated glucose uptake was significantly reduced by IRF3-2D overexpression. Similarly, wtIRF3 overexpression resulted in a trend toward reduced insulin-stimulated glucose uptake that did not reach statistical significance (Figure 4.5A). Conversely, shRNA mediated IRF3 knockdown resulted in enhanced insulin-stimulated glucose uptake, while basal glucose uptake was not affected (Figure 4.5B).

In addition to glucose uptake, insulin also stimulates lipogenesis in fat cells. Lentiviral-mediated overexpression of both wtIRF3 and IRF3-2D reduced insulin-stimulated lipogenesis, while basal lipogenesis remained unchanged (Figure 4.5C). Consistent with these observations, knockdown of IRF3 resulted in improved insulin-stimulated lipogenesis (Figure 4.5D). These data indicate IRF3 plays an important role in adipocyte insulin action and glucose homeostasis. Thus, the enhanced glucose metabolism observed in HFD-fed *Irf3*$^{-/-}$ mice is at least in part due to the role of IRF3 in the adipose tissue.

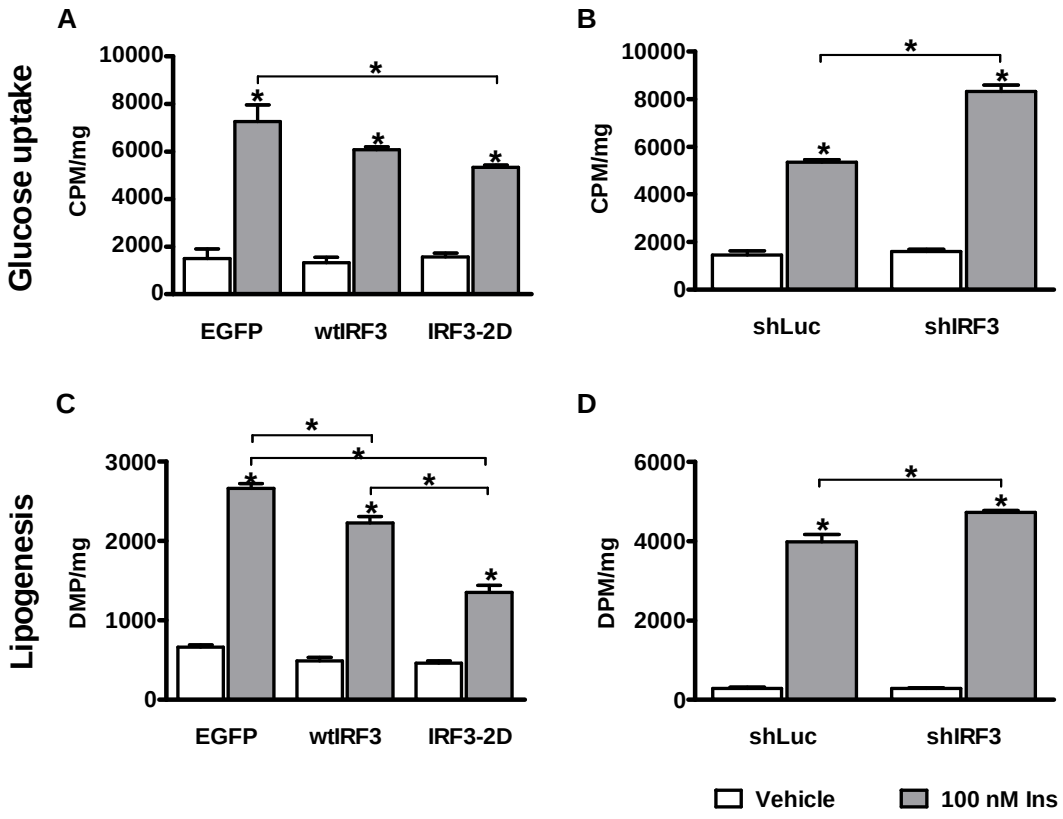

Figure 4. 5 IRF3 reduces insulin-stimulated glucose uptake in 3T3-L1 adipocytes.

A-B) Glucose uptake assay in 3T3-L1 adipocytes 8 days after lentiviral mediated IRF3 A) overexpression or B) knockdown. C-D) Lipogenesis assay in 3T3-L1 adipocytes 8 days after lentiviral mediated IRF3 C) overexpression or D) knockdown. N=6, *P<0.05

Adipocytes derived from Irf3$^{-/-}$ MEFs exhibit enhanced insulin action.

Although shRNA-mediated IRF3 knockdown in 3T3-L1 adipocytes results in enhanced glucose uptake and lipogenesis, it is possible that this effect is due to off-target effects of the shRNA hairpin. To eliminate this possibility, we employed an

additional *in vitro* model, namely immortalized mouse embryonic fibroblasts (MEFs) isolated from WT and *Irf3*$^{-/-}$ mice and differentiated into adipocytes *in vitro*.

Since IRF3 is known to be anti-adipogenic, WT and *Irf3*$^{-/-}$ MEFs may not differentiate equally. To overcome this problem, MEFs were transduced with a retrovirus overexpressing PPARγ and treated with rosiglitazone, a potent PPAR*γ* ligand, during adipogenic differentiation. Together these two measures drive adipogenesis to completion, as measured by Oil-Red-O staining, which showed that both WT and *Irf3*$^{-/-}$ MEFs achieved equal levels of differentiation (Figure 4.6A). Additionally, the expression of representative adipocyte genes were measured by Q-RTPCR and showed no difference between adipocytes derived from WT and *Irf3*$^{-/-}$ MEFs (Figure 4.6B).

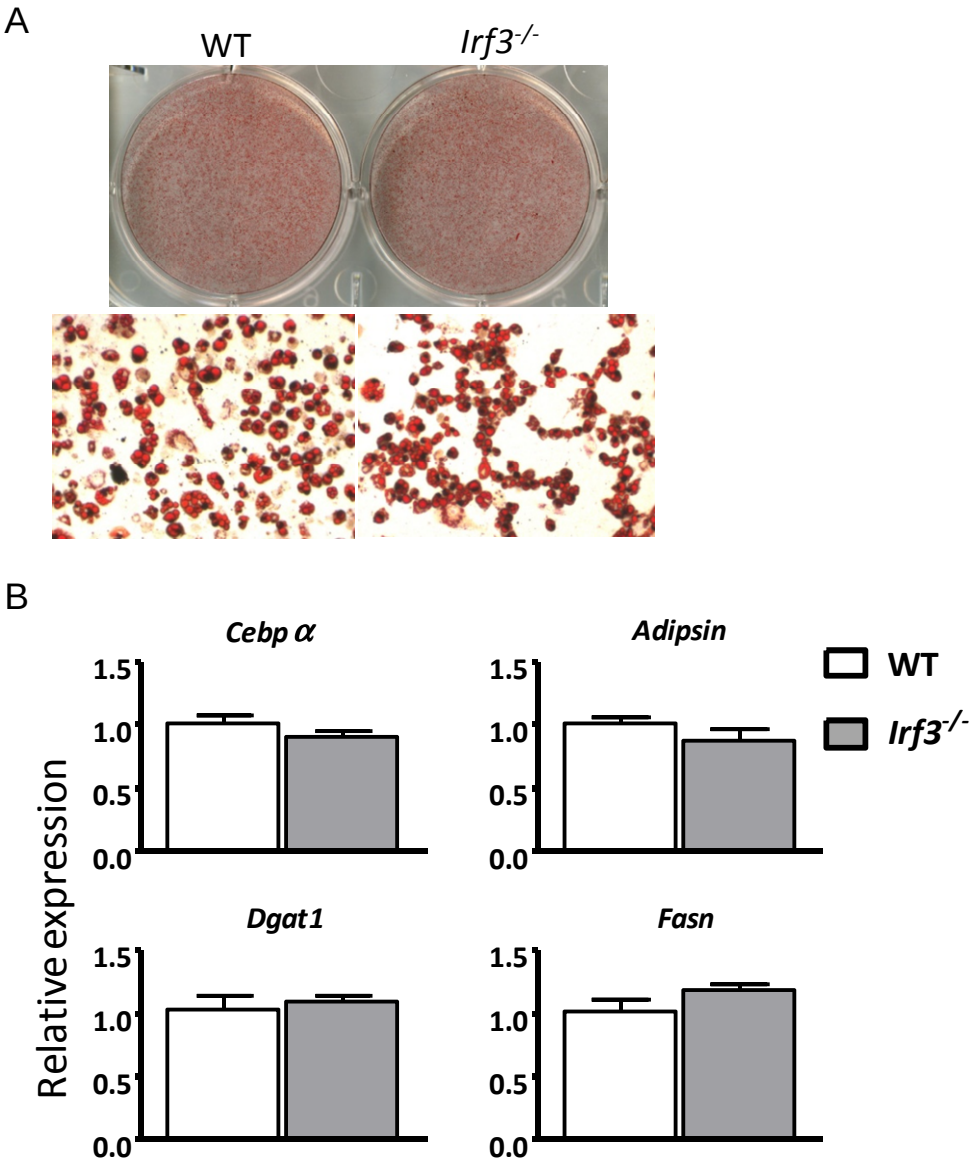

Figure 4. 6 WT and *Irf3*$^{-/-}$ MEFs achieved equal levels of adipogenesis.

MEF derived adipocytes 7 days after adipogenic differentiation. A) Oil-Red-O staining. Whole field scan (top) and 10X magnified image (bottom). B) Q-RTPCR of adipocyte genes, N=4.

Glucose uptake and lipogenesis assays were performed using MEF-derived adipocytes. *Irf3*$^{-/-}$ adipocytes showed enhanced insulin-stimulated glucose uptake compared to WT, while basal glucose uptake was unchanged (Figure 4.7A). To confirm that this is an IRF3-specific effect, *Irf3*$^{-/-}$ MEF adipocytes were rescued by reintroducing IRF3-2D or EGFP control via lentiviral transduction. Reintroduction of IRF3-2D in *Irf3*$^{-/-}$ MEF adipocytes diminished insulin-stimulated glucose uptake compared to EGFP control (Figure 4.7B).

Additionally, lipogenesis was also assessed in *Irf3*$^{-/-}$ MEF adipocytes. *Irf3*$^{-/-}$ adipocytes showed improved insulin-stimulated lipogenesis compared to WT, while basal lipogenesis was unaffected (Figure 4.7C). In the rescue experiment, *Irf3*$^{-/-}$ adipocytes overexpressing IRF3-2D showed reduced insulin-stimulated lipogenesis compared to those overexpressing EGFP control (Figure 4.7D). These data are entirely consistent with and validate the observations made in 3T3-L1 adipocytes. Taken together, these results indicate that IRF3 is a suppressor of insulin-stimulated glucose homeostasis in adipocytes.

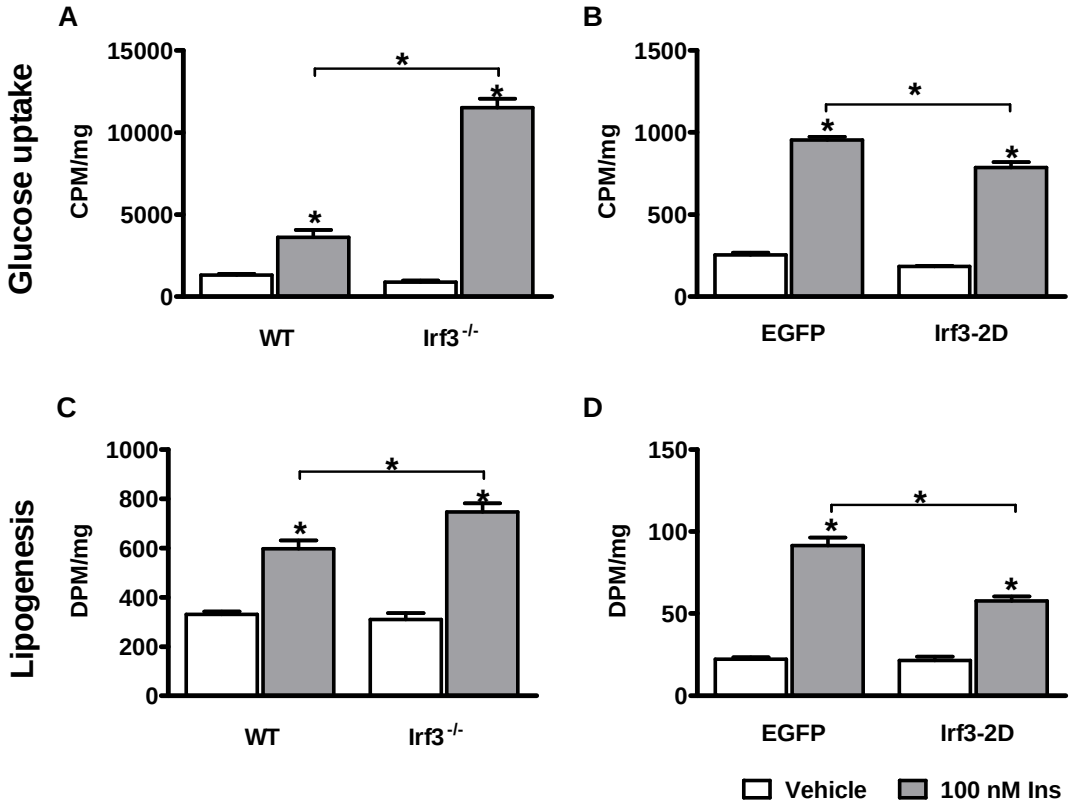

Figure 4. 7 Adipocytes derived *Irf3*$^{-/-}$ MEFs have enhanced insulin-stimulated glucose uptake.

A-B) Glucose uptake assay in MEF-derived adipocytes adipocytes A) 10 days after adipogenic differentiation or B) 8 days after IRF3 overexpression. C-D) Lipogenesis assay in MEF-derived adipocytes C) 10 days after adipogenic differentiation or D) 8 days after IRF3 overexpression. N=6, *P<0.05.

IRF3 affects glucose uptake at different doses of insulin.

To elucidate the mechanism through which IRF3 interferes with insulin action, insulin-stimulated glucose uptake was performed in 3T3-L1 cells after shRNA-mediated

IRF3 knockdown using a range of insulin doses from 1nM to 100nM. Regardless of the dose of insulin used, IRF3 knockdown enhanced insulin-stimulated glucose uptake (Figure 4.8). This was interesting to us because proportionate increase in glucose uptake at all insulin levels after a manipulation has been suggested to indicate a role for that factor in late insulin action, post-insulin receptor (IR) activation[232].

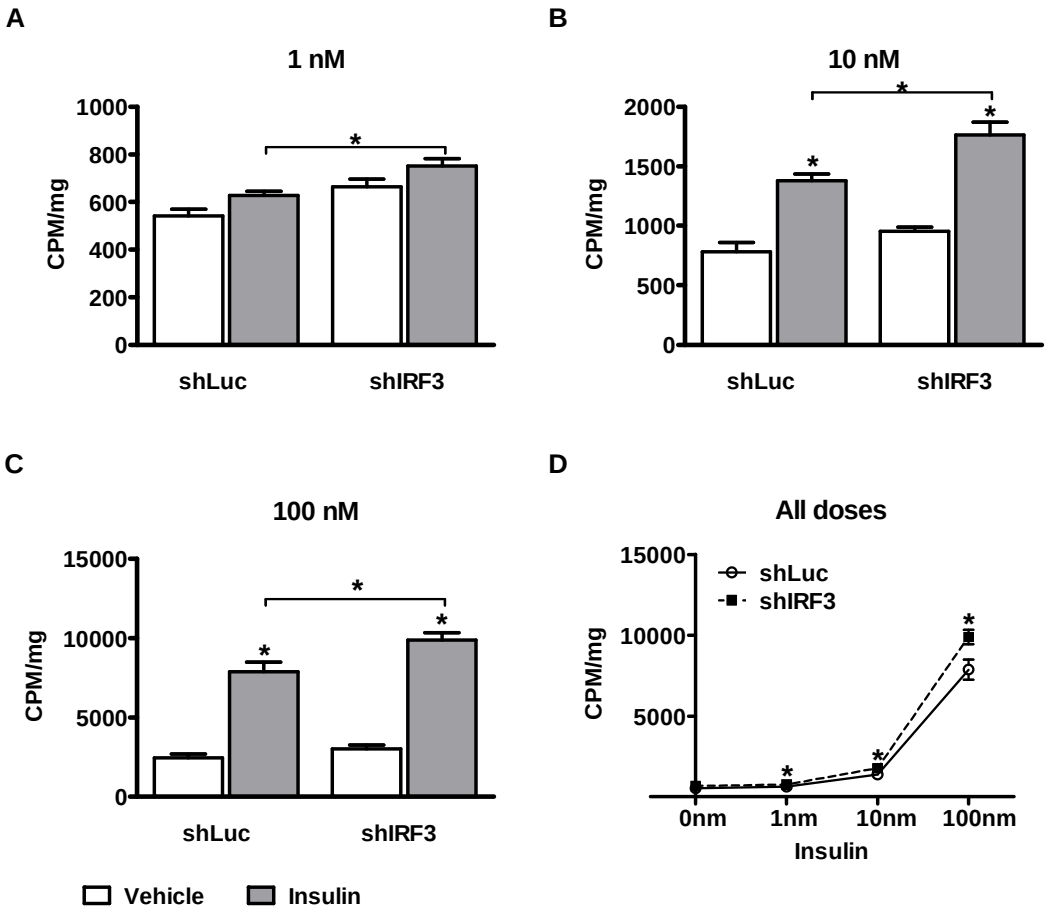

Figure 4.8 IRF3 knockdown enhances glucose uptake at different doses of insulin.

Dose-dependent insulin-stimulated glucose uptake in 3T3-L1 adipocytes. A) 1nM insulin B) 10nM insulin C) 100nM insulin and D) a composite view across all insulin doses. N=6, *P<0.05.

The insulin signaling pathway involves many different nodes[221]. Insulin binding leads to dimerization and auto-phosphorylation of IR. Phosphorylated IR subsequently phosphorylates IRS1 and IRS2, which then recruit PI-3k to the cell surface. PI-3k converts PIP_2 to PIP_3, leading to the downstream activation Pdk1, which ultimately leads to Akt phosphorylation and activation. Activated Akt recruits the Glut4 glucose transporter to the cell surface to facilitate glucose transport into the cell[212, 221, 224]. To determine whether IRF3 regulates the insulin signaling pathway we used Western blots to detect the abundance of phosphorylated Akt in the visceral adipose tissue of high fat-fed male *Irf3*$^{-/-}$ and WT mice five minutes after intraperitoneal insulin injection. No difference was found in the amount of phosphorylated Akt between *Irf3*$^{-/-}$ and WT mice (data not shown). Since Akt is a late node in the insulin signaling pathway, this data suggests that IRF3 is not affecting the insulin signaling pathway in adipocytes. However, we are still studying the effect of IRF3 on pre-Akt nodes, such as possible changes in IRS phosphorylation and activation.

Irf3$^{-/-}$ *WAT has increased levels of Glut4.*

Since IRF3 is a transcription factor, it is likely that IRF3 is hampering insulin stimulated glucose homeostasis by transcriptionally regulating target genes involved in insulin action. The results from the microarray analysis in 3T3-L1 adipocytes (Figure 2.1) were used to find such target genes. An analysis was performed to search for genes that are regulated in opposite directions by IRF3-2D and shIRF3, and are also known to

be players in insulin-stimulated glucose uptake. The two top candidates that emerged were *Adipoq* and *Slc2a4*. Both genes were down-regulated after IRF3-2D overexpression and up-regulated by shIRF3 in 3T3-L1 adipocytes. *Adipoq* encodes the hormone adiponectin, which has an insulin-sensitizing function. *Slc2a4* encodes the Glut4 glucose transporter, which is necessary for insulin-stimulated glucose uptake in adipocytes.

To confirm the microarray results, Q-RTPCR was used to determine the expression of *Adipoq* and *Slc2a4*. Indeed, both genes were potently down-regulated by IRF3-2D overexpression and significantly up-regulated after IRF3 knockdown in 3T3-L1 adipocytes (Figure 4.9A and B). Additionally, the expression of these genes was also assessed in mouse WAT. In agreement with the *in vitro* data, both *Adipoq* and *Slc2a4* were up-regulated in WAT from *Irf3*$^{-/-}$ mice compared to WT in both chow and high fat-fed conditions (Figure 4.9C and D).

While *Adipoq* is an adipocyte-specific gene, *Slc2a4* is also expressed in skeletal muscle, which is a key organ in insulin-stimulated glucose homeostasis. To determine whether IRF3 is a regulator of *Slc2a4* in skeletal muscle, the expression of *Slc2a4* in muscle was assessed by Q-RTPCR and no difference was found between *Irf3*$^{-/-}$ and WT mice on HFD (Figure 4.9E). This result indicates that the effect of IRF3 on global insulin-stimulated glucose homeostasis is likely not mediated via regulation of *Slc2a4* expression in skeletal muscle.

Although *Slc2a4* expression is up-regulated in *Irf3*$^{-/-}$ WAT, Glut4 protein levels must also be elevated to confer an insulin-sensitizing phenotype. Indeed, Western

blotting showed that Glut4 protein was significantly elevated in WAT of *Irf3*$^{-/-}$ mice compared to WT littermates under HFD conditions (Figure 4.9F). WT and *Irf3*$^{-/-}$ MEF derived adipocytes were used as an *in vitro* model, and Glut4 protein was also markedly increased in *Irf3*$^{-/-}$ cells compared to WT (Figure 4.9G).

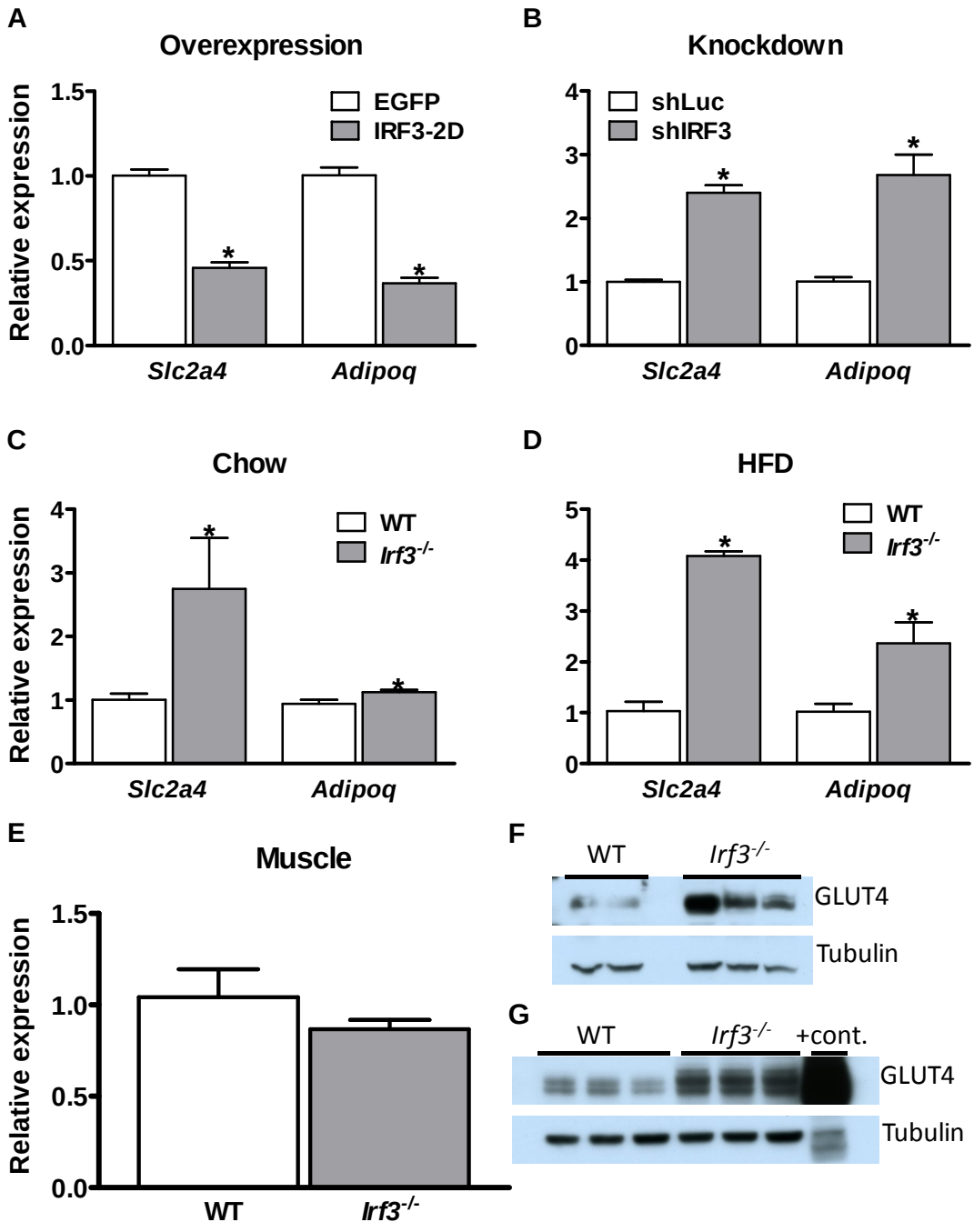

Figure 4. 9 IRF3 regulates *Slc2a4* expression in adipocytes.

A-E) Q-RTPCR of *Slc2a4* and *Adipoq* expression in A) 3T3-L1 adipocytes after IRF3 overexpression, B) 3T3-L1 adipocytes after IRF3 knockdown, C) epididymal WAT of

Figure 4.9 (Continued). chow-fed male mice, D) epididymal WAT of HFD-fed male mice, E) skeletal muscle of HFD-fed male mice. N=4, *P<0.05. F) Western blot of epididymal WAT from HFD-fed male mice, G) Western blot of MEF-derived adipocytes with WAT from the GLUT4 transgenic mouse as positive control.

Irf3$^{-/-}$ mice do not show increased serum adiponectin.

To study adiponectin protein levels, serum adiponectin was measured via ELISA in both chow and HFD-fed mice. Our results show the expected reduction in serum adiponectin level after HFD. However, adiponectin levels are not elevated in *Irf3$^{-/-}$* mice, and in fact are somewhat lower than in WT animals, suggesting that IRF3's role in insulin-stimulated glucose homeostasis is not mediated by systemic changes in serum adiponectin.

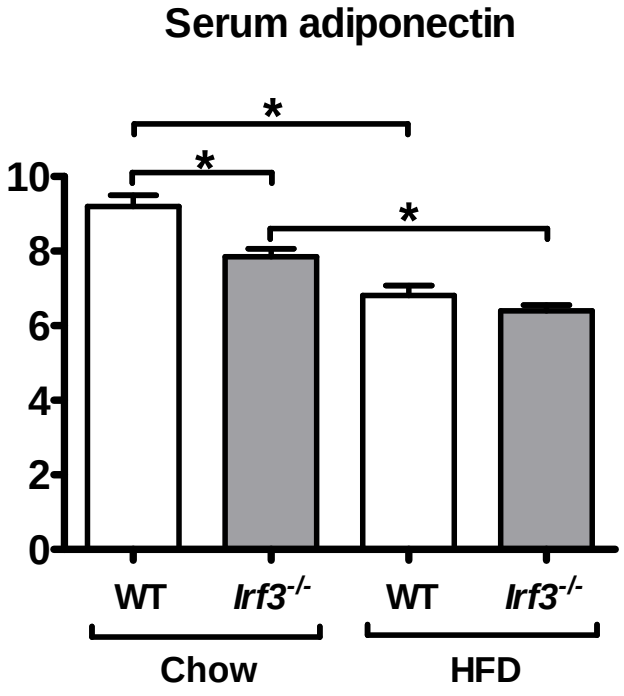

Figure 4. 1 0

Figure 4.10 (Continued). Serum adiponectin is not elevated in *Irf3*$^{-/-}$ mice.

Fasting serum adiponectin of chow and HFD fed male mice. N=8, *P<0.05.

IRF3 transcriptionally regulates the Slc2a4 promoter.

Because IRF3 is a transcription factor, it is possible that it exerts its effect on Glut4 expression by directly transcriptional regulation of the *Slc2a4* gene. Analysis of the *Slc2a4* proximal promoter using the Mulan multiple sequence local alignment and visualization tool (http://mulan.decode.org) identified several potential ISRE sites, with the most proximal ISRE located at 801 base pairs upstream of the transcription start site. To test whether IRF3 regulates *Slc2a4* via this ISRE site, promoter luciferase constructs containing 808 base pairs of the Slc2a4 promoter were cloned and luciferase assays were performed in 3T3-L1 adipocytes after wtIRF3 or IRF3-2D overexpression. Compared to EGFP control, overexpression of wtIRF3 significantly reduced luciferase activity driven by the *Slc2a4* proximal promoter, and IRF3-2D reduced luciferase activity to an even greater extent. When the putative ISRE site was deleted, neither wtIRF3 nor IRF3-2D overexpression reduced luciferase activity (Figure 4.11). These results indicate IRF3 hinders glucose homeostasis at least in part by transcriptionally regulating the expression of Glut4 in adipocytes.

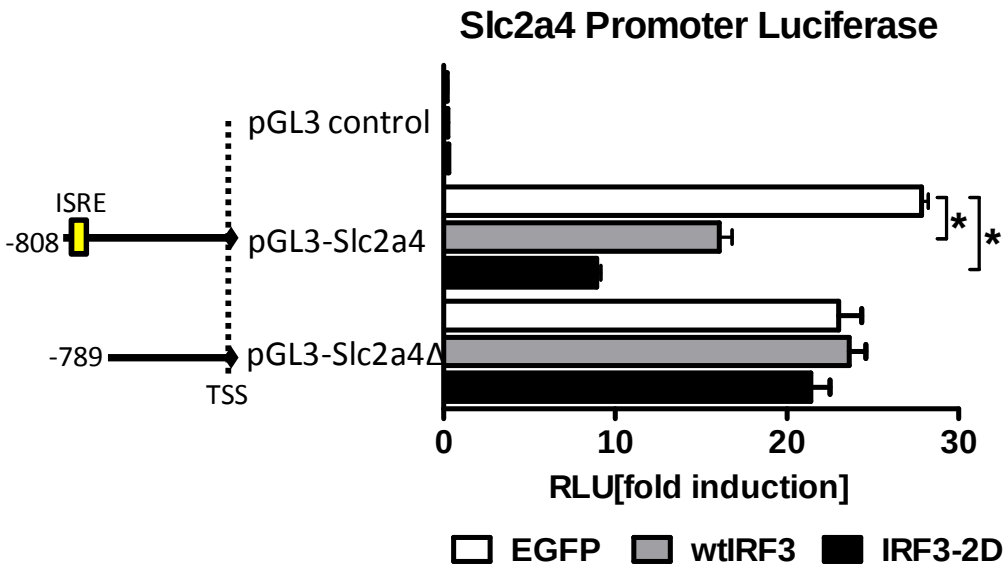

Figure 4. 1 1 IRF3 regulates the *Slc2a4* promoter.

Luciferase promoter assay of the *Slc2a4* promoter after EGFP or IRF3 overexpression in 3T3-L1 adipocytes. pGL3 control: pGL3 basic empty vector, pGL3-Slc2a4: pGL3 vector containing the *Slc2a4* proximal promoter including the ISRE site at -801bp, pGL3-Slc2a4Δ: pGL3 vector containing 789bp of the *Slc2a4* proximal promoter so that the ISRE site is deleted. N=4, *P<0.05.

Discussion

Here we characterized the role of IRF3 in glucose homeostasis. Analysis of *Irf3*$^{-/-}$ mice after high fat feeding showed enhanced glucose and insulin tolerance in the GTT and ITT, accompanied by decreased fasting serum insulin levels. Unlike the *Tlr4*$^{-/-}$ and the *Ikkε*$^{-/-}$ mice, *Irf3*$^{-/-}$ mice did not have reduced body weight. Even though *Irf3*$^{-/-}$ mice

did exhibit a small decrease in fat mass and complementary increase in lean mass, which we proposed above is correlated with an increase in beige adipocytes, such a small change in body composition is not likely to be sufficient to increase systemic insulin sensitivity to such a degree. Furthermore our results in Chapter 2 suggested that IRF3 deletion did not alter macrophage infiltration of WAT or the whole body systemic inflammatory state. Hence the enhanced glucose homeostasis in *Irf3*$^{-/-}$ mice is not likely due to reduced inflammation. As a result, we hypothesized that IRF3 may hinder glucose homeostasis through an additional mechanism in white adipose tissue.

Using 3T3-L1 adipocytes and MEF-derived adipocytes as *in vitro* adipocyte models, we found IRF3 overexpression to reduce insulin-stimulated glucose uptake and lipogenesis, and IRF3 knockdown or knockout to have the opposite effect. Subsequent Q-RTPCR experiments found *Slc2a4* mRNA and the Glut4 protein it encodes to be reduced in adipocytes after IRF3 overexpression and induced by IRF3 knockdown; *Irf3*$^{-/-}$ WAT also showed elevated Glut4 levels. A luciferase assay was used to show that IRF3 suppresses *Slc2a4* expression via an ISRE site 801 base pairs upstream of the Slc2a4 transcriptional start site (Figure 4.12).

Figure 4. 1 2 IRF3 suppresses adipocyte glucose uptake by transcriptionally downregulating adipose Glut4.

One intriguing question arising from these results is the sexual dimorphism observed in the enhanced insulin handling phenotype of the *Irf3*$^{-/-}$ mice. A possible explanation for this discrepancy is the differences in hormones between the male and female mice[233]. Specifically, estrogen, the primary female sex hormone has been implicated to play a role in whole body insulin sensitivity. Treating postmenopausal women with estrogen increased their insulin sensitivity as measured by both GTT and ITT; however, another study showed that estrogen can cause insulin resistance in young women[234, 235]. Treating insulin receptor mutant mice with estrogen enhances their resistance to oxidative stress, while ovariectomy leads to increased susceptibility to oxidative stress, which has been shown to contribute to insulin resistance[127, 236]. To test whether the sexual dimorphism of the *Irf3*$^{-/-}$ mice insulin handling phenotype results from a difference in estrogen levels, we can remove the effect of estrogen by performing ovariectomy on WT and *Irf3*$^{-/-}$ female mice, then determine whether the *Irf3*$^{-/-}$ mice exhibit enhanced insulin sensitivity on HFD compared to WT.

It is still unknown whether IRF3 regulates the *Slc2a4* promoter by direct binding or via an intermediate protein, although the involvement of the ISRE makes direct binding the most likely scenario. We would like to use chromatin immunoprecipitation (ChIP) to confirm direct binding, but we have not been able to locate a ChIP-grade mouse IRF3 antibody. An alternative strategy would be to perform ChIP after ectopic expression of a tagged form of IRF3 in 3T3-L1 adipocytes. We will design primers against computationally predicted ISRE regions in the *Slc2a4* promoter and perform PCR on the ChIP products. Regions directly bound by IRF3 should be successfully amplified.

The Glut4 glucose transporter is regulated transcriptionally as well as post-translationally[228, 237]. Under basal conditions GLUT4 resides intracellularly, but upon insulin stimulation, Glut4 containing vesicles fuse with the plasma membrane facilitating contact with extracellular glucose[237]. It would be interesting to determine whether increased Glut4 protein in *Irf3*$^{-/-}$ adipocytes also translates to increased Glut4 transport to the plasma membrane. To test this hypothesis we can use GFP-tagged Glut4 to visualize Glut4 location in the adipocyte. Glut4-GFP and IRF3-2D will be overexpressed in 3T3-L1 adipocytes and Glut4 localization will be visualized under a confocal microscope. If IRF3 is a regulator of Glut4 translocation then we will see differences in Glut4 trafficking in IRF3-2D overexpressing cells compared to negative control.

Another intriguing question is the tissue specific regulation of Glut4 expression by IRF3 only in adipocytes but not in muscle. One way this can occur is that IRF3 regulation of Glut4 requires cofactors that are only present in adipocytes but not in muscle. For instance it is known that there are transcription factors that regulate Glut4 only in adipocytes such as Srebp-1c and LXRα[228]. Alternatively transcription factors that regulate Glut4 only in muscle include muscle-specific Glut4 enhancer factor (GEF) and myogenic bHLH factors (MyoD)[223, 228]. To test this hypothesis we can perform immunoprecipitation (IP) of IRF3 followed by mass spectrometry. Performing this experiment in both muscle and adipocytes will determine the different cofactors bound to IRF3 in each tissue.

These results will also help us answer the question of whether IRF3 directly binds to the *Slc2a4* promoter or regulates Glut4 via an intermediate transcription factor,

which binds the *Slc2a4* promoter. By studying the list of cofactors bound to IRF3 in adipocytes we can look for transcription factors that are previously known to be direct transcription regulators of Glut4. If such a factor is identified we can further test whether this factor is required for IRF3 regulation of Glut4 by knocking down this factor in 3T3-L1 adipocytes followed by IRF3-2D overexpression and testing whether IRF3-2D can still cause insulin resistance compared to negative control.

In addition to *Slc2a4*, we also identified *Adipoq* to be down-regulated by IRF3 overexpression and up-regulated in IRF3 knockdown and knockout adipocytes. However, when we measured serum adiponectin levels in *Irf3*$^{-/-}$ mice, we did not see the expected increase. Adiponectin is an adipokine that's secreted by the adipose tissue and acts on the liver and muscle. It enhances insulin sensitivity, leading to a decrease in hepatic gluconeogenesis and an increase in skeletal muscle glucose uptake[238-240]. Adiponectin binding to its receptors in liver and muscle leads to downstream activation of Ampk and Pparα[238]. Ampk activation inhibits gluconeogenesis while stimulating fatty acid oxidation, and Pparα activation stimulates energy dissipation through increased fatty acid oxidation and by lowering oxidative stress and inflammation[238, 241].

Circulating adiponectin is found in three different isoforms: global trimers, low-molecular weight hexamers, and high-molecular weight 18-mers[238]. Metabolic diseases such as T2D, hypertension, atherosclerosis, and endothelial dysfunction are associated with low circulating adiponectin levels[238, 240, 242, 243]. However, the risk for T2D is inversely associated with only high molecular weight adiponectin[242, 244, 245]. In addition, only the high molecular weight isoform of adiponectin is associated with insulin

sensitizing effects, while the other two isoforms are implicated in the central effects of adiponectin action[238]. Therefore it is still possible that IRF3 may influence glucose homeostasis through affecting the level of high molecular weight adiponectin, but the ELISA assay used in this study was unable to distinguish between the different isoforms of adiponectin.

In summary, we identified IRF3 to be a transcriptional suppressor of the expression of the Glut4 glucose transporter in adipocytes. Deletion of IRF3 resulted in up to four-fold up-regulation of the gene and protein, which points to the importance of IRF3 in glucose homeostasis.

Chapter 5

Conclusions and future directions

Conclusions

In the past 20 years there has been a growing recognition of the close link between the immune and the metabolic systems[97]. Obesity has been found to be associated with chronic low-grade systemic inflammation as well as inflammation of peripheral metabolic tissues including adipose tissue, liver, and muscle. This state of inflammation is a crucial contributing factor to the comorbidities of obesity, including insulin resistance and T2D[97].

Numerous studies have shown that obesity results in elevated expression of inflammatory cytokines such as TNF-α, IL-6, IL-10, and IL-1β in the adipose tissue, which contribute to obesity-induced insulin resistance[4]. Additionally, many kinases involved in the proinflammatory signaling pathway, such as JNK, IKKβ, and PKC are also activated during obesity and act to promote insulin resistance[141, 143-145]. However, few studies have looked into the transcriptional pathways that regulate the immune-metabolic interaction. Here we show that IRF3, an important transcription factor in the viral-mediated interferon response pathway, is a player in this transcriptional pathway crosstalk.

First of all, using whole genome microarray and Q-RTPCR analysis we found IRF3 to be a potent inducer of immune response genes in adipocytes. Unexpectedly, however, we did not see altered MCP-1 levels or a decrease in the extent of macrophage infiltration in the WAT of *Irf3*$^{-/-}$ mice. Despite this, we did in fact find that IRF3 has potent effects on adipose tissue biology and metabolism.

Upon examination of the adipose tissue of *Irf3*$^{-/-}$ mice, we found IRF3 to be a potential suppressor of beige cell development from poised precursors in inguinal WAT. Specifically, *Irf3*$^{-/-}$ mice were found to have increased number of UCP-1-expressing beige cells in the inguinal WAT compared to WT mice at room temperature and thermoneutral conditions, but not in cold challenged conditions. When exposed to cold challenge, *Irf3*$^{-/-}$ mice exhibited short-term protection from a sharp drop in body temperature. These mice also exhibited increased food intake and energy expenditure as well as a shift away from glucose toward fatty acid as a source of fuel in *Irf3*$^{-/-}$ mice on HFD. Together these data suggest that IRF3 is a regulator of energy homeostasis by suppressing the "browning" of adipocytes.

Lastly we found IRF3 to be a transcriptional regulator of glucose homeostasis. Specifically, *Irf3*$^{-/-}$ mice exhibited enhanced insulin sensitivity and glucose tolerance on HFD. *In vitro* experiments in cultured adipocytes found this phenomenon to be at least partially due to an adipocyte-specific role of IRF3 to suppress the expression of Glut4 (Figure 5.1).

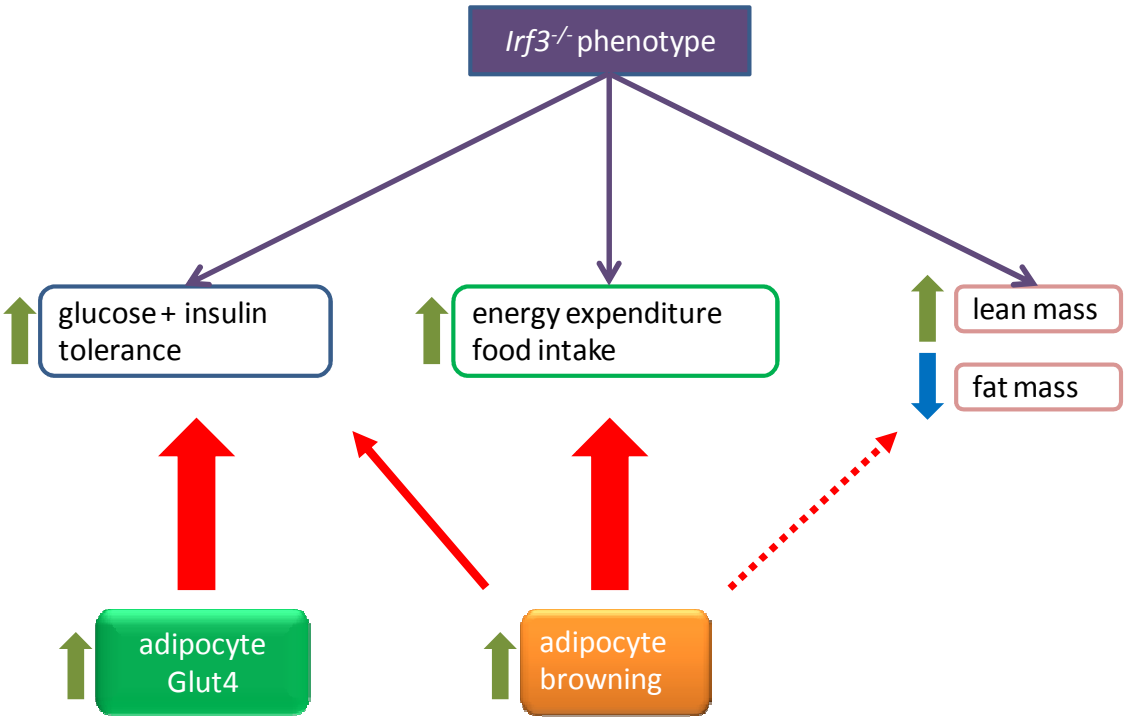

Figure 5. 1 IRF3 regulates glucose and energy homeostasis by suppressing adipocyte browning and Glut4 expression.

Because of the close link between the immune and the metabolic systems, is it possible that some of the phenotypes manifested in the *Irf3*$^{-/-}$ mice are in part due to IRF3's role in immune response? Nguyen et al. recently showed that M2 macrophages are required to sustain adaptive thermogenesis[246]. They found cold exposure to be an inducer of adipocyte M2 macrophages. These macrophages produce catecholamines that promote upregulation of *Pgc1α, Ucp1, and Acsl1.* Disruption of the IL-4/IL-13 pathway, which is required for M2 macrophage polarization, resulted in blunted adaptive thermogenesis, and thus these mice were unable to maintain core body temperature in response to cold challenge[246].

IRF3 is a strong positive regulator of M1 macrophage activation[54, 61]. Therefore *Irf3*$^{-/-}$ mice may exhibit elevated M2 macrophage polarization accompanied by decreased M1 macrophage polarization in the adipose tissue. This can lead to increased catecholamine in the adipose tissue, which may lead to the increased thermogenesis and adipocyte "browning" phenotype of the *Irf3*$^{-/-}$ mice. To determine whether M2 macrophage activation is indeed contributing to the increased thermogenesis and adipocyte "browning" in *Irf3*$^{-/-}$ mice, we can study whether there is increased M2 macrophage activation in the adipose tissue of *Irf3*$^{-/-}$ mice. This can be done by fractionating the adipose tissue and using FACS sorting to count the number of M1 macrophages, which are CD11c+ and M2 macrophages, which are CD11c-. If *Irf3*$^{-/-}$ mice have increased CD11c- macrophages in the white adipose tissue then M2 macrophage polarization is a contributing factor to the increased beige adipocyte phenotype in *Irf3*$^{-/-}$ mice.

In this study we observed both increased adipose tissue "browning" and enhanced glucose handling in *Irf3*$^{-/-}$ mice. Although we have identified increased Glut4 expression as a direct cause for enhanced glucose handling, it is still possible that the increase in adipose tissue "browning" is also a contributor to the glucose handling phenotype. Previous studies have shown that diabetes is associated with decreased expression of the brown adipocyte-selective gene Pgc1α[247], while resveratrol treatment, which increases Pgc1α activity, protects mice from diet induced obesity and insulin resistance[248]. Clinical observations also show that insulin resistant patients exhibit reduction in a panel of brown adipogenic genes including Pgc1α, Ucp1, Rxrγ, etc[249].

To determine how much the increase in adipocyte "browning" is contributing to the enhanced insulin sensitivity in *Irf3*$^{-/-}$ mice, we can assess how much lack of IRF3 increases insulin sensitivity in the absence of browning. This can be achieved by mating *Irf3*$^{-/-}$ mice onto an adipocyte-specific Prdm16 knockout background. Since lack of Prdm16 in the adipocyte will inhibit the development of brown adipocytes, we can compare the insulin sensitivity of the double-knockout mice with those expressing IRF3 to determine the extent to which IRF3 can affect insulin sensitivity without adipocyte "browning".

Future directions

One might wonder whether hyperactivation of IRF3 is involved in the onset of obesity since obesity is closely associated with the dysregulation of glucose and energy homeostasis. We have studied the expression of IRF3 in lean and obese mice and found no difference, consistent with the observation that IRF3 is constitutively expressed, and is not typically regulated at the transcriptional level[57]. IRF3 is, however, highly regulated by post-translational modifications[75]. Latent IRF3 resides in the cytoplasm, and under stimulation it is phosphorylated at the C-terminus, dimerizes, and translocates into the nucleus to activate transcription of downstream genes[63, 68, 69, 71]. Therefore the best way to study IRF3 activity is to look at its phosphorylation or translocation. Unfortunately there is currently no usable mouse-specific antibody on the market that specifically detects phosphorylated IRF3. We have also attempted to isolate the nuclear fraction from adipose tissue to detect nuclear IRF3. However, since obese adipose tissue is filled

with infiltrating macrophages, which also highly express IRF3, one must fractionate the adipose tissue to separate the adipocytes from the macrophages. Due to the low amount of nuclear protein in the obese adipocyte and the loss of yield from the fractionation process we have, as yet, been unable to detect adipose nuclear IRF3. We are now pursuing a mass-spectroscopy-based strategy to address the question of whether adipose IRF3 activity is elevated in obesity.

In this study we identified two important roles for IRF3 in the adipose tissue. However, it still remains a question whether some of the phenotypes we observed are entirely due to IRF3's role in the adipocyte or if there were confounding effects from other cell types. The lack of a floxed IRF3 mouse model limits our ability to completely work out IRF3's role in metabolism. A tissue specific knockout model would allow us to dissect the role of IRF3 in each metabolic tissue, especially its differential role in WAT and BAT. To this end, we plan to create a floxed IRF3 mouse model as the next stage of this project.

We are also interested in the pathways that lead to IRF3 activation in adipocytes. IRF3 activation is well studied in immune cells, where IRF3 acts downstream of TLR4. Activation of TLR4 after viral or bacterial infection results in activation of the kinases Tbk1 and Ikkε, which together phosphorylate and activate IRF3[91]. Both TLR4 and Ikkε have been found to be expressed in adipocytes. TLR4 has been shown to be a direct target of free fatty acids[80]. Metabolic characterization of *Tlr4*$^{-/-}$ mice and mice lacking TLR4 in hematopoietic cells show increased insulin sensitivity[80, 250]. Ikkε is also linked to metabolism in that obesity increases liver and adipose Ikkε expression[95]. *Ikkε*$^{-/-}$ mice are

protected from diet induced obesity and insulin resistance. Additionally, they exhibit increased food intake, body temperature, and energy expenditure[95]. These data correlate with our observations in the *Irf3*$^{-/-}$ mice *in vivo* as well as in *Irf3*$^{-/-}$ adipocytes *in vitro*. This suggests that IRF3 may act downstream of TLR4 and Ikkε in adipocytes. We plan to begin by performing *in vitro* experiments in 3T3-L1 adipocytes to study if overexpression or knockdown of TLR4 or Ikkε results in similar effects as that of IRF3. Then use epistasis experiments to determine if knockdown of IRF3 in 3T3-L1 adipocytes abolishes the effects of TLR4 and Ikkε.

In the process of characterizing the *Irf3*$^{-/-}$ mouse, we found them to be resistant to HFD-induced liver steatosis. This points to a potential role for IRF3 in liver metabolism. Seo et al. recently found viperin, a viral response protein encoded by the *Rsad2* gene, to have a role in inhibiting fatty acid oxidation[251]. Interestingly, viperin expression was significantly up-regulated by IRF3 overexpression and down-regulated by IRF3 knockdown in our microarray in 3T3-L1 adipocytes. Therefore we hypothesize a potential pathway where IRF3 acts through viperin to regulate fatty acid oxidation in the liver. This will be one of our new directions in the study of IRF3 in metabolism.

In conclusion we found IRF3 to be a regulator of adipose metabolism, specifically suppressing adipocyte "browning" and insulin-stimulated glucose handling. Although further studies are still needed to fully delineate IRF3's role in metabolism, these results clearly indicate that IRF3 is a critical transcriptional regulator of the crosstalk between the immune and the metabolic systems.

References

1. Waki, H. & Tontonoz, P. Endocrine functions of adipose tissue. *Annual review of pathology* **2**, 31-87 (2007).

2. Pelleymounter, M. *et al.* Effects of the obese gene product on body weight regulation in ob/ob mice. *Science (New York, N.Y.)* **269**, 540-543 (1995).

3. Friedman, J. The function of leptin in nutrition, weight, and physiology. *Nutrition reviews* **60** (2002).

4. Ouchi, N., Parker, J., Lugus, J. & Walsh, K. Adipokines in inflammation and metabolic disease. *Nature reviews. Immunology* **11**, 85-182 (2011).

5. Goossens, G.H., Blaak, E.E. & Van Baak, M.A. Possible involvement of the adipose tissue renin-angiotensin system in the pathophysiology of obesity and obesity-related disorders. *Obesity Reviews* **4**, 43-55 (2003).

6. Vázquez-Vela, M., Torres, N. & Tovar, A. White adipose tissue as endocrine organ and its role in obesity. *Archives of medical research* **39**, 715-743 (2008).

7. Rosen, E. & Spiegelman, B. Adipocytes as regulators of energy balance and glucose homeostasis. *Nature* **444**, 847-900 (2006).

8. Cinti, S. The adipose organ. *Prostaglandins, leukotrienes, and essential fatty acids* **73**, 9-24 (2005).

9. Kissebah, A. & Peiris, A. Biology of regional body fat distribution: relationship to non-insulin-dependent diabetes mellitus. *Diabetes/metabolism reviews* **5**, 83-192 (1989).

10. Després, J. *et al.* The insulin resistance-dyslipidemic syndrome: contribution of visceral obesity and therapeutic implications. *International journal of obesity and related metabolic disorders : journal of the International Association for the Study of Obesity* **19 Suppl 1**, 86 (1995).

11. Greenwood, M. & Hirsch, J. Postnatal development of adipocyte cellularity in the normal rat. *Journal of lipid research* **15**, 474-557 (1974).

12. Cannon, B. & Nedergaard, J. Brown adipose tissue: function and physiological significance. *Physiological reviews* **84**, 277-636 (2004).

13. Liesa, M., Palacín, M. & Zorzano, A. Mitochondrial dynamics in mammalian health and disease. *Physiological reviews* **89**, 799-1644 (2009).

14. Fromme, T. & Klingenspor, M. Uncoupling protein 1 expression and high-fat diets. *American journal of physiology. Regulatory, integrative and comparative physiology* **300**, 8 (2011).

15. Lee, P., Greenfield, J., Ho, K. & Fulham, M. A critical appraisal of the prevalence and metabolic significance of brown adipose tissue in adult humans. *American journal of physiology. Endocrinology and metabolism* **299**, 6 (2010).

16. Cypess, A. *et al.* Identification and importance of brown adipose tissue in adult humans. *The New England journal of medicine* **360**, 1509-1526 (2009).

17. Virtanen, K. *et al.* Functional brown adipose tissue in healthy adults. *The New England journal of medicine* **360**, 1518-1543 (2009).

18. van Marken Lichtenbelt, W.D. *et al.* Cold-Activated Brown Adipose Tissue in Healthy Men. *New England Journal of Medicine* **360**, 1500-1508 (2009).

19. Cinti, S. Transdifferentiation properties of adipocytes in the adipose organ. *American journal of physiology. Endocrinology and metabolism* **297**, 86 (2009).

20. Scarpace, P.J., Mooradian, A.D. & Morley, J.E. Age-Associated Decrease in Beta-Adrenergic Receptors and Adenylate Cyclase Activity in Rat Brown Adipose Tissue. *Journal of Gerontology* **43**, B65-B70 (1988).

21. Heaton, J.M. The distribution of brown adipose tissue in the human. *J Anat* **112**, 35-39 (1972).

22. Mercer, S.W. & Trayhurn, P. Effect of high fat diets on energy balance and thermogenesis in brown adipose tissue of lean and genetically obese ob/ob mice. *J Nutr* **117**, 2147-2153 (1987).

23. Gesta, S., Tseng, Y.-H. & Kahn, C. Developmental origin of fat: tracking obesity to its source. *Cell* **131**, 242-298 (2007).

24. Kajimura, S. *et al.* Initiation of myoblast to brown fat switch by a PRDM16-C/EBP-beta transcriptional complex. *Nature* **460**, 1154-1162 (2009).

25. Seale, P. *et al.* PRDM16 controls a brown fat/skeletal muscle switch. *Nature* **454**, 961-968 (2008).

26. Seale, P. *et al.* Transcriptional control of brown fat determination by PRDM16. *Cell Metabolism* **6**, 38-92 (2007).

27. Seale, P. *et al.* Prdm16 determines the thermogenic program of subcutaneous white adipose tissue in mice. *The Journal of clinical investigation* **121**, 96-201 (2011).

28. Kajimura, S. *et al.* Regulation of the brown and white fat gene programs through a PRDM16/CtBP transcriptional complex. *Genes & development* **22**, 1397-1806 (2008).

29. Timmons Ja Fau - Wennmalm, K. *et al.* - Myogenic gene expression signature establishes that brown and white adipocytes originate from distinct cell lineages. *Proc Natl Acad Sci U S A* **104**, 4401-4406 (2007).

30. Forner, F. *et al.* Proteome differences between brown and white fat mitochondria reveal specialized metabolic functions. *Cell Metabolism* **10**, 324-359 (2009).

31. Rangwala, S. & Lazar, M. Transcriptional control of adipogenesis. *Annual review of nutrition* **20**, 535-594 (2000).

32. Rosen, E. *et al.* C/EBPalpha induces adipogenesis through PPARgamma: a unified pathway. *Genes & development* **16**, 22-28 (2002).

33. Spiegelman, B. PPAR-gamma: adipogenic regulator and thiazolidinedione receptor. *Diabetes* **47**, 507-521 (1998).

34. Gearing, K., Göttlicher, M., Teboul, M., Widmark, E. & Gustafsson, J. Interaction of the peroxisome-proliferator-activated receptor and retinoid X receptor. *Proceedings of the National Academy of Sciences of the United States of America* **90**, 1440-1444 (1993).

35. Issemann, I., Prince, R., Tugwood, J. & Green, S. The peroxisome proliferator-activated receptor:retinoid X receptor heterodimer is activated by fatty acids and fibrate hypolipidaemic drugs. *Journal of molecular endocrinology* **11**, 37-84 (1993).

36. Wu, Z. *et al.* Cross-regulation of C/EBP alpha and PPAR gamma controls the transcriptional pathway of adipogenesis and insulin sensitivity. *Molecular cell* **3**, 151-159 (1999).

37. Lowe, C., O'Rahilly, S. & Rochford, J. Adipogenesis at a glance. *Journal of cell science* **124**, 2681-2687 (2011).

38. Rosen, E. & MacDougald, O. Adipocyte differentiation from the inside out. *Nature reviews. Molecular cell biology* **7**, 885-981 (2006).

39. Graves, R., Tontonoz, P. & Spiegelman, B. Analysis of a tissue-specific enhancer: ARF6 regulates adipogenic gene expression. *Molecular and cellular biology* **12**, 1202-1210 (1992).

40. Tontonoz, P., Hu, E., Graves, R., Budavari, A. & Spiegelman, B. mPPAR gamma 2: tissue-specific regulator of an adipocyte enhancer. *Genes & development* **8**, 1224-1258 (1994).

41. Christy, R. *et al.* Differentiation-induced gene expression in 3T3-L1 preadipocytes: CCAAT/enhancer binding protein interacts with and activates the promoters of two adipocyte-specific genes. *Genes & development* **3**, 1323-1358 (1989).

42. Tontonoz, P., Hu, E. & Spiegelman, B. Stimulation of adipogenesis in fibroblasts by PPAR gamma 2, a lipid-activated transcription factor. *Cell* **79**, 1147-1203 (1994).

43. Kaestner, K., Christy, R. & Lane, M. Mouse insulin-responsive glucose transporter gene: characterization of the gene and trans-activation by the CCAAT/enhancer binding protein. *Proceedings of the National Academy of Sciences of the United States of America* **87**, 251-256 (1990).

44. Gray, S. *et al.* The Krüppel-like factor KLF15 regulates the insulin-sensitive glucose transporter GLUT4. *The Journal of biological chemistry* **277**, 34322-34330 (2002).

45. Rosen, E.D., Walkey, C.J., Puigserver, P. & Spiegelman, B.M. Transcriptional regulation of adipogenesis. *Genes & development* **14**, 1293-1307 (2000).

46. Cristancho, A. & Lazar, M. Forming functional fat: a growing understanding of adipocyte differentiation. *Nature reviews. Molecular cell biology* **12**, 722-756 (2011).

47. Krebs Je Fau - Peterson, C.L. & CL, P. - Understanding "active" chromatin: a historical perspective of chromatin remodeling. *Crit Rev Eukaryot Gene Expr* **10**, 1-12 (2000).

48. Navas Pa Fau - Peterson, K.R., Peterson Kr Fau - Li, Q., Li Q Fau - McArthur, M., McArthur M Fau - Stamatoyannopoulos, G. & G, S. - The 5'HS4 core element of the human beta-globin locus control region is required for high-level globin gene expression in definitive but not in primitive erythropoiesis. *J Mol Biol* **312**, 17-26 (2001).

49. Crawford Ge Fau - Davis, S. *et al.* - DNase-chip: a high-resolution method to identify DNase I hypersensitive sites using tiled microarrays. *Nat Methods* **3**, 503-509 (2006).

50. Eguchi, J. *et al.* Interferon regulatory factors are transcriptional regulators of adipogenesis. *Cell Metab* **7**, 86-94 (2008).

51. Smith, A., Sumazin, P. & Zhang, M. Identifying tissue-selective transcription factor binding sites in vertebrate promoters. *Proceedings of the National Academy of Sciences of the United States of America* **102**, 1560-1565 (2005).

52. Crawford, G.E. *et al.* Genome-wide mapping of DNase hypersensitive sites using massively parallel signature sequencing (MPSS). *Genome Res* **16**, 123-131 (2006).

53. Xu Z Fau - Yu, S., Yu S Fau - Hsu, C.-H., Hsu Ch Fau - Eguchi, J., Eguchi J Fau - Rosen, E.D. & ED, R. - The orphan nuclear receptor chicken ovalbumin upstream promoter-transcription factor II is a critical regulator of adipogenesis. *Proc Natl Acad Sci U S A* **105**, 2421-2426 (2008).

54. Honda, K. & Taniguchi, T. IRFs: master regulators of signalling by Toll-like receptors and cytosolic pattern-recognition receptors. *Nat Rev Immunol* **6**, 644-658 (2006).

55. Lohoff, M. & Mak, T.W. Roles of interferon-regulatory factors in T-helper-cell differentiation. *Nat Rev Immunol* **5**, 125-135 (2005).

56. Bragança, J. & Civas, A. Type I interferon gene expression: differential expression of IFN-A genes induced by viruses and double-stranded RNA. *Biochimie* **80**, 673-760 (1998).

57. Ozato, K., Tailor, P. & Kubota, T. The interferon regulatory factor family in host defense: mechanism of action. *J Biol Chem* **282**, 20065-20069 (2007).

58. Eguchi, J. *et al.* Transcriptional control of adipose lipid handling by IRF4. *Cell Metabolism* **13**, 249-308 (2011).

59. Grandvaux, N. *et al.* Transcriptional profiling of interferon regulatory factor 3 target genes: direct involvement in the regulation of interferon-stimulated genes. *Journal of virology* **76**, 5532-5541 (2002).

60. Holm, G. *et al.* Retinoic acid-inducible gene-I and interferon-beta promoter stimulator-1 augment proapoptotic responses following mammalian reovirus infection via interferon regulatory factor-3. *The Journal of biological chemistry* **282**, 21953-22014 (2007).

61. Doyle, S. *et al.* IRF3 mediates a TLR3/TLR4-specific antiviral gene program. *Immunity* **17**, 251-263 (2002).

62. Qin, B. *et al.* Crystal structure of IRF-3 reveals mechanism of autoinhibition and virus-induced phosphoactivation. *Nature structural biology* **10**, 913-934 (2003).

63. Takahasi, K. *et al.* X-ray crystal structure of IRF-3 and its functional implications. *Nature structural biology* **10**, 922-929 (2003).

64. Mori, M. *et al.* Identification of Ser-386 of interferon regulatory factor 3 as critical target for inducible phosphorylation that determines activation. *The Journal of biological chemistry* **279**, 9698-10400 (2004).

65. Servant, M. *et al.* Identification of distinct signaling pathways leading to the phosphorylation of interferon regulatory factor 3. *The Journal of biological chemistry* **276**, 355-418 (2001).

66. Clément, J.-F. *et al.* Phosphorylation of IRF-3 on Ser 339 generates a hyperactive form of IRF-3 through regulation of dimerization and CBP association. *Journal of virology* **82**, 3984-4080 (2008).

67. Kim, T., Song, Y., Min, I. & Yim, J. Activation of interferon regulatory factor 3 in response to DNA-damaging agents. *The Journal of biological chemistry* **274**, 30686-30695 (1999).

68. Servant, M.J. *et al.* Identification of the minimal phosphoacceptor site required for in vivo activation of interferon regulatory factor 3 in response to virus and double-stranded RNA. *J Biol Chem* **278**, 9441-9447 (2003).

69. Chen, W. *et al.* Contribution of Ser386 and Ser396 to activation of interferon regulatory factor 3. *Journal of molecular biology* **379**, 251-311 (2008).

70. Lin, R., Mamane, Y. & Hiscott, J. Structural and functional analysis of interferon regulatory factor 3: localization of the transactivation and autoinhibitory domains. *Molecular and cellular biology* **19**, 2465-2539 (1999).

71. Qin, B. *et al.* Crystal structure of IRF-3 in complex with CBP. *Structure (London, England : 1993)* **13**, 1269-1346 (2005).

72. Kumar, K., McBride, K., Weaver, B., Dingwall, C. & Reich, N. Regulated nuclear-cytoplasmic localization of interferon regulatory factor 3, a subunit of double-stranded RNA-activated factor 1. *Molecular and cellular biology* **20**, 4159-4227 (2000).

73. Weaver, B., Kumar, K. & Reich, N. Interferon regulatory factor 3 and CREB-binding protein/p300 are subunits of double-stranded RNA-activated transcription factor DRAF1. *Molecular and cellular biology* **18**, 1359-1427 (1998).

74. Yoneyama, M. *et al.* Direct triggering of the type I interferon system by virus infection: activation of a transcription factor complex containing IRF-3 and CBP/p300. *The EMBO journal* **17**, 1087-1182 (1998).

75. Lin, R., Heylbroeck, C., Pitha, P.M. & Hiscott, J. Virus-dependent phosphorylation of the IRF-3 transcription factor regulates nuclear translocation, transactivation potential, and proteasome-mediated degradation. *Mol Cell Biol* **18**, 2986-2996 (1998).

76. Wathelet, M. *et al.* Virus infection induces the assembly of coordinately activated transcription factors on the IFN-beta enhancer in vivo. *Molecular cell* **1**, 507-525 (1998).

77. Schafer, S., Lin, R., Moore, P., Hiscott, J. & Pitha, P. Regulation of type I interferon gene expression by interferon regulatory factor-3. *The Journal of biological chemistry* **273**, 2714-2734 (1998).

78. Higgs, R. *et al.* The E3 ubiquitin ligase Ro52 negatively regulates IFN-beta production post-pathogen recognition by polyubiquitin-mediated degradation of IRF3. *Journal of immunology (Baltimore, Md. : 1950)* **181**, 1780-1786 (2008).

79. Saira, K., Zhou, Y. & Jones, C. The infected cell protein 0 encoded by bovine herpesvirus 1 (bICP0) induces degradation of interferon response factor 3 and, consequently, inhibits beta interferon promoter activity. *J Virol* **81**, 3077-3086 (2007).

80. Shi, H. *et al.* TLR4 links innate immunity and fatty acid-induced insulin resistance. *J Clin Invest* **116**, 3015-3025 (2006).

81. Takeuchi, O. *et al.* Differential Roles of TLR2 and TLR4 in Recognition of Gram-Negative and Gram-Positive Bacterial Cell Wall Components. *Immunity* **11**, 443-451 (1999).

82. Kurt-Jones, E.A. *et al.* Pattern recognition receptors TLR4 and CD14 mediate response to respiratory syncytial virus. *Nat Immunol* **1**, 398-401 (2000).

83. Adachi, O. *et al.* Targeted disruption of the MyD88 gene results in loss of IL-1- and IL-18-mediated function. *Immunity* **9**, 143-193 (1998).

84. Kawai, T., Adachi, O., Ogawa, T., Takeda, K. & Akira, S. Unresponsiveness of MyD88-deficient mice to endotoxin. *Immunity* **11**, 115-137 (1999).

85. Fitzgerald, K. *et al.* Mal (MyD88-adapter-like) is required for Toll-like receptor-4 signal transduction. *Nature* **413**, 78-161 (2001).

86. Horng, T., Barton, G., Flavell, R. & Medzhitov, R. The adaptor molecule TIRAP provides signalling specificity for Toll-like receptors. *Nature* **420**, 329-362 (2002).

87. Oshiumi, H., Matsumoto, M., Funami, K., Akazawa, T. & Seya, T. TICAM-1, an adaptor molecule that participates in Toll-like receptor 3-mediated interferon-beta induction. *Nature immunology* **4**, 161-168 (2003).

88. Yamamoto, M. *et al.* Role of adaptor TRIF in the MyD88-independent toll-like receptor signaling pathway. *Science (New York, N.Y.)* **301**, 640-643 (2003).

89. Yamamoto, M. *et al.* TRAM is specifically involved in the Toll-like receptor 4-mediated MyD88-independent signaling pathway. *Nature immunology* **4**, 1144-1194 (2003).

90. Akira, S., Uematsu, S. & Takeuchi, O. Pathogen recognition and innate immunity. *Cell* **124**, 783-1584 (2006).

91. Fitzgerald, K. *et al.* IKKepsilon and TBK1 are essential components of the IRF3 signaling pathway. *Nature immunology* **4**, 491-497 (2003).

92. Lei, C.-Q. *et al.* Glycogen synthase kinase 3β regulates IRF3 transcription factor-mediated antiviral response via activation of the kinase TBK1. *Immunity* **33**, 878-967 (2010).

93. Sharma, S. *et al.* Triggering the interferon antiviral response through an IKK-related pathway. *Science (New York, N.Y.)* **300**, 1148-1199 (2003).

94. Saberi, M. *et al.* Hematopoietic cell-specific deletion of toll-like receptor 4 ameliorates hepatic and adipose tissue insulin resistance in high-fat-fed mice. *Cell Metab* **10**, 419-429 (2009).

95. Chiang, S.H. *et al.* The protein kinase IKKepsilon regulates energy balance in obese mice. *Cell* **138**, 961-975 (2009).

96. Fain, J.N. Release of interleukins and other inflammatory cytokines by human adipose tissue is enhanced in obesity and primarily due to the nonfat cells. *Vitamins and hormones* **74**, 443-477 (2006).

97. Wellen, K.E. & Hotamisligil, G.S. Inflammation, stress, and diabetes. *J Clin Invest* **115**, 1111-1119 (2005).

98. Pradhan Ad, M.J.E.R.N.B.J.E.R.P.M. C-reactive protein, interleukin 6, and risk of developing type 2 diabetes mellitus. *JAMA: The Journal of the American Medical Association* **286**, 327-334 (2001).

99. Schäffler, A., Schölmerich, J. & Salzberger, B. Adipose tissue as an immunological organ: Toll-like receptors, C1q/TNFs and CTRPs. *Trends in immunology* **28**, 393-402 (2007).

100. Shoelson, S.E., Lee, J. & Goldfine, A.B. Inflammation and insulin resistance. *J Clin Invest* **116**, 1793-1801 (2006).

101. Xu, H. *et al.* Chronic inflammation in fat plays a crucial role in the development of obesity-related insulin resistance. *The Journal of clinical investigation* **112**, 1821-1851 (2003).

102. Hirsch, J. & Batchelor, B. Adipose tissue cellularity in human obesity. *Clin Endocrinol Metab* **5**, 299-311 (1976).

103. van Harmelen, V. *et al.* Effect of BMI and age on adipose tissue cellularity and differentiation capacity in women. *International journal of obesity and related metabolic disorders : journal of the International Association for the Study of Obesity* **27**, 889-984 (2003).

104. Lijnen, H. *et al.* 2002).

105. Chinetti-Gbaguidi, G. & Staels, B. Macrophage polarization in metabolic disorders: functions and regulation. *Current opinion in lipidology* **22**, 365-437 (2011).

106. Weisberg, S. *et al.* Obesity is associated with macrophage accumulation in adipose tissue. *The Journal of clinical investigation* **112**, 1796-2604 (2003).

107. Christiansen, T., Richelsen, B. & Bruun, J.M. Monocyte chemoattractant protein-1 is produced in isolated adipocytes, associated with adiposity and reduced after weight loss in morbid obese subjects. *Int J Obes (Lond)* **29**, 146-150 (2005).

108. Sartipy, P. & Loskutoff, D.J. Monocyte chemoattractant protein 1 in obesity and insulin resistance. *Proc Natl Acad Sci U S A* **100**, 7265-7270 (2003).

109. Feuerer, M. *et al.* Lean, but not obese, fat is enriched for a unique population of regulatory T cells that affect metabolic parameters. *Nat Med* **15**, 930-939 (2009).

110. Winer, S. *et al.* Normalization of obesity-associated insulin resistance through immunotherapy. *Nat Med* **15**, 921-929 (2009).

111. Winer, D.A. *et al.* B cells promote insulin resistance through modulation of T cells and production of pathogenic IgG antibodies. *Nat Med* **17**, 610-617 (2011).

112. Liu, J. *et al.* Genetic deficiency and pharmacological stabilization of mast cells reduce diet-induced obesity and diabetes in mice. *Nat Med* **15**, 940-945 (2009).

113. Wu, D. *et al.* Eosinophils Sustain Adipose Alternatively Activated Macrophages Associated with Glucose Homeostasis. *Science* **332**, 243-247 (2011).

114. Winer, S. *et al.* Normalization of obesity-associated insulin resistance through immunotherapy. *Nature medicine* **15**, 921-930 (2009).

115. Hotamisligil, G.S., Budavari, A., Murray, D. & Spiegelman, B.M. Reduced tyrosine kinase activity of the insulin receptor in obesity-diabetes. Central role of tumor necrosis factor-alpha. *The Journal of clinical investigation* **94**, 1543-1549 (1994).

116. Hofmann, C. *et al.* Altered gene expression for tumor necrosis factor-alpha and its receptors during drug and dietary modulation of insulin resistance. *Endocrinology* **134**, 264-270 (1994).

117. Hotamisligil, G.S. *et al.* IRS-1-Mediated Inhibition of Insulin Receptor Tyrosine Kinase Activity in TNF-α- and Obesity-Induced Insulin Resistance. *Science* **271**, 665-670 (1996).

118. Hotamisligil, G.S., Arner, P., Caro, J.F., Atkinson, R.L. & Spiegelman, B.M. Increased adipose tissue expression of tumor necrosis factor-alpha in human obesity and insulin resistance. *The Journal of clinical investigation* **95**, 2409-2415 (1995).

119. Kern, P.A. *et al.* The expression of tumor necrosis factor in human adipose tissue. Regulation by obesity, weight loss, and relationship to lipoprotein lipase. *The Journal of clinical investigation* **95**, 2111-2119 (1995).

120. Saghizadeh, M., Ong, J.M., Garvey, W.T., Henry, R.R. & Kern, P.A. The expression of TNF alpha by human muscle. Relationship to insulin resistance. *The Journal of clinical investigation* **97**, 1111-1116 (1996).

121. Dandona, P. *et al.* Tumor Necrosis Factor-α in Sera of Obese Patients: Fall with Weight Loss. *Journal of Clinical Endocrinology & Metabolism* **83**, 2907-2910 (1998).

122. Liu, L.S., Spelleken, M., Röhrig, K., Hauner, H. & Eckel, J. Tumor necrosis factor-alpha acutely inhibits insulin signaling in human adipocytes: implication of the p80 tumor necrosis factor receptor. *Diabetes* **47**, 515-522 (1998).

123. Hotamisligil, G., Shargill, N. & Spiegelman, B. Adipose expression of tumor necrosis factor-alpha: direct role in obesity-linked insulin resistance. *Science* **259**, 87-91 (1993).

124. Cheung, A.T. *et al.* An in Vivo Model for Elucidation of the Mechanism of Tumor Necrosis Factor-α (TNF-α)-Induced Insulin Resistance: Evidence for Differential Regulation of Insulin Signaling by TNF-α. *Endocrinology* **139**, 4928-4935 (1998).

125. Hotamisligil, G. The role of TNFalpha and TNF receptors in obesity and insulin resistance. *Journal of internal medicine* **245**, 621-626 (1999).

126. Uysal, K.T., Wiesbrock, S.M., Marino, M.W. & Hotamisligil, G.S. Protection from obesity-induced insulin resistance in mice lacking TNF-[alpha] function. *Nature* **389**, 610-614 (1997).

127. Houstis N Fau - Rosen, E.D., Rosen Ed Fau - Lander, E.S. & ES, L. - Reactive oxygen species have a causal role in multiple forms of insulin resistance. *Nature* **440**, 944-948 (2006).

128. Rudich, A. *et al.* Prolonged oxidative stress impairs insulin-induced GLUT4 translocation in 3T3-L1 adipocytes. *Diabetes* **47**, 1562-1569 (1998).

129. Lin, Y. *et al.* The Hyperglycemia-induced Inflammatory Response in Adipocytes. *Journal of Biological Chemistry* **280**, 4617-4626 (2005).

130. Feinstein, R., Kanety, H., Papa, M.Z., Lunenfeld, B. & Karasik, A. Tumor necrosis factor-alpha suppresses insulin-induced tyrosine phosphorylation of insulin receptor and its substrates. *Journal of Biological Chemistry* **268**, 26055-26058 (1993).

131. Kanety, H., Feinstein, R., Papa, M.Z., Hemi, R. & Karasik, A. Tumor Necrosis Factor -induced Phosphorylation of Insulin Receptor Substrate-1 (IRS-1). *Journal of Biological Chemistry* **270**, 23780-23784 (1995).

132. Jain, R., Police, S., Phelps, K. & Pekala, P. Tumour necrosis factor-alpha regulates expression of the CCAAT-enhancer-binding proteins (C/EBPs) alpha and beta and determines the occupation of the C/EBP site in the promoter of the insulin-responsive glucose-transporter gene in 3T3-L1 adipocytes. *The Biochemical journal* **338 (Pt 3)**, 737-780 (1999).

133. Lumeng, C. & Saltiel, A. Inflammatory links between obesity and metabolic disease. *The Journal of clinical investigation* **121**, 2111-2118 (2011).

134. Wen, H. *et al.* Fatty acid-induced NLRP3-ASC inflammasome activation interferes with insulin signaling. *Nat Immunol* **12**, 408-415 (2011).

135. McGillicuddy, F.C. *et al.* Lack of Interleukin-1 Receptor I (IL-1RI) Protects Mice From High-Fat Diet–Induced Adipose Tissue Inflammation Coincident With Improved Glucose Homeostasis. *Diabetes* **60**, 1688-1698 (2011).

136. Vandanmagsar, B. *et al.* The NLRP3 inflammasome instigates obesity-induced inflammation and insulin resistance. *Nat Med* **17**, 179-188 (2011).

137. Jager, J., Grémeaux, T., Cormont, M., Le Marchand-Brustel, Y. & Tanti, J.-F. Interleukin-1β-Induced Insulin Resistance in Adipocytes through Down-Regulation of Insulin Receptor Substrate-1 Expression. *Endocrinology* **148**, 241-251 (2007).

138. A, D. - Inflammasome activation: from inflammatory disease to infection. *Biochem Soc Trans* **39**, 669-673 (2011).

139. Dinarello, C.A. Interleukin-1 in the pathogenesis and treatment of inflammatory diseases. *Blood* **117**, 3720-3732 (2011).

140. Stienstra, R. *et al.* The Inflammasome-Mediated Caspase-1 Activation Controls Adipocyte Differentiation and Insulin Sensitivity. *Cell Metabolism* **12**, 593-605 (2010).

141. Hirosumi, J. *et al.* A central role for JNK in obesity and insulin resistance. *Nature* **420**, 333-336 (2002).

142. Kim, J.K. *et al.* Prevention of fat-induced insulin resistance by salicylate. *The Journal of clinical investigation* **108**, 437-446 (2001).

143. Arkan, M.C. *et al.* IKK-[beta] links inflammation to obesity-induced insulin resistance. *Nat Med* **11**, 191-198 (2005).

144. Ravichandran, L.V., Esposito, D.L., Chen, J. & Quon, M.J. Protein Kinase C-ζ Phosphorylates Insulin Receptor Substrate-1 and Impairs Its Ability to Activate Phosphatidylinositol 3-Kinase in Response to Insulin. *Journal of Biological Chemistry* **276**, 3543-3549 (2001).

145. Li, Y. *et al.* Protein Kinase C θ Inhibits Insulin Signaling by Phosphorylating IRS1 at Ser1101. *Journal of Biological Chemistry* **279**, 45304-45307 (2004).

146. Itani, S.I., Ruderman, N.B., Schmieder, F. & Boden, G. Lipid-Induced Insulin Resistance in Human Muscle Is Associated With Changes in Diacylglycerol, Protein Kinase C, and IκB-α. *Diabetes* **51**, 2005-2011 (2002).

147. Baeuerle, P.A. & Baltimore, D. NF-κB: Ten Years After. *Cell* **87**, 13-20 (1996).

148. Delhase, M., Hayakawa, M., Chen, Y. & Karin, M. Positive and Negative Regulation of IκB Kinase Activity Through IKKβ Subunit Phosphorylation. *Science* **284**, 309-313 (1999).

149. Patel, S. & Santani, D. Role of NF-kappa B in the pathogenesis of diabetes and its associated complications. *Pharmacol Rep* **61**, 595-603 (2009).

150. Morigi, M. *et al.* Leukocyte-endothelial interaction is augmented by high glucose concentrations and hyperglycemia in a NF-kB-dependent fashion. *J Clin Invest* **101**, 1905-1915 (1998).

151. Dias, A.S. *et al.* Quercetin Decreases Oxidative Stress, NF-κB Activation, and iNOS Overexpression in Liver of Streptozotocin-Induced Diabetic Rats. *The Journal of Nutrition* **135**, 2299-2304 (2005).

152. Ajuwon, K.M. & Spurlock, M.E. Palmitate Activates the NF-κB Transcription Factor and Induces IL-6 and TNFα Expression in 3T3-L1 Adipocytes. *The Journal of Nutrition* **135**, 1841-1846 (2005).

153. Rodríguez-Calvo, R. *et al.* Activation of Peroxisome Proliferator–Activated Receptor β/δ Inhibits Lipopolysaccharide-Induced Cytokine Production in Adipocytes by Lowering Nuclear Factor-κB Activity via Extracellular Signal–Related Kinase 1/2. *Diabetes* **57**, 2149-2157 (2008).

154. Ruan, H., Pownall, H.J. & Lodish, H.F. Troglitazone Antagonizes Tumor Necrosis Factor-α-induced Reprogramming of Adipocyte Gene Expression by Inhibiting the Transcriptional Regulatory Functions of NF-κB. *Journal of Biological Chemistry* **278**, 28181-28192 (2003).

155. Ajuwon, K.M. & Spurlock, M.E. Adiponectin inhibits LPS-induced NF-κB activation and IL-6 production and increases PPARγ2 expression in adipocytes. *American Journal of Physiology - Regulatory, Integrative and Comparative Physiology* **288**, R1220-R1225 (2005).

156. Sato, M. *et al.* Distinct and essential roles of transcription factors IRF-3 and IRF-7 in response to viruses for IFN-alpha/beta gene induction. *Immunity* **13**, 539-548 (2000).

157. Sakaguchi S Fau - Negishi, H. *et al.* - Essential role of IRF-3 in lipopolysaccharide-induced interferon-beta gene expression and endotoxin shock. *Biochem Biophys Res Commun* **306**, 860-866 (2003).

158. Lumeng, C.N., Bodzin, J.L. & Saltiel, A.R. Obesity induces a phenotypic switch in adipose tissue macrophage polarization. *The Journal of clinical investigation* **117**, 175-184 (2007).

159. Lumeng, C.N., DeYoung, S.M., Bodzin, J.L. & Saltiel, A.R. Increased Inflammatory Properties of Adipose Tissue Macrophages Recruited During Diet-Induced Obesity. *Diabetes* **56**, 16-23 (2007).

160. Castrillo, A. *et al.* Crosstalk between LXR and toll-like receptor signaling mediates bacterial and viral antagonism of cholesterol metabolism. *Mol Cell* **12**, 805-816 (2003).

161. Abe, M. *et al.* Effects of Statins on Adipose Tissue Inflammation. *Arteriosclerosis, Thrombosis, and Vascular Biology* **28**, 871-877 (2008).

162. Zhao, W. *et al.* Peroxisome proliferator-activated receptor gamma negatively regulates IFN-beta production in Toll-like receptor (TLR) 3- and TLR4-stimulated macrophages by preventing interferon regulatory factor 3 binding to the IFN-beta promoter. *The Journal of biological chemistry* **286**, 5519-5547 (2011).

163. Zebisch, K., Voigt, V., Wabitsch, M. & Brandsch, M. Protocol for effective differentiation of 3T3-L1 cells to adipocytes. *Analytical Biochemistry* **425**, 88-90 (2012).

164. Green, H. & Meuth, M. An established pre-adipose cell line and its differentiation in culture. *Cell* **3**, 127-133 (1974).

165. Green, H. & Kehinde, O. Spontaneous heritable changes leading to increased adipose conversion in 3T3 cells. *Cell* **7**, 105-118 (1976).

166. Green, H. & Kehinde, O. An established preadipose cell line and its differentiation in culture. II. Factors affecting the adipose conversion. *Cell* **5**, 19-46 (1975).

167. Negishi, H. *et al.* Negative regulation of Toll-like-receptor signaling by IRF-4. *Proceedings of the National Academy of Sciences of the United States of America* **102**, 15989-15994 (2005).

168. Subramanian A Fau - Tamayo, P. *et al.* - Gene set enrichment analysis: a knowledge-based approach for interpreting genome-wide expression profiles. *Proc Natl Acad Sci U S A* **102**, 15545-15550 (2005).

169. Knaus, U. Rho GTPase signaling in inflammation and transformation. *Immunologic Research* **21**, 103-109 (2000).

170. Kopp, A. *et al.* Toll-like receptor ligands cause proinflammatory and prodiabetic activation of adipocytes via phosphorylation of extracellular signal-regulated kinase and c-Jun N-terminal kinase but not interferon regulatory factor-3. *Endocrinology* **151**, 1097-1205 (2010).

171. Christiansen, T., Richelsen, B. & Bruun, J.M. Monocyte chemoattractant protein-1 is produced in isolated adipocytes, associated with adiposity and reduced after weight loss in morbid obese subjects. *Int J Obes Relat Metab Disord* **29**, 146-150 (2004).

172. Gerhardt, C.C., Romero, I.A., Cancello, R., Camoin, L. & Strosberg, A.D. Chemokines control fat accumulation and leptin secretion by cultured human adipocytes. *Molecular and Cellular Endocrinology* **175**, 81-92 (2001).

173. Smith, M.J.H., Ford-Hutchinson, A.W. & Bray, M.A. Leukotriene B: a potential mediator of inflammation. *Journal of Pharmacy and Pharmacology* **32**, 517-518 (1980).

174. Chakrabarti, S.K. *et al.* Evidence for activation of inflammatory lipoxygenase pathways in visceral adipose tissue of obese Zucker rats. *American Journal of Physiology - Endocrinology And Metabolism* **300**, E175-E187 (2011).

175. Spite, M. *et al.* Deficiency of the Leukotriene B4 Receptor, BLT-1, Protects against Systemic Insulin Resistance in Diet-Induced Obesity. *The Journal of Immunology* **187**, 1942-1949 (2011).

176. Stephens, J.M. & Pekala, P.H. Transcriptional repression of the GLUT4 and C/EBP genes in 3T3-L1 adipocytes by tumor necrosis factor-alpha. *Journal of Biological Chemistry* **266**, 21839-21845 (1991).

177. Ohshima, S. *et al.* Interleukin 6 plays a key role in the development of antigen-induced arthritis. *Proceedings of the National Academy of Sciences* **95**, 8222-8226 (1998).

178. Nguyen, M.T.A. *et al.* A Subpopulation of Macrophages Infiltrates Hypertrophic Adipose Tissue and Is Activated by Free Fatty Acids via Toll-like Receptors 2 and 4 and JNK-dependent Pathways. *Journal of Biological Chemistry* **282**, 35279-35292 (2007).

179. Patsouris, D. *et al.* Ablation of CD11c-Positive Cells Normalizes Insulin Sensitivity in Obese Insulin Resistant Animals. *Cell Metabolism* **8**, 301-309 (2008).

180. Nishimura, S. *et al.* CD8+ effector T cells contribute to macrophage recruitment and adipose tissue inflammation in obesity. *Nat Med* **15**, 914-920 (2009).

181. H, K. - Eosinophils: multifaceted biological properties and roles in health and disease. *Immunol Rev* **242**, 161-177 (2011).

182. Hall, K.D. *et al.* Energy balance and its components: implications for body weight regulation. *The American Journal of Clinical Nutrition* **95**, 989-994 (2012).

183. Lean, M.E. Brown adipose tissue in humans. *Proc Nutr Soc* **48**, 243-256 (1989).

184. Farmer, S.R. Transcriptional Control of Gene Expression in Different Adipose Tissue Depots
Novel Insights into Adipose Cell Functions, in. (eds. Y. Christen, K. Clément & B.M. Spiegelman) 93-100 (Springer Berlin Heidelberg, 2010).

185. Zhou, Z. *et al.* Cidea-deficient mice have lean phenotype and are resistant to obesity. *Nat Genet* **35**, 49-56 (2003).

186. Hammel, H.T. & Pierce, J.B. Regulation of Internal Body Temperature. *Annual Review of Physiology* **30**, 641-710 (1968).

187. Tinsley, F.C., Taicher, G.Z. & Heiman, M.L. Evaluation of a Quantitative Magnetic Resonance Method for Mouse Whole Body Composition Analysis. *Obesity* **12**, 150-160 (2004).

188. Nixon, J.P. *et al.* Evaluation of a Quantitative Magnetic Resonance Imaging System for Whole Body Composition Analysis in Rodents. *Obesity* **18**, 1652-1659 (2010).

189. Ntambi, J.M. & Young-Cheul, K. Adipocyte Differentiation and Gene Expression. *The Journal of Nutrition* **130**, 3122S-3126S (2000).

190. Guo, X. & Liao, K. Analysis of gene expression profile during 3T3-L1 preadipocyte differentiation. *Gene* **251**, 45-53 (2000).

191. Zhang, Y. *et al.* Positional cloning of the mouse obese gene and its human homologue. *Nature* **372**, 425-432 (1994).

192. Campfield, L.A., Smith, F.J., Guisez, Y., Devos, R. & Burn, P. Recombinant mouse OB protein: evidence for a peripheral signal linking adiposity and central neural networks. *Science* **269**, 546-549 (1995).

193. Coleman, D.L. Obese and diabetes: two mutant genes causing diabetes-obesity syndromes in mice. *Diabetologia* **14**, 141-148 (1978).

194. Pelleymounter, M.A. *et al.* Effects of the obese gene product on body weight regulation in ob/ob mice. *Science* **269**, 540-543 (1995).

195. Chen, H. *et al.* Evidence That the Diabetes Gene Encodes the Leptin Receptor: Identification of a Mutation in the Leptin Receptor Gene in db/db Mice. *Cell* **84**, 491-495 (1996).

196. Stephens, T.W. *et al.* The role of neuropeptide Y in the antiobesity action of the obese gene product. *Nature* **377**, 530-532 (1995).

197. Bjorbaek, C. Central leptin receptor action and resistance in obesity. *J Investig Med* **57**, 789-794 (2009).

198. Menachery, V.D., Pasieka, T.J. & Leib, D.A. Interferon Regulatory Factor 3-Dependent Pathways Are Critical for Control of Herpes Simplex Virus Type 1 Central Nervous System Infection. *Journal of virology* **84**, 9685-9694 (2010).

199. Kim, H. *et al.* Double-stranded RNA mediates interferon regulatory factor 3 activation and interleukin-6 production by engaging Toll-like receptor 3 in human brain astrocytes. *Immunology* **124**, 480-488 (2008).

200. Marsh, B. *et al.* Systemic Lipopolysaccharide Protects the Brain from Ischemic Injury by Reprogramming the Response of the Brain to Stroke: A Critical Role for IRF3. *The Journal of Neuroscience* **29**, 9839-9849 (2009).

201. Davidson, B.L. *et al.* Recombinant adeno-associated virus type 2, 4, and 5 vectors: Transduction of variant cell types and regions in the mammalian central nervous system. *Proceedings of the National Academy of Sciences* **97**, 3428-3432 (2000).

202. Nakamura, K. & Morrison, S.F. A thermosensory pathway that controls body temperature. *Nat Neurosci* **11**, 62-71 (2008).

203. Morrison, S.F., Nakamura, K. & Madden, C.J. Central control of thermogenesis in mammals. *Experimental Physiology* **93**, 773-797 (2008).

204. Ellis, J.M. *et al.* Adipose Acyl-CoA Synthetase-1 Directs Fatty Acids toward β-Oxidation and Is Required for Cold Thermogenesis. *Cell Metabolism* **12**, 53-64 (2010).

205. Enerback, S. *et al.* Mice lacking mitochondrial uncoupling protein are cold-sensitive but not obese. *Nature* **387**, 90-94 (1997).

206. Puigserver, P. *et al.* A cold-inducible coactivator of nuclear receptors linked to adaptive thermogenesis. *Cell* **92**, 829-839 (1998).

207. Maeda, N. *et al.* Diet-induced insulin resistance in mice lacking adiponectin/ACRP30. *Nature medicine* **8**, 731-738 (2002).

208. Kubota, N. *et al.* Disruption of adiponectin causes insulin resistance and neointimal formation. *The Journal of biological chemistry* **277**, 25863-25869 (2002).

209. Ma, K. *et al.* Increased beta -oxidation but no insulin resistance or glucose intolerance in mice lacking adiponectin. *The Journal of biological chemistry* **277**, 34658-34719 (2002).

210. Banerjee, R. *et al.* Regulation of fasted blood glucose by resistin. *Science (New York, N.Y.)* **303**, 1195-1203 (2004).

211. Steppan, C. & Lazar, M. The current biology of resistin. *Journal of internal medicine* **255**, 439-486 (2004).

212. Saltiel, A.R. & Kahn, C.R. Insulin signalling and the regulation of glucose and lipid metabolism. *Nature* **414**, 799-806 (2001).

213. Kasuga, M., Karlsson, F. & Kahn, C. Insulin stimulates the phosphorylation of the 95,000-dalton subunit of its own receptor. *Science* **215**, 185-187 (1982).

214. Kasuga, M., Zick, Y., Blithe, D.L., Crettaz, M. & Kahn, C.R. Insulin stimulates tyrosine phosphorylation of the insulin receptor in a cell-free system. *Nature* **298**, 667-669 (1982).

215. White, M.F., Maron, R. & Kahn, C.R. Insulin rapidly stimulates tyrosine phosphorylation of a Mr-185,000 protein in intact cells. *Nature* **318**, 183-186 (1985).

216. Sun, X.J. *et al.* Structure of the insulin receptor substrate IRS-1 defines a unique signal transduction protein. *Nature* **352**, 73-77 (1991).

217. Patti, M. & Kahn, C. The insulin receptor--a critical link in glucose homeostasis and insulin action. *Journal of basic and clinical physiology and pharmacology* **9**, 89-198 (1998).

218. Shepherd, P., Withers, D. & Siddle, K. Phosphoinositide 3-kinase: the key switch mechanism in insulin signalling. *The Biochemical journal* **333 (Pt 3)**, 471-561 (1998).

219. Wymann, M.P. & Pirola, L. Structure and function of phosphoinositide 3-kinases. *Biochim Biophys Acta* **1436**, 127-150 (1998).

220. Jiang, Z.Y. *et al.* Insulin signaling through Akt/protein kinase B analyzed by small interfering RNA-mediated gene silencing. *Proceedings of the National Academy of Sciences* **100**, 7569-7574 (2003).

221. Taniguchi, C., Emanuelli, B. & Kahn, C. Critical nodes in signalling pathways: insights into insulin action. *Nature reviews. Molecular cell biology* **7**, 85-181 (2006).

222. Thorens, B. Glucose sensing and the pathogenesis of obesity and type 2 diabetes. *International journal of obesity (2005)* **32 Suppl 6**, 71 (2008).

223. Zorzano, A., Palacín, M. & Gumà, A. Mechanisms regulating GLUT4 glucose transporter expression and glucose transport in skeletal muscle. *Acta physiologica Scandinavica* **183**, 43-101 (2005).

224. White, M. & Kahn, C. The insulin signaling system. *The Journal of biological chemistry* **269**, 1-5 (1994).

225. Hill, M.M. *et al.* A Role for Protein Kinase Bβ/Akt2 in Insulin-Stimulated GLUT4 Translocation in Adipocytes. *Molecular and cellular biology* **19**, 7771-7781 (1999).

226. Bogan, J.S. & Kandror, K.V. Biogenesis and regulation of insulin-responsive vesicles containing GLUT4. *Current Opinion in Cell Biology* **22**, 506-512 (2010).

227. Robinson, L., Pang, S., Harris, D., Heuser, J. & James, D. Translocation of the glucose transporter (GLUT4) to the cell surface in permeabilized 3T3-L1 adipocytes: effects of ATP insulin, and GTP gamma S and localization of GLUT4 to clathrin lattices. *The Journal of Cell Biology* **117**, 1181-1196 (1992).

228. Charron, M., Katz, E. & Olson, A. GLUT4 gene regulation and manipulation. *The Journal of biological chemistry* **274**, 3253-3259 (1999).

229. Carvalho, E., Kotani, K., Peroni, O.D. & Kahn, B.B. Adipose-specific overexpression of GLUT4 reverses insulin resistance and diabetes in mice lacking GLUT4 selectively in muscle. *American Journal of Physiology - Endocrinology And Metabolism* **289**, E551-E561 (2005).

230. HOFMANN, C., LORENZ, K. & COLCA, J.R. Glucose Transport Deficiency in Diabetic Animals Is Corrected by Treatment with the Oral Antihyperglycemic Agent Pioglitazone. *Endocrinology* **129**, 1915-1925 (1991).

231. Todaro Gj Fau - Green, H. & H., G. - Quantitative studies of the growth of mouse embryo cells in culture and their development into established lines. *J Cell Biol* **17**, 299-313 (1963).

232. Ronald Kahn, C. Insulin resistance, insulin insensitivity, and insulin unresponsiveness: A necessary distinction. *Metabolism* **27**, 1893-1902 (1978).

233. Hirschberg, A.L. Sex hormones, appetite and eating behaviour in women. *Maturitas* **71**, 248-256 (2012).

234. Godsland If Fau - Walton, C. *et al.* - Insulin resistance, secretion, and metabolism in users of oral contraceptives. *J Clin Endocrinol Metab* **74**, 64-70 (1992).

235. Lindheim Sr Fau - Buchanan, T.A. *et al.* - Comparison of estimates of insulin sensitivity in pre- and postmenopausal women using the insulin tolerance test and the frequently sampled intravenous glucose tolerance test. *J Soc Gynecol Investig* **1**, 150-154 (1994).

236. Baba T Fau - Shimizu, T. *et al.* - Estrogen, insulin, and dietary signals cooperatively regulate longevity signals to enhance resistance to oxidative stress in mice. *J Biol Chem* **280**, 16417-16426 (2005).

237. STEPHENS, J.M. & PILCH, P.F. The Metabolic Regulation and Vesicular Transport of GLUT4, the Major Insulin-Responsive Glucose Transporter. *Endocrine Reviews* **16**, 529-546 (1995).

238. Brochu-Gaudreau, K. *et al.* Adiponectin action from head to toe. *Endocrine* **37**, 11-32 (2010).

239. Deng, Y. & Scherer, P.E. Adipokines as novel biomarkers and regulators of the metabolic syndrome. *Annals of the New York Academy of Sciences* **1212**, E1-E19 (2010).

240. Maury, E. & Brichard, S.M. Adipokine dysregulation, adipose tissue inflammation and metabolic syndrome. *Molecular and Cellular Endocrinology* **314**, 1-16 (2010).

241. Boyle, J. *et al.* AMP-activated protein kinase is activated in adipose tissue of individuals with type 2 diabetes treated with metformin: a randomised glycaemia-controlled crossover study. *Diabetologia* **54**, 1799-1809 (2011).

242. Bredella, M.A. *et al.* Determinants of bone mineral density in obese premenopausal women. *Bone* **48**, 748-754 (2011).

243. Rasouli, N. & Kern, P.A. Adipocytokines and the Metabolic Complications of Obesity. *Journal of Clinical Endocrinology & Metabolism* **93**, s64-s73 (2008).

244. Hirose, H., Yamamoto, Y., Seino-Yoshihara, Y., Kawabe, H. & Saito, I. Serum high-molecular-weight adiponectin as a marker for the evaluation and care of subjects with metabolic syndrome and related disorders. *Journal of Atherosclerosis and Thrombosis* **17**, 1201-1211 (2010).

245. Nakashima, R., Yamane, K., Kamei, N., Nakanishi, S. & Kohno, N. Low serum levels of total and high-molecular-weight adiponectin predict the development of metabolic syndrome in Japanese-Americans. *J Endocrinol Invest* **34**, 615-619 (2011).

246. Nguyen, K.D. *et al.* Alternatively activated macrophages produce catecholamines to sustain adaptive thermogenesis. *Nature* **480**, 104-108 (2011).

247. Patti Me Fau - Butte, A.J. *et al.* - Coordinated reduction of genes of oxidative metabolism in humans with insulin resistance and diabetes: Potential role of PGC1 and NRF1. *Proc Natl Acad Sci U S A* **100**, 8466-8471 (2003).

248. Lagouge, M. *et al.* Resveratrol Improves Mitochondrial Function and Protects against Metabolic Disease by Activating SIRT1 and PGC-1±. *Cell* **127**, 1109-1122 (2006).

249. Yang, X., Enerback, S. & Smith, U. Reduced Expression of FOXC2 and Brown Adipogenic Genes in Human Subjects with Insulin Resistance. *Obesity* **11**, 1182-1191 (2003).

250. Saberi, M. *et al.* Hematopoietic cell-specific deletion of toll-like receptor 4 ameliorates hepatic and adipose tissue insulin resistance in high-fat-fed mice. *Cell Metabolism* **10**, 419-448 (2009).

251. Seo, J.-Y., Yaneva, R., Hinson, E. & Cresswell, P. Human cytomegalovirus directly induces the antiviral protein viperin to enhance infectivity. *Science (New York, N.Y.)* **332**, 1093-1100 (2011).